Two-Phase Natural-Circulation Experiments in a Test Facility Modeled After Three Mile Island Unit-2

MASTER

EPRI

EPRI NP-2069
Project 1731-1
Final Report
October 1981

Keywords:
Two-Phase Flow
Natural Circulation
Reflux
Once-Through Steam Generators
Noncondensible Gases
Condensation

Prepared by
SRI International
Menlo Park, California

ELECTRIC POWER RESEARCH INSTITUTE

DISCLAIMER

Two-Phase Natural-Circulation Experiments in a Test Facility Modeled After Three Mile Island Unit-2

NP-2069
Research Project 1731-1

Final Report, October 1981

Prepared by

SRI INTERNATIONAL
333 Ravenswood Avenue
Menlo Park, California 94025

Principal Investigator
R. L. Kiang

Prepared for

Electric Power Research Institute
3412 Hillview Avenue
Palo Alto, California 94304

EPRI Project Manager
J.-P. Sursock

Analysis and Testing Program
Nuclear Power Division

ORDERING INFORMATION

Requests for copies of this report should be directed to Research Reports Center (RRC), Box 50490, Palo Alto, CA 94303, (415) 965-4081. There is no charge for reports requested by EPRI member utilities and affiliates, contributing nonmembers, U.S utility associations, U.S. government agencies (federal, state, and local), media, and foreign organizations with which EPRI has an information exchange agreement. On request, RRC will send a catalog of EPRI reports.

NOTICE

This report was prepared by the organization(s) named below as an account of work sponsored by the Electric Power Research Institute, Inc (EPRI) Neither EPRI, members of EPRI, the organization(s) named below, nor any person acting on behalf of any of them (a) makes any warranty, express or implied, with respect to the use of any information, apparatus, method, or process disclosed in this report or that such use may not infringe privately owned rights, or (b) assumes any liabilities with respect to the use of, or for damages resulting from the use of, any information, apparatus, method, or process disclosed in this report

Prepared by
SRI International
Menlo Park, California

EPRI PERSPECTIVE

PROJECT DESCRIPTION

In the days that followed the Three Mile Island (TMI) accident, much concern was raised about the possibility of cooling the core by natural circulation means in presence of noncondensible gases. These gases could collect in the top of the steam generator and seriously impede the flow motion.

The project (RP1731-1) was initiated to explore the possibility of cooling the core by means of two-phase natural circulation which produces sufficient vapor to traverse the plug and restore flow motion.

A scaled version of TMI primary loop, with once-through heat exchangers, was rapidly erected, and tests proceeded almost continuously during the next few days.

PROJECT OBJECTIVES

The objectives of the tests were to determine (1) the significant variables affecting two-phase natural circulation and reflux condensation modes, (2) the transition between these two modes, and (3) the limits of operation.

PROJECT RESULTS

The major result of the tests is that both two-phase natural circulation and reflux condensation are very tolerant of noncondensible gases. In addition, the tests provided extremely valuable insights about the detailed mechanisms at work and an important data bank which could be (and has been) used for code qualification.

The report should be helpful to individuals interested in small-break analysis, natural circulation, code verification, and procedure evaluation.

Jean-Pierre Sursock, Project Manager
Nuclear Power Division

ABSTRACT

A series of natural circulation experiments was conducted in a test facility that was configured after the primary and the secondary cooling systems of Three Mile Island Unit-2 (TMI-2). The results support the feasibility of core residual heat removal by two-phase natural circulation. Tests with noncondensable gas in the primary system indicate that two-phase natural circulation is quite tolerant of the presence of noncondensable gas. Two different modes of natural circulation were discovered. Mode 1, during which only saturated steam flows in the hot leg, accomplishes the heat removal via phase changes in the vessel and in the steam generator tubes. Mode 2, during which a percolating flow exists in the hot leg, removes the heat by means of a much faster circulation in the primary loop.

ACKNOWLEDGMENT

The conception of the project, the design and fabrication of the test facility, and the performance of the experiments were accomplished in a very short period of time not long after the accident at TMI-2. A large number of people contributed to this project. In particular, the contributions of the following individuals are recognized: Peter Newgard; Joseph Eckerle; Manchi Colah; Philip Jeuck, 3rd; Brian Grossi; Thomas Maxwell; George Ganschow; Mark Benz. The author would also like to acknowledge the personal involvement of Drs. R.T. Fernandez and J-P Sursock of EPRI during the course of the project.

CONTENTS

NOMENCLATURE

A_{HL}	Cross-sectional area of a hotleg
c	Circumference of a tube
C_p	Specific heat of water
d_{HL}	Inside diameter of a hotleg
d_{CL}	Inside diameter of a coldleg
d_T	Inside diameter of a heat exchanger tube
h	Enthalpy
l_{HL}	Length of a hotleg
l_{CL}	Length of a coldleg
l_T	Length of a heat exchanger tube
$\dot{m}$	Mass flow rate of steam
$\dot{m}_p$	Primary flow rate
$\dot{m}_s$	Secondary flow rate
N_T	Number of active tubes in a heat exchanger
p	Pressure in the reactor vessel
P_{in}	Power input
$\dot{q}$	Rate of heat transfer
T	Temperature
U	Overall heat loss coefficient
V	Volume
z	Elevation

Subscripts

p	Primary system
s	Secondary system
RV	Reactor vessel
SG	Steam generator
HL	Hotleg
CL	Coldleg
LHL	Left-loop hotleg
RHL	Right-loop hotleg
LI	Secondary inlet to the left steam generator
LO	Secondary outlet to the left steam generator
LSGP	Upper plenum of left steam generator
LSGT	Instrumented tube in the left steam generator
UP	Upper plenum of reactor vessel
SS	Shell-side of heat exchanger
SAT	Saturation condition

W	Water
N_2	Nitrogen
m	Model
f	Full scale

EXECUTIVE SUMMARY

The feasibility of two-phase natural circulation in a test facility modeled after Three Mile Island Unit-2 (TMI-2) was assessed in this experimental program.

The test facility consisted of a steel vessel containing three electric heaters, two vertical counterflow heat exchangers, and the connecting hotlegs and coldlegs between the vessel and the heat exchangers. There was no pump in the system. All experiments were performed with the primary system under two-phase conditions of various void fractions, and with the secondary coolant in the heat exchangers kept subcooled. With a solid secondary, the heat exchangers are not used as steam generators. However, since the test facility was modeled after the TMI-2 cooling system, we have retained the TMI terminology and refered to the two heat exchangers as steam generators.

The tests were run with varying amounts of water in the primary system, varying power input to the heaters, different secondary flow rates, and measured amounts of noncondensable gas in the primary system. The major findings of the experiments are summarized below.

Steady-state heat removal is readily achievable by means of two-phase natural circulation in the primary system and forced circulation in the secondary system, provided one allows the primary system pressure to seek its own equilibrium value. Throughout the test facility, the highest recorded temperature is always the saturation temperature corresponding to the pressure in the vessel. Only one time during the entire test program, after a copious amount of nitrogen gas was injected into the primary system, did the system fail to reach an equilibrium. Even on that occasion, the test was terminated because the design pressure limit of the facility (~ 100 psig) was approached. Had the pressure limit been higher, an equilibrium state might have been achieved. In any case, we found that under a two-phase natural circulation condition, the system was quite tolerant of noncondensable gas.

One of the more interesting results of these experiments is the discovery and the substantial explanation of two fundamental modes of natural circulation. If the water inventory in the primary system is sufficiently low so that the hotlegs are entirely clear of water, the system will equilibrate at a mode characterized by a step-like temperature profile on the secondary side of the active steam generator(s). This mode of operation has been designated as Mode 1. During this mode of operation, steam and water in the primary system are segregated in such a way that steam exists primarily in the upper half and water in the lower half of the system. The condensation of steam and the subsequent cooling of condensate take place in a short vertical section of the active steam generator(s). The slight "vacuum" generated by the condensation process continuously draws steam from the vessel, thus keeping the primary-loop flow going. This is sometimes referred to as the "reflux condensation" mode.

If the water inventory in the primary system is high, such that the hotlegs are substantially filled with water, the flow through the hotlegs is postulated to be two phase and to resemble the percolating action in a coffee maker. This percolating flow can be detected by its characteristic noise as well as the unsteady water levels in the steam generator tubes, which are instrumented with sight-gauges. Once the two-phase mixture enters the tubes of a steam generator, the heat transfer between the primary and the secondary coolants takes place over a much longer section of the steam generator when compared with that of Mode 1. As a result, the temperature profile along the secondary side of the steam generator assumes a much gentler curve. The shape of this curve, which indicates where the heat transfer occurs, is dependent on the ratio of primary to secondary flow rates. That ratio appears to be dictated by either the water inventory or the amount of noncondensable gas in the primary system. When either the water inventory or the amount of gas is relatively low, the bulk of heat transfer occurs near the lower tube sheet. We have designated this mode of operation as Mode 2a. In this mode, the ratio of primary to secondary flow is greater than one. As the amount of water or gas is increased, heat transfer takes place along the entire length of the steam generator. This mode, characterized by a nearly linear temperature profile along the steam generator, is designated as Mode 2b. When this mode is in existence, the ratio of primary to secondary flow is believed to be close to one. For very high water or gas content, heat transfer occurs primarily near the upper tube sheet. The ratio of primary to secondary flow during this mode, to be called Mode 2c, is less than one.

Section 1

BACKGROUND AND OBJECTIVES

One of the proposed natural cooling schemes to bring the crippled Three-Mile Island Unit 2 (TMI-2) reactor core to a cold shutdown after the 28 March 1979 accident was via two-phase natural circulation. The envisioned heat-removal process was as follows. Primary cooling water entering the reactor vessel from either or both steam generators would be heated and brought to boiling by the residual heat of the core. The steam or steam/water mixture thus generated would be convected via buoyancy effect through the hotleg(s) to the steam generator(s). The primary coolant would then be cooled in the once-through steam generator(s) (OTSG) by forced circulation of water on the secondary side(s) of the steam generator(s). The two-phase natural circulation differs from the single-phase natural circulation in two respects:

- The water inventory in the primary system is less than that in the single-phase operation.
- Steam, as well as water, is present in the primary system.

The major advantage of this scheme over single-phase natural circulation is the possibility of overcoming potential negative effects of noncondensable gas in the primary system.

A 1/18-scale model of the TMI-2 cooling system was designed and fabricated. During the subsequent test series, approximately 50 sets of data were collected, most of them under steady-state two-phase natural circulation conditions. The objectives of these experiments were to:

- Ascertain whether steady-state heat removal is achievable.
- Define limits, if they exist, outside of which steady-state heat removal is not possible.
- Compile relevant experimental data for future analysis.

Section 2

DESIGN CONSIDERATIONS

The TMI-2 cooling system to be modeled includes the reactor vessel, the two hotlegs, the two vertical once-through steam generators, and the coldlegs. To ease model fabrication, a number of simplifications were implemented. The two coldlegs of each loop were combined into one coldleg. The elevated "dog-leg" portion of the coldleg was modeled, but with the primary coolant pump eliminated. The coaxial arrangement of the downcomer was not duplicated. Instead, the annular flow path was replaced by a vertical extension of the coldleg external of the vessel. The pressurizer was not modeled. During the last two days of testing, a glass vessel was added and connected to the left hotleg: It was not designed to regulate the system pressure, but rather to act as a drain tank.

The basic scaling criterion selected for the model was that the enthalpy flux in the hotleg be kept the same between the model and the full-scale plant. If $\dot{m}_p$ denotes the mass flow rate in the hotleg, h denotes the enthalpy of the primary coolant at a cross-sectional area of the hotleg, and A_{HL} denotes the cross-sectional area of the hotleg, we require that

$$\left(\frac{\dot{m}_p h}{A_{HL}}\right)_m = \left(\frac{\dot{m}_p h}{A_{HL}}\right)_f \quad , \tag{2-1}$$

where subscripts m and f denote model and full-scale plant respectively. This criterion in turn determines how the residual power of the core should be scaled:

$$\frac{(P_{in})_m}{(P_{in})_p} = \frac{(A_{HL})_m}{(A_{HL})_p} = \frac{(d_{HL}^2)_m}{(d_{HL}^2)_p} \quad . \tag{2-2}$$

In our model, the power input was provided by immersion electric heaters.

The availability of 2-inch copper pipes and their fittings made it convenient to construct the model hotlegs and coldlegs out of these pipes. Since the diameter of the full-scale hotleg is 36 inches, the resulting scale factor is*

$$\frac{(d_{HL})_m}{(d_{HL})_p} = \frac{2}{36} = \frac{1}{18} \quad . \tag{2-3}$$

In order to permit use of off-the-shelf items, many dimensions of the model, such as the diameter of the vessel and the height of the steam generators, were not scaled exactly, but whenever possible, the relative elevations and the internal volumes of various components are scaled according to the scale factor. Table 2-1 summarizes the model parameters and the corresponding TMI-2 values.

*To be exact, the 2-inch pipe has an ID of 1.985 inches. Hence, the exact scale factor is 1/18.14.

Table 2-1

MODEL PARAMETERS AND VALUES

Item	Notation	TMI-2 English Units	TMI-2 Metric Units	Model English Units	Model Metric Units
Steam generation	$\dot{m}$	~ 2.1 lbm/s	9.53 g/s	0.0064 lbm/s	2.9 g/s
Steam flux in hotleg	$\dot{m}/A_{HL}$	0.30 (lbm/s)/ft^2	0.15 (g/s)/cm^2	0.30 (lbm/s)/ft^2	0.15 (g/s)/cm^2
Hotleg ID	d_{HL}	36 inches	91.4 cm	1.985 inches	5.0 cm
Coldleg ID	d_{CL}	28 inches	71.1 cm	1.985 inches	5.0 cm
Core power	P_{in}	1894 Btu/s	2,000 kW	5.87 Btu/s	6.2 kW
Primary system volume	V_p	11,970 ft^3	344,975 liters	2.01 ft^3	57.9 liters
Volume of hotleg (one)	V_{HL}	526 ft^3	15,159 liters	0.140 ft^3	3.98 liters
Volume of coldleg (one)	V_{CL}	745 ft^3	21,471 liters	0.144 ft^3	4.14 liters
Volume of reactor vessel (RV)	V_{RV}	3,909 ft^3	112,657 liters	0.655 ft^3	18.9 liters
Sum of tube volume	V_T	1,368 ft^3	39,426 liters	0.229 ft^3	6.6 liters
Length of hotleg	l_{HL}			6.5 ft	198 cm
Length of coldleg	l_{CL}			6.7 ft	204 cm
Heat exchanger tube ID	d_T			0.328 inch	0.83 cm
Heat exchanger tube length	l_T			57.5 inches	146 cm
Number of heat exchanger tubes	N_T			78	
RV upper plenum volume	V_{UP}	1,111 ft^3	31,460 liters	0.19 ft^3	5.5 liters
Heat exchanger shell-side volume	V_{ss}			0.52 ft^3	15.2 liters
Vessel ID				6.065 inches	15.4 cm
Vessel OD				6.625 inches	16.8 cm
Vessel height				42.5 inches	108 cm
Number of heat exchangers		2		2	
Number of coldlegs		4		2	

Section 3

DESCRIPTION OF TEST FACILITY

A sketch of the test facility is shown in Figure 3-1. A photograph of the test facility before the installation of sightgauges and fiberglass insulation is shown in Figure 3-2. The two loops are designated left and right loops. Substitution of a vertical extension of the coldleg for the annular downcomer flow path is visible in both figures.

As seen in Figure 3-1, there are three immersion heaters in the model reactor vessel. The maximum power available for these experiments was approximately 9 kW. For most of the tests, power was reduced to 6.2 kW, which corresponds to a full-scale core decay heat of 2 mW.

The model hotlegs and coldlegs are made of standard 2-inch copper pipes and their corresponding elbows and fittings. They have an inside diameter (ID) of 1.985 inch (5.0 cm) and an outside diameter (OD) of 2.125 inch (5.4 cm). The two model steam generators are commercial counterflow heat exchangers, Model BCF 5-030-06-060, manufactured by the Heat Transfer Division of American-Standard, Buffalo, New York. Each heat exchanger has 116 vertical tubes. The tubes are 0.375 inch (0.95 cm) OD, 0.328 inch (0.83 cm) ID, and 60 inches (152 cm) long. In order to scale the total tube volume of a TMI-2 steam generator, 38 of the 116 tubes are blocked, leaving 78 active tubes. The shell of the heat exchanger has an OD of 6.125 inches (15.6 cm) and an ID of 6.0 inches (15.2 cm). There are nine half baffles along the length of the heat exchanger so that the secondary flow, which goes from bottom to top, is wavy.

Two bypasses with valves were installed, each connecting a coldleg to the vessel (see Figure 3-1). These bypasses were to simulate the leakage between the cold annulus and the hot core region within the TMI-2 reactor vessel.

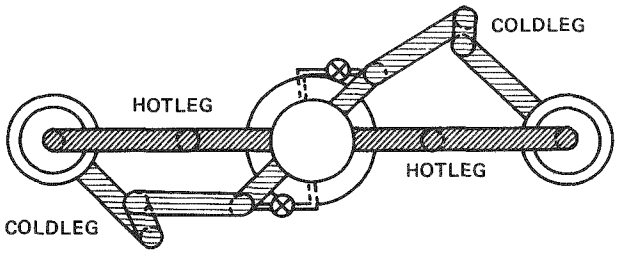

(a) TOP VIEW

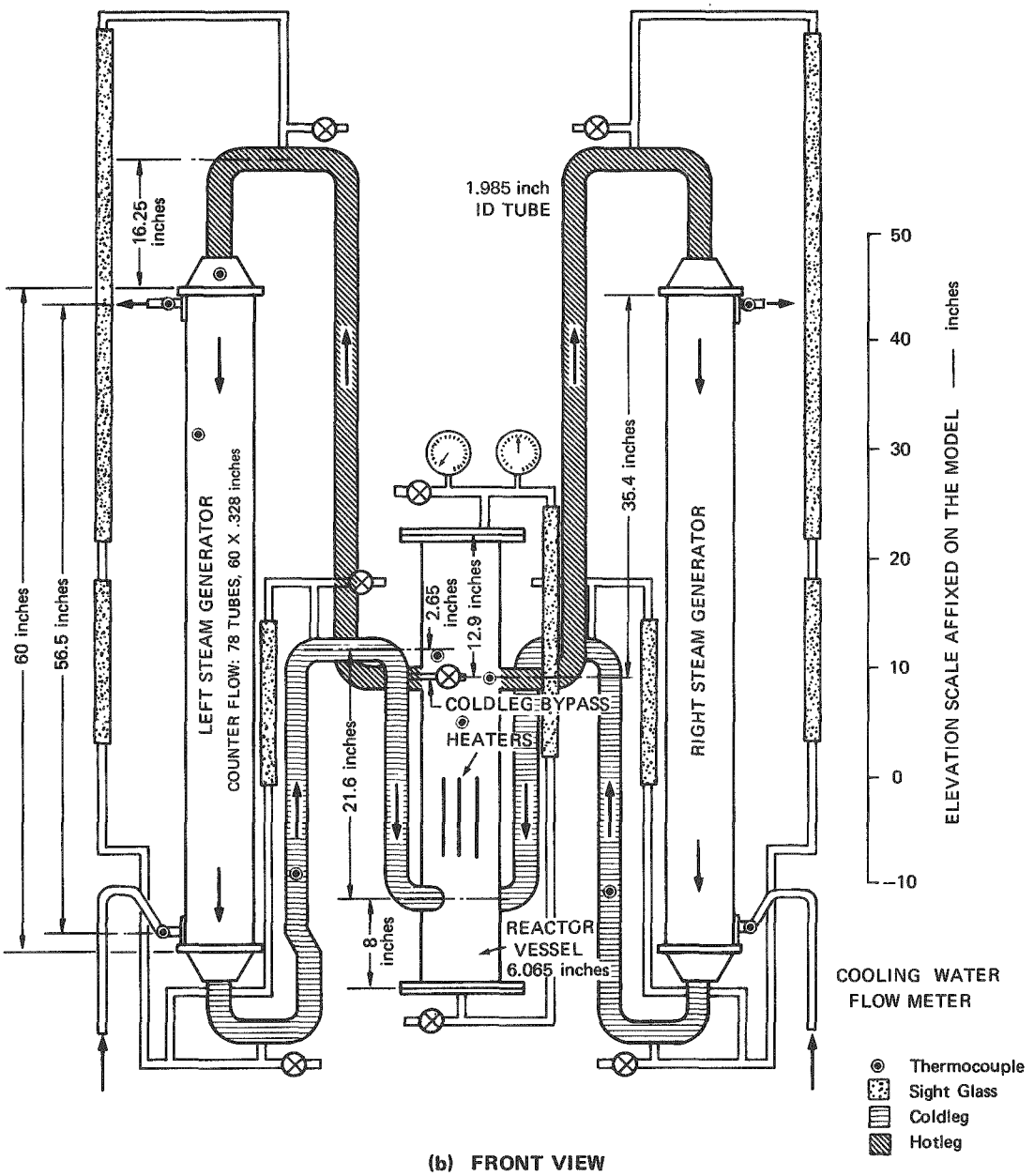

(b) FRONT VIEW

Figure 3-1. TMI-2 Cooling System Model, 1/18-Scale

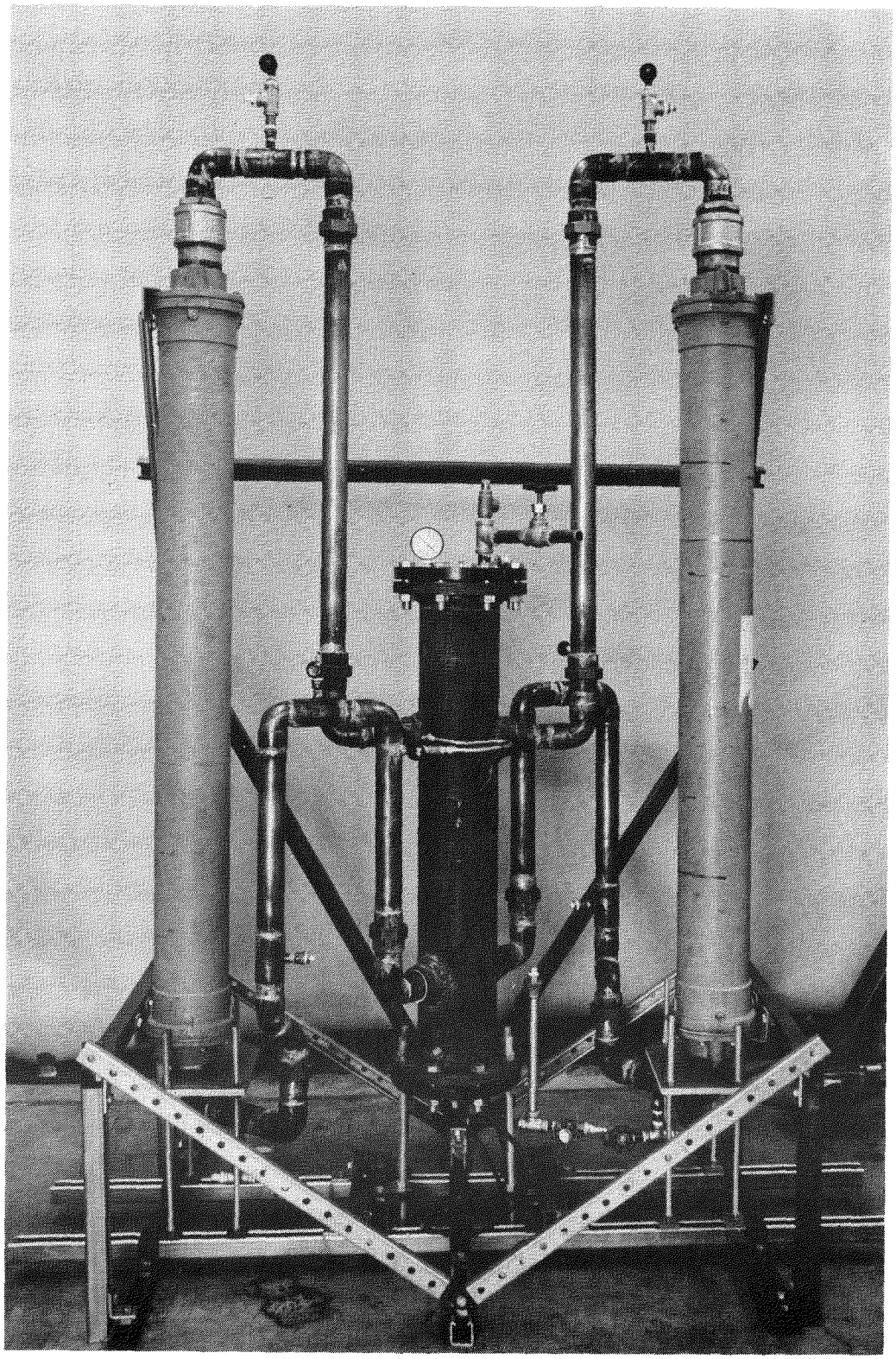

Figure 3-2. TMI-2 Model Test Facility

Section 4

INSTRUMENTATION

Pressure in the system was monitored by two Bourdon gauges connected to the top of the reactor vessel. One gauge had a range of 30-inch vacuum (0 kPa) to 15 psig (205 kPa) with a reading accuracy of ± 0.1 psi (± 0.7 kPa). The second gauge had a range of 30-inch vacuum (0 kPa) to 100 psig (791 kPa) with a reading accuracy of ± 0.5 psi (± 3.5 kPa). Pressure in the steam generators could be inferred from the reactor vessel pressure and the water levels in the sightgauges. As seen in Figure 3-1, there were a total of seven sightgauges. One for the reactor vessel, one for each coldleg, and two for each steam generator. Two sightgauges were used for each steam generator because the length of the available glass tubes is limited.

Temperatures in the system were measured by nine thermocouples* and a digital surface pyrometer. The thermocouples were of Chromel-Constantan type (Type E); they have an accuracy of ± 1°F (± 0.6°C). The surface pyrometer is a product of Service Techtonics Instruments; it has an accuracy of ± 2°F (± 1°C). The locations of the thermocouples are shown in Figure 3-1. Their designations are as follows:

T_{RV} Reactor vessel

T_{LO} Left SG cooling water outlet

T_{LI} Left SG cooling water inlet

T_{RO} Right SG cooling water outlet

T_{RI} Right SG cooling water inlet

---

*On the last few tests, Tests 43 to 50, two more thermocouples were installed: one in the top plenum of the left steam generator and one inside one of the 78 tubes of the left steam generator (30-inch level), as shown in Figure 3-1.

T_{LCL} Left coldleg

T_{RCL} Right coldleg

T_{LSGT} Primary tube of left steam generator

T_{LSGP} Upper plenum of left steam generator.

On each of the steam generators, a vertical slit was cut in the insulation jacket to expose the metal surface. The surface pyrometer was used to measure the skin temperatures of the steam generators.

The secondary flow rate was measured by using a graduated beaker and a stop watch. Other instrumentation included voltmeters and ammeters to monitor the electric power input to the heaters, a variac to regulate the total power input, and standard digital voltmeters to display the output from the thermocouples.

Section 5

DESCRIPTION OF EXPERIMENTS AND SUMMARY OF TEST DATA

A general test procedure was adopted after the first few days of exploratory tests: At the start of each day's experiment, the secondary sides of both steam generators were filled with tap water while a vacuum pump was used to evacuate the primary system of the model. After the evacuation, deaerated hot water was fed into the bottom of the vessel until the water inventory in the primary system, as indicated by levels in various sightgauges, reached a predetermined amount. This vacuum-fill process was adopted to minimize the amount of uncontrolled noncondensable gas in the system. The primary system pressure at the end of the filling operation was usually at 3 psia (20.7 kPa), which corresponds to a vapor temperature of 141°F (60.6°C). At that point, the heaters were turned on, usually to maximum power so that the system pressure could be brought as quickly as possible to above atmospheric pressure, thus minimizing the amount of air (noncondensable) seeping into the system. Once the system pressure exceeded the atmospheric pressure, we reset the power input to the desired level and turned on the secondary cooling water to either or both steam generators. From then on, the system was allowed to equilibrate while the power and the cooling water flow were periodically monitored and maintained at constant values.*

When the system pressure ceased to change with time, an equilibrium state was assumed to have been reached. A full set of data was then recorded. Such a data package, each with a designated test number, included

- System pressure (i.e., pressure in the reactor vessel)
- Water level in each sightgauge
- Power input

*Both quantities fluctuate to a certain extent as a result of variations in line voltage and line pressure.

- Cooling water flow rate(s)
- Readings of all nine thermocouples*
- Temperature profile along each of the two steam generators.

After the equilibrium data were collected, a change in the test condition was then made and the system was allowed to reach a new equilibrium. The parameters that characterize a test condition are:

- Volume of water in the primary system. (Empirical formulas that allow one to calculate water volume from level data are given in Appendix A.)
- Power input.
- Cooling water flow rates and inlet temperatures.
- Amount of noncondensable gas, namely, nitrogen.†
- Number of loops.
- The existence of a bypass, or equivalently, the opening of the cross-connection between the reactor vessel and the coldleg.

In the early days of testing, an attempt was made to stabilize the system at a preselected pressure by adjusting the cooling water flow. Although this scheme should work theoretically, we discovered that because of the large thermal mass and the thermal insulation of the test facility,‡ one would have to wait for hours before the effect of flow rate change manifested itself. It was found more practical to treat the cooling water flow rate as an independent variable and let the system pressure be a dependent variable.

Fifty-one sets of test data, that is, 50 sets of equilibrium or near equilibrium and one nonequilibrium data set, were recorded in the 15 days of testing. For easy reference, tests with special features are compiled in Table 5-1. Table 5-2 lists most of the measured quantities in all the tests in both English (Table 5-2a) and SI (Table 5-2b) units.

---

*Eleven thermocouple readings in Tests 43 through 50.

†Mass of nitrogen we injected into the system was known, but it was not possible to determine the fraction that was dissolved and the fraction that remained to be gaseous in the system.

‡Total heat loss of the test facility is estimated in Appendix B.

Table 5-1

SPECIAL TEST FEATURES

Test Number	Special Feature
0,1	Data package incomplete; high P_{in}
4,18,43	Mode 2c temperature profiles
8	Low P_{in}; coldlegs uncovered
7,9,10,11,12	Mode 1 profiles; increasing amount of N_2
13	No temperature profiles
13,14,15	Mode 2; increasing water inventory
16,17	Mode 2; increasing water inventory
19	Fail to reach equilibrium because of excess N_2
20	High P_{in}
23	Cross-connections fully opened
24	Cross-connections reclosed
25	Low secondary flow
27,28,30	Two-loop operation
31,32,33,34,35	Mode 1 profiles; increasing amount of N_2
36,37	No temperature profiles; increasing amount of N_2 into left coldleg
39	Following cooling flow perturbation
41,42	Mode 2; increasing amount of N_2
43,44,45	Mode 2; increasing amount of N_2
46,47,48,49,50	Tests with pressurizer (drain tank)
18,26,29,38,39, 40,41,43	Repeated tests intended

Table 5-2a

SUMMARY OF TEST RESULTS (English units)

Test Number	Mode	V_W (in^3)	V_{N2} (in^3)	P_{in} (Btu/s)	Q_L (in^3/s)	Q_R (in^3/s)	P (psia)	T_{RV} (°F)	T_{LCL} (°F)	T_{LI} (°F)	T_{LO} (°F)	T_{RCL} (°F)	T_{RI} (°F)	T_{RO} (°F)	Z_{LSG} (inch)	Z_{RV} (inch)	Z_{RSG} (inch)	Comments
0	1	1590	0	8.06	0-1.10	0	~19	225	--	--	--	--	--	--	8.0	5.0	5.8	Widely fluctuating secondary flow
1	2b	2190	0	8.54	0.51	0	~40	267	--	--	--	--	--	--	31.5	8.0	24.0	Suspect nonequilibrium
2	2a	2450	0	5.79	0.65	0	24.9	241	130	67	222	135	135	187	38.0	9.3	42.0	System pressure dropping, suspect nonequilibrium
3	2b	2450	0	6.07	1.09	0	19.3	227	82	65	199	143	147	186	40.5	8.0	40.0	System pressure dropping, suspect nonequilibrium
4	2c	2720	0	5.88	1.01	0	31.7	254	64	61	209	95	100	200	51.8	10.3	52.0	Very high water inventory
5	2b	2200	0	5.84	0.96	0	15.3	216	89	62	195	146	155	191	36.0	8.3	20.0	Reduced water inventory from Test 4
6	--	2200	9	6.07	0.95	0	20.7	231	85	64	198	138	142	203	41.0	8.4	~18	No temperature profiles measured, N_2 added into LHL
7	1	1660	0	5.97	0.77	0	14.7	214	66	62	207	112	115	187	9.0	6.0	7.0	Low water inventory
8	1	1660	0	1.45	0.67	0	3.7	154	69	64	130	113	103	137	8.5	7.8	8.0	Low power, coldlegs uncovered, test not in equilibrium
9	1	1660	66	6.00	0.74	0	14.0	210	69	66	206	107	110	184	10.5	6.0	7.5	LSG profile revealed air seeped into system
10	1	1660	110	5.99	0.68	0	15.2	214	69	67	209	111	112	190	10.3	6.3	7.0	N_2 added into LHL
11	1	1660	195	5.99	0.70	0	18.2	223	70	68	213	113	116	196	10.3	6.3	7.5	More N_2 added into LHL
12	1	1660	225	6.03	0.66	0	19.5	227	70	68	204	114	118	200	10.3	6.3	7.0	More N_2 added into LHL
13	--	2190	0	5.94	0.77	0	13.0	208	156	65	192	125	126	176	37.5	8.0	~18	No temperature profiles measured
14	2a	2410	0	5.95	0.76	0	14.2	213	142	67	193	128	128	162	39.5	8.3	38.3	Increased water inventory from Test 13
15	2a	2670	0	5.98	0.76	0	25.5	242	112	68	199	120	134	169	51.5	8.8	52.0	Increased water inventory from Test 14
16	2a	2130	0	6.01	1.01	0	8.7	189	126	64	176	100	100	172	35.3	8.4	12.8	
17	2a	2420	0	5.96	1.01	0	11.2	200	105	62	175	115	116	151	39.5	8.5	39.0	Increased water inventory from Test 16
18	2c	2510	0	5.86	1.02	0	28.0	247	66	59	160	96	97	185	41.0	8.3	47.5	High water inventory
19	--	2510	22	5.86	1.02	0	~85	316	--	--	--	--	--	--	--	--	--	N_2 added; test terminated when pressure approached 85 psia
20	1	1570	0	8.06	0.59	0	25.3	241	65	64	236	81	89	222	5.8	4.8	4.8	High power, low water inventory
21	1	1570	0	5.90	0.57	0	15.8	215	65	65	211	81	91	198	5.8	4.8	4.8	Nominal power
22	1	1570	0	6.08	0.54	0	15.0	215	69	65	211	99	92	198	7.0	5.5	8.0	Cross-connections open, RCL uncovered
23	1	1570	0	6.11	0.52	0	17.3	221	67	66	216	98	95	203	6.8	5.3	9.5	Cross-connections open, RCL uncovered
24	1	1570	0	6.04	0.51	0	18.8	225	67	67	220	91	98	207	5.9	4.6	4.6	Cross-connections closed
25	2a	2310	0	5.91	0.35	0	20.1	229	201	82	215	129	126	208	38.3	8.1	29.5	
26	2b	2490	0	5.92	0.95	0	15.5	215	86	62	176	127	127	173	42.0	8.4	44.0	Increased water inventory and cooling flow from Test 25
27	2a/2b	2490	0	5.91	0.38	0.31	17.2	221	139	64	183	70	64	120	40.0	8.3	45.5	Two-loop operation
28	2a/2c	2490	0	5.84	0.46	0.40	16.5	219	128	64	184	66	64	117	39.8	8.3	46.0	Two-loop operation with increased cooling flow rates
29	2a	2480	0	5.85	0.99	0	12.6	206	97	63	174	118	119	165	40.0	8.5	44.3	
30	2a/2c	2480	0	5.86	0.51	0.45	13.6	210	136	64	176	65	64	111	39.5	8.4	45.5	Two-loop operation
31	1	1640	0	5.83	0.67	0	9.9	195	61	60	191	80	90	183	8.3	6.3	7.3	Low water inventory
32	1	1640	151	5.89	0.72	0	10.2	197	62	61	193	82	94	185	7.8	6.3	7.0	N_2 added into LHL
33	1	1640	308	5.89	0.70	0	11.2	201	63	62	195	84	96	189	8.0	6.3	7.0	More N_2 added into LHL
34	1	1640	358	5.99	0.76	0	16.0	218	64	63	187	85	98	204	8.5	6.1	7.0	More N_2 added into LHL
35	1	1640	365	5.91	0.70	0	21.7	234	65	63	187	86	100	219	8.5	6.1	7.1	More N_2 added into LHL
36	--	1640	383	5.96	0.87	0	23.5	238	65	63	175	88	101	224	9.9	6.5	7.3	N_2 added to LCL, LCL uncovered
37	--	1640	361	5.93	0.74	0	28.5	248	66	64	189	98	103	233	16.0	6.1	6.8	More N_2 added to LCL, LCL uncovered
38	2a	2490	0	5.84	0.95	0	10.8	198	112	60	179	94	99	156	39.3	8.4	43.5	
39	2a	2490	0	6.08	0.91	0	13.5	207	112	61	177	125	126	157	39.8	8.4	48.0	After perturbation in cooling flow
40	2b	2510	0	6.00	0.92	0	14.4	212	80	59	171	111	112	173	41.5	8.6	46.0	
41	2b	2510	0	5.91	0.95	0	15.7	216	85	60	168	123	126	180	41.0	8.5	46.5	No significant change of test conditions from Test 40
42	2c	2510	18	5.86	0.90	0	31.8	254	73	61	179	117	128	195	41.5	8.0	47.5	N_2 added into LHL
43	2a	2410	0	5.91	0.98	0	13.7	208	103	61	179	108	107	155	37.0	8.5	40.0	Two additional TC's installed, $T_{LSGP} \lesssim T_{SAT}$, T_{LSGT} subcooled
43A	2a	2410	0	5.84	0.95	0	13.1	206	105	62	174	110	109	153	38.0	8.5	39.0	No significant change of test conditions from Test 43
44	2a	2410	31	5.51	0.94	0	17.2	219	87	63	179	121	122	167	35.0	8.5	41.0	N_2 added into LHL
45	2b	2410	49	5.91	0.86	0	20.0	228	86	65	174	132	135	174	36.0	8.5	41.0	More N_2 added into LHL
46	2a	2120	21	5.90	0.93	0	16.2	215	102	67	181	131	135	196	34.5	8.7	11.9	Water displaced into pressurizer (drain tank)
47	2a	2140	0	5.96	0.94	0	10.7	197	138	69	183	117	121	181	34.8	8.3	14.8	Additional 520 in^3 of water in pressurizer
48	2a	2480	0	6.01	0.98	0	15.0	214	108	70	185	128	131	166	40.5	8.5	43.5	Connecting of pressurizer caused water to flow from pressurizer into system
49	2a	2430	0	5.99	0.96	0	14.7	212	109	61	178	129	125	161	40.0	8.6	38.3	Venting of pressurizer caused water to drain to pressurizer
50	2a	2110	0	9.38	0.95	0	17.5	222	188	69	212	144	139	205	35.0	8.0	11.8	High power, water continued to flow into pressurizer, nonequilibrium

Table 5-2b

SUMMARY OF TEST RESULTS (SI units)

Test Number	Mode	V_W (1)	V_{N_2} (1)	P_{in} (kW)	Q_L (cc/s)	Q_R (cc/s)	P (kPa)	T_{RV} (°C)	T_{LCL} (°C)	T_{LI} (°C)	T_{LO} (°C)	T_{RCL} (°C)	T_{RI} (°C)	T_{RO} (°C)	Z_{LSG} (cm)	Z_{RV} (cm)	Z_{TSG} (cm)	Comments
0	1	26.1	0	8.50	0-18	0	~131	107	--	--	--	--	--	--	20.3	12.7	14.7	Widely fluctuating secondary flow
1	2b	35.9	0	9.00	8.3	0	~276	131	--	--	--	--	--	--	80.0	20.3	61.0	Suspect nonequilibrium
2	2a	40.1	0	6.10	10.6	0	171	116	54	19	106	57	57	86	96.5	23.6	106.7	System pressure dropping, suspect nonequilibrium
3	2b	40.1	0	6.40	17.9	0	133	108	28	18	93	62	64	86	102.9	20.3	101.6	System pressure dropping, suspect nonequilibrium
4	2c	44.6	0	6.20	16.5	0	219	123	18	16	98	35	38	93	131.6	26.2	132.1	Very high water inventory
5	2b	36.1	0	6.16	15.8	0	105	102	32	17	91	63	68	88	91.4	21.1	50.8	Reduced water inventory from Test 4
6	--	36.1	0.15	6.40	15.6	0	143	111	29	18	92	59	61	95	104.1	21.3	~46	No temperature profiles measured, N_2 added into LHL
7	1	27.2	0	6.29	12.6	0	101	101	19	17	97	44	46	86	22.9	15.2	17.8	Low water inventory
8	1	27.2	0	1.53	11.0	0	25	68	21	18	54	45	39	58	21.6	19.8	20.3	Low power, coldlegs uncovered, test not in equilibrium
9	1	27.2	1.1	6.32	12.2	0	97	99	21	19	97	42	43	84	26.7	15.2	19.1	LSG profile revealed air seeped into system
10	1	27.2	1.8	6.31	11.2	0	105	101	21	19	98	44	44	88	26.2	16.0	17.8	N_2 added into LHL
11	1	27.2	3.2	6.31	11.4	0	125	106	21	20	101	45	47	91	26.2	16.0	18.1	More N_2 added into LHL
12	1	27.2	3.7	6.36	10.8	0	134	108	21	20	96	46	48	93	26.2	16.0	17.8	More N_2 added into LHL
13	--	35.9	0	6.26	12.7	0	90	98	69	18	89	52	52	80	95.3	20.3	~46	No temperature profiles measured
14	2a	39.5	0	6.27	12.5	0	98	101	61	19	89	53	53	72	100.3	21.1	97.3	Increased water inventory from Test 13
15	2a	43.8	0	6.30	12.5	0	176	117	44	20	93	49	57	76	130.8	22.4	132.1	Increased water inventory from Test 14
16	2a	34.9	0	6.33	16.5	0	60	87	52	18	80	38	38	78	89.7	21.3	32.5	
17	2a	39.7	0	6.28	16.5	0	77	93	41	17	79	46	47	66	100.3	21.6	99.1	Increased water inventory from Test 16
18	2c	41.2	0	6.18	16.7	0	193	119	19	15	71	36	36	85	104.1	21.1	120.7	High water inventory
19	--	41.2	0.36	6.18	16.7	0	~586	158	--	--	--	--	--	--	--	--	--	N_2 added, test terminated when pressure approached 85 psia
20	1	25.7	0	8.49	9.6	0	174	116	18	18	113	27	32	106	14.7	12.2	12.2	High power, low water inventory
21	1	25.7	0	6.22	9.4	0	109	102	18	18	99	27	33	92	14.7	12.2	12.2	Nominal power
22	1	25.7	0	6.41	8.9	0	103	102	21	18	99	37	33	92	17.8	14.0	20.3	Cross-connections open, RCL uncovered
23	1	25.7	0	6.44	8.5	0	119	105	19	19	102	37	35	95	17.3	13.5	24.1	Cross-connections open, RCL uncovered
24	1	25.7	0	6.37	8.3	0	130	107	19	19	104	33	37	97	15.0	11.7	11.7	Cross-connections closed
25	2a	37.9	0	6.23	5.8	0	139	109	94	28	102	54	52	98	97.3	20.6	74.9	
26	2b	40.8	0	6.24	15.6	0	107	102	30	17	80	53	53	78	106.7	21.3	111.8	Increased water inventory and cooling flow from Test 25
27	2a/2b	40.8	0	6.23	6.3	5.1	119	105	59	18	84	21	18	49	101.6	21.1	115.6	Two-loop operation
28	2a/2c	40.8	0	6.16	7.6	6.6	114	104	53	18	84	19	18	47	101.1	21.1	116.8	Two-loop operation with increased cooling flow rates
29	2a	40.7	0	6.17	16.2	0	87	97	36	17	79	48	48	74	101.6	21.6	112.5	
30	2a/2c	40.7	0	6.18	8.3	7.4	94	99	58	18	80	18	18	44	100.3	21.3	115.6	Two-loop operation
31	1	26.9	0	6.15	11.0	0	68	91	16	16	88	27	32	84	21.1	16.0	18.5	Low water inventory
32	1	26.9	2.5	6.21	11.8	0	70	92	17	16	89	28	34	85	19.8	16.0	17.8	N_2 added into LHL
33	1	26.9	5.0	6.21	11.4	0	77	94	17	17	91	29	36	87	20.3	16.0	17.8	More N_2 added into LHL
34	1	26.9	5.9	6.31	12.5	0	110	103	18	17	86	29	37	96	21.6	15.5	17.8	More N_2 added into LHL
35	1	26.9	6.0	6.23	11.4	0	150	112	18	17	86	30	38	104	21.6	15.5	18.0	More N_2 added into LHL
36	--	26.9	6.2	6.28	14.3	0	162	114	18	17	79	31	38	107	25.1	16.5	18.5	N_2 added to LCL, LCL uncovered
37	--	26.9	5.9	6.25	12.2	0	197	120	19	18	87	37	39	112	40.6	15.5	17.3	More N_2 added to LCL, LCL uncovered
38	2a	40.8	0	6.16	15.6	0	74	92	44	16	82	34	37	69	99.8	21.3	110.5	
39	2a	40.8	0	6.41	14.9	0	93	97	44	16	81	52	52	69	101.1	21.3	121.9	After perturbation in cooling flow
40	2b	41.2	0	6.32	15.1	0	99	100	27	15	77	44	44	78	105.4	21.8	116.8	
41	2b	41.2	0	6.23	15.6	0	108	102	29	16	76	51	52	82	104.1	21.6	118.1	No significant change of test conditions from Test 40
42	2c	41.2	0.29	6.18	14.7	0	219	123	23	16	82	47	53	91	105.4	20.3	120.7	N_2 added into LHL
43	2a	39.5	0	6.23	16.1	0	94	98	39	16	82	42	42	68	94.0	21.6	101.6	Two additional TC's installed, $T_{LSGP} \lesssim T_{SAT}$, T_{LSGT} subcooled
43A	2a	39.5	0	6.16	15.6	0	90	97	41	17	79	43	43	67	96.5	21.6	99.1	No significant change of test conditions from Test 43
44	2a	39.5	0.51	5.81	15.4	0	119	104	31	17	82	49	50	75	88.9	21.6	104.1	N_2 added into LHL
45	2b	39.5	0.80	6.23	14.1	0	138	109	30	18	79	56	57	79	91.4	21.6	104.1	More N_2 added into LHL
46	2a	34.8	0.30	6.22	15.2	0	112	102	39	19	83	55	57	91	87.6	22.1	30.2	Water displaced into pressurizer (drain tank)
47	2a	35.1	0	6.28	15.4	0	74	92	59	21	84	47	49	83	88.4	21.1	37.6	Additional 520 in^3 of water in pressurizer
48	2a	40.6	0	6.33	16.1	0	103	101	42	21	85	53	55	74	102.9	21.6	110.5	Connecting of pressurizer caused water to flow from pressurizer into system
49	2a	39.7	0	6.31	15.8	0	101	100	43	16	81	54	52	72	101.6	21.8	97.3	Venting of pressurizer caused water to drain to pressurizer
50	2a	34.5	0	9.89	15.6	0	121	106	87	21	100	62	59	96	88.9	20.3	30.0	High power, water continued to flow into pressurizer, nonequilibrium

Section 6

INTERPRETATION OF TEST RESULTS

TWO MODES AND FOUR CHARACTERISTIC TEMPERATURE PROFILES

As mentioned in Section 5, a vertical slit was cut in the fiberglass insulation of each of the two steam generators. The temperature profiles measured along these slits reveal that there are two distinct modes of two-phase natural circulation. Mode 1 is characterized by a step-like temperature profile along the functional steam generator (see Figure 6-1). The nearly constant temperature at either end of the Mode 1 profile indicates little or no heat transfer between the primary and the secondary coolants in these two regions. Nearly all the heat transfer takes place in the midsection of the steam generator, where the upward-flowing secondary coolant takes a temperature jump of approximately 140°F (78°C). This relatively short heat-transfer section of about 8 inches (20 cm) lies just above the water level in the tubes of the active steam generator.

When the water inventory in the primary system is increased, the step-like temperature profile is replaced by profiles of milder temperature variations. In fact, the temperature profile can assume one of three shapes. A sample of each is shown in Figure 6-1. These three profiles have been labeled Modes 2a, 2b, and 2c. An examination of these three profiles led to the inevitable conclusion that the bulk of the heat transfer takes place near the bottom tube sheet for Mode 2a, along the entire steam generator for Mode 2b, and near the top tube sheet for Mode 2c. In the following subsections, we shall offer physical explanations of the various two-phase natural circulation phenomena that are consistent with these observed temperature profiles. For complete documentation of the test results, measured profiles from most of the 50 tests are presented in Appendix C. (A broken pyrometer was the reason for the missing few.)

MODE 1 NATURAL CIRCULATION

The Mode 1 temperature profile is observed only when the water inventory in the primary system is sufficiently low so that the hotlegs are entirely clear of water. In this mode of operation, the steam and water in the primary system are segregated in such a way that steam exists in the upper half and water in the

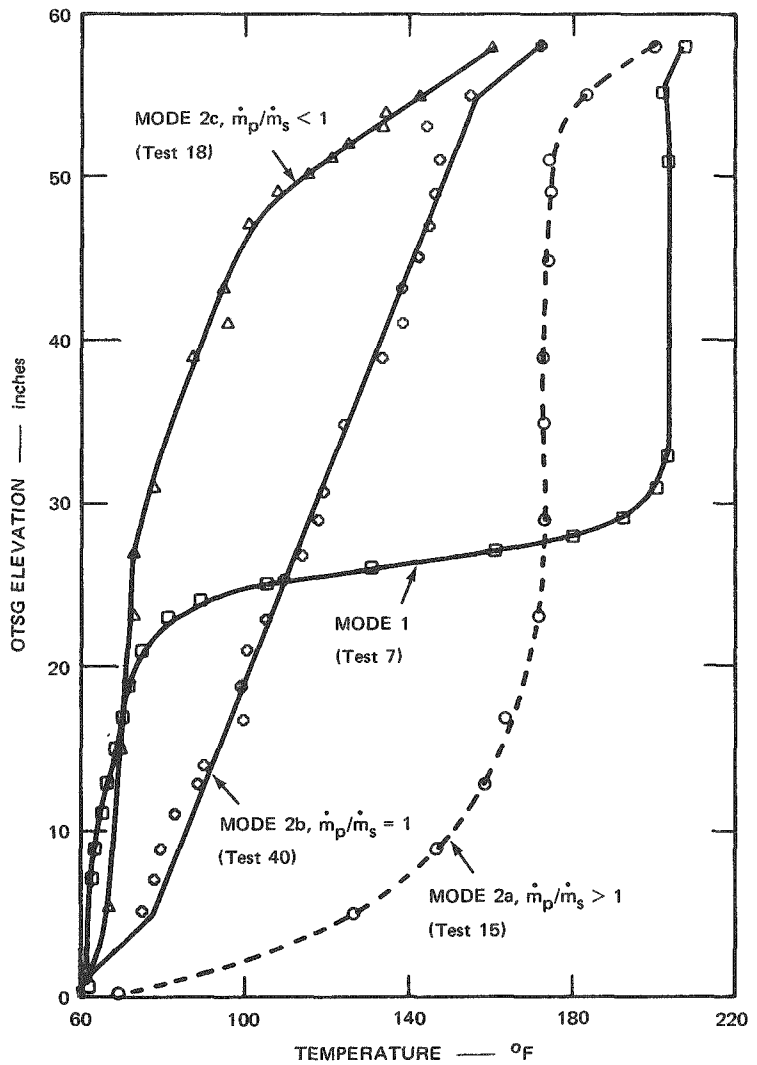

Figure 6-1. Axial Temperature Profiles of Various Modes

lower half of the system. For our understanding of the Mode 1 process, we are indebted to Dr. Robert Murray of SRI. According to Dr. Murray, the condensation of steam and the subsequent cooling of condensate take place in a short vertical section of the active steam generator. Above or below this section, the temperature of the primary and the secondary coolants is essentially the same, resulting in little heat transfer. This explanation thus accounts for the step-like temperature profile measured along the active steam generator. The slight "vacuum" generated by the condensation process continuously draws steam from the vessel, thus maintaining the primary loop flow.

A particularly interesting discovery regarding Mode 1 is the observed correlation between the elevation of the heat transfer section and the amount of noncondensable gas in the system. When there is little noncondensable in the steam domain of the primary system, this section of sharp temperature gradient lies just above the water-steam interface in the steam generator tubes. If there exists noncondensable gas, the gas molecules are dragged by the flow of steam and are eventually accumulated above the water-steam interface. This forces the condensation to occur above the slug of noncondensable gas. As a result, the heat transfer section is displaced upward. As a matter of fact, we can deliberately raise the elevation of this section by injecting nitrogen gas into the candy-cane portion of the hotleg. The evidence of this manipulation can be seen in Tests 9 through 12, and also in Tests 31 through 35, of Appendix C.

The understanding of the Mode 1 process and the discovery that, because of intermolecular drag, the noncondensable gas always gets swept along until it is piled above the water-steam interface, have some profound implications. They are:

- The concern that accumulation of noncondensable gas in the candy-cane would block the natural circulation loop flow is unfounded.
- The two-phase natural circulation is amazingly tolerant of noncondensable gas, especially in the Mode 1 process. The fact that Tests 12 and 35 are in equilibrium despite the presence of a large amount of nitrogen gas in the steam generator tubes is a testimony to the above statement.

It should be noted that as long as one allows the system pressure to seek its own equilibrium, the loop circulation will reestablish itself at a higher equilibrium pressure even if a fresh infusion of noncondensable gas in the candy-cane temporarily blocks the natural circulation. This self-regulating process also works when noncondensable gas in the dogleg part of the coldleg blocks the loop circulation. Experimental evidence of this is found in Tests 36 and 37.

SIGNIFICANCE OF THE RATIO OF PRIMARY TO SECONDARY FLOW RATES

In a once-through counterflow heat exchanger, the temperature profile along the heat exchanger not only reveals the location of heat transfer, as discussed earlier, but also sheds light on the magnitude of the ratio of primary to secondary flow rates. The following analysis will demonstrate this point.

Referring to Figure 6-2(a), let us examine the single-phase heat transfer between the primary and the secondary coolants in a vertical section between z and z + dz.

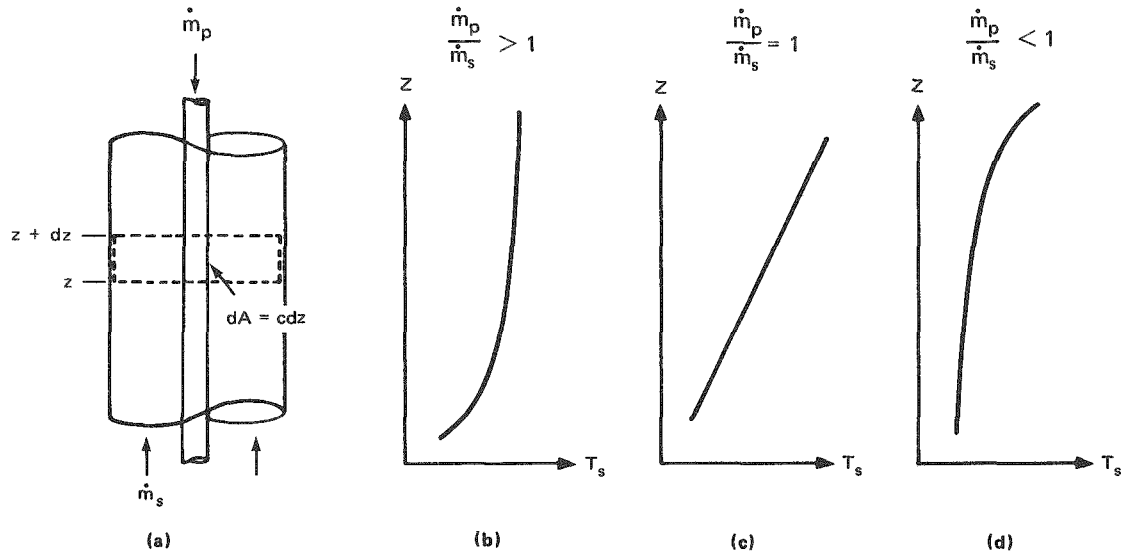

Figure 6-2. Secondary Coolant Temperature Profiles in a Counterflow Heat Exchanger

The rate of heat transfer should be proportional to the temperature difference between the primary and the secondary coolants, and the heat transfer surface area. That is,

$$d\dot{q} = U(T_p - T_s)\ (cdz) \quad , \tag{6-1}$$

where U denotes the overall heat transfer coefficient and c is the circumference of the tube. This transfer reduces the heat content in the primary coolant and increases the heat content in the secondary coolant:

$$d\dot{q} = \dot{m}_p C_p [T_p(z + dz) - T_p(z)] \quad , \tag{6-2}$$

$$d\dot{q} = \dot{m}_s C_p [T_s(z + dz) - T_s(z)] \quad . \tag{6-3}$$

Combining the last three equations, one obtains two differential equations for the two unknowns T_p and T_s.

$$\dot{m}_p C_p \frac{dT_p}{dz} = U(T_p - T_s)c \quad , \tag{6-4}$$

$$\dot{m}_s C_p \frac{dT_s}{dz} = U(T_p - T_s)c \quad . \tag{6-5}$$

Since the skin temperature profiles measured along the model steam generators reflect the secondary coolant temperature, we shall eliminate T_p from Eqs. 6-4 and 6-5. The resulting differential equation for T_s is

$$\frac{d^2T_s}{dz^2} = \frac{Uc}{\dot{m}_p C_p}\left(1 - \frac{\dot{m}_p}{\dot{m}_s}\right)\frac{dT_s}{dz} \quad . \tag{6-6}$$

It is possible to infer the principal features of the secondary temperature profile without solving Eq. 6-6.* From the flow directions, we know that dT_s/dz is always positive. Thus,

$$\frac{\dot{m}_p}{\dot{m}_s} > 1 \text{ implies } \frac{d^2T_s}{dz^2} < 0 \quad ,$$

---

*The solution of Eq. 6-6 is:

$$T_s(z) = C_1 \frac{\dot{m}_p C_p}{Uc}\left(1 - \frac{\dot{m}_p}{\dot{m}_s}\right)^{-1} e^{\frac{Uc}{\dot{m}_p C_p}\left(1 - \frac{\dot{m}_p}{\dot{m}_s}\right)z} + C_2 \quad ,$$

where C_1 and C_2 are integration constants to be determined by the boundary conditions.

$$\frac{\dot{m}_p}{\dot{m}_s} = 1 \text{ implies } \frac{d^2T_s}{dz^2} = 0 \quad ,$$

$$\frac{\dot{m}_p}{\dot{m}_s} < 1 \text{ implies } \frac{d^2T_s}{dz^2} > 0 \quad .$$

The fact that d^2T_s/dz^2 is related to curvature leads to the following statements:

For $\dot{m}_p/\dot{m}_s > 1$, $T_s(z)$ is concave upward in a T_s - z plot;

For $\dot{m}_p/\dot{m}_s = 1$, $T_s(z)$ is a straight line in a T_s - z plot;

For $\dot{m}_p/\dot{m}_s < 1$, $T_s(z)$ is concave downward in a T_s - z plot.

These features are illustrated in Figure 6-2(b), (c), and (d). Comparing these three figures with the Mode 2 temperature profiles shown in Figure 6-1, it is obvious that

For Mode 2a, $\dot{m}_p/\dot{m}_s > 1$;

For Mode 2b, $\dot{m}_p/\dot{m}_s = 1$;

For Mode 2c, $\dot{m}_p/\dot{m}_s < 1$.*

MODE 2 NATURAL CIRCULATION

High water inventory in the primary system is a prerequisite to establish either of the three Mode 2 temperature profiles. By high water inventory, we mean the collapsed water levels in the hotlegs to be above the hotleg nozzles. This also means that before the heaters in the vessel are turned on, the vessel is either full of water or has a level that lies above the hotleg nozzles. Once boiling starts, the generated steam will rise to the upper plenum of the vessel. The added steam causes the pressure to increase, and the rising pressure in turn depresses the water level in the vessel until part of the hotleg nozzle is uncovered. Excess steam then percolates up one or both hotlegs, thus preventing

---

*These relationships between the modes and the ratio of flow rates were first discovered by Dr. Jean-Pierre Sursock of EPRI in an analysis of the heat transfer processes in a once-through steam generator.

the pressure in the vessel from building up indefinitely. Although our model is nontransparent, this percolating action is easily detectable by its characteristic sound. Mode 2 can alternately be called a percolating mode.

It is not difficult to visualize that the violent nature of the percolating action in the hotleg causes water, as well as steam, to flow over the candy-cane and into the steam generator. The primary flow rate during a Mode 2 operation is thus much higher than that during a Mode 1 operation. As an example, we have made estimates of the $\dot{m}_p$ for Tests 9 and 14. The former is a Mode 1 operation, and the latter a Mode 2a operation (cf. Table 5-2); otherwise, both tests have much the same power input and secondary flow rate, and they have nearly identical equilibrium pressure. For Test 9 (Mode 1), $\dot{m}_p$ is about 3.6×10^{-3} lbm/s (1.6 g/s); and for test 14 (Mode 2a), $\dot{m}_p$ is about 3.8×10^{-2} lbm/s (17.3 g/s).

Once the two-phase mixture enters the active steam generator, steam is quickly condensed. The heat released by the condensation of steam causes an increase in the secondary coolant temperature near the top tube sheet. This temperature increase is readily observable in the Mode 2 temperature profiles shown in Figure 6-1. It is particularly evident for Modes 2a and 2b. The subsequent water-to-water (single-phase) heat transfer depends on the ratio of primary to secondary flow rate as we have discussed in the last subsection. For Mode 2a which is postulated to have an $\dot{m}_p/\dot{m}_s$ greater than one, this heat transfer takes place in the lower half of the steam generator. For Mode 2b, with an $\dot{m}_p/\dot{m}_s$ equals to one, this heat transfer takes place all along the steam generator. Finally, for Mode 2c with $\dot{m}_p/\dot{m}_s$ less than one, this heat transfer takes place in the upper half of the steam generator.

For quite some time after these tests were performed, it was not clear under what test conditions each of the three submodes, 2a, 2b, and 2c, would prevail. The revelation came only after a painstaking examination and cross comparison of all the data taken. The conclusion we have come to is that these three submodes represent a continuous spectrum of two-phase natural circulation processes. The transitions among the three are gradual. For this reason, we have classified all three of them as Mode 2. The transitions from Mode 2a through 2b, to 2c can be effected by increased water inventory, increased noncondensable gas, or increased secondary cooling flow. The evidences will be provided in the next section.

Table 6-1 summarizes the characteristics and postulated physical processes of the various modes of two-phase natural circulation discussed earlier.

Table 6-1

IDENTIFIED MODES OF TWO-PHASE NATURAL CIRCULATION

Mode	Prerequisite	Mass Flow Rate	Hydraulic Process in Primary Loop	Heat Transfer Process in Active OTSG	
				Primary Side	Secondary Side
1	Low water inventory	$\dot{m}_p/\dot{m}_s \ll 1$	Liquid levels and static pressures in the OTSG and reactor vessel are about equal. All levels are below hotleg nozzle. Steam exits the hotleg port, flows to the OTSG, condenses in a short axial length of the tubes, and returns via the coldleg to the reactor vessel. Excess noncondensable gas accumulates above the water surface inside the OTSG tubes.	Condensation heat transfer above the liquid (and noncondensable gas) level; single-phase convective heat transfer below this level. Coolant temperature exiting the tubes closely approaches the secondary coolant inlet temperature.	Forced convection heat transfer throughout. Coolant temperature has a sharp gradient in the condensation zone as it absorbs most energy in this region.
2a	High water inventory	$\dot{m}_p/\dot{m}_s > 1$	OTSG and reactor-vessel-liquid levels oscillate mildly. Vapor in the upper head depresses the reactor-vessel-liquid level to the hotleg ports. Water displaced from vessel causes higher levels in the OTSGs. Two-phase percolating flow up the hotleg enhances primary flow rate, resulting in less steam production than in Mode 1. Steam condenses near the top of the OTSG. Subcooled liquid returns to the reactor vessel.	Condensation heat transfer from the smaller amount of steam in the two-phase mixture near the top of the OTSG; single-phase convective heat transfer below the liquid level in the tubes. Coolant exits the tubes with generally less subcooling than for Mode 1.	Forced convective transfer throughout, with generally milder temperature gradients than for Mode 1. Most heat is transferred in the lower half of the OTSGs.
2b	Higher water inventory than Mode 2a	$\dot{m}_p/\dot{m}_s = 1$	Similar to above, but the primary flow rate is nearly equal to the secondary flow rate.	Similar to above, but heat transfer is more or less uniform along the OTSG.	Similar to above, but heat transfer is more or less uniform along the OTSG.
2c	Highest water inventory, or excess noncondensable gas	$\dot{m}_p/\dot{m}_s < 1$	Similar to above, but the primary flow rate is less than the secondary flow rate.	Similar to above, but most heat is transferred in the upper half of the OTSG.	Similar to above, but most heat is transferred in the upper half of the OTSG.

Section 7

EFFECTS OF VARIOUS OPERATING PARAMETERS

One of the objectives of this experimental program was to identify limiting conditions beyond which two-phase natural circulation could no longer expect to keep the heater temperature from rising. We found no such limit, save for one instance (Test 19) in which the limit may be associated with the design limit of the test facility rather than the thermodynamics. In the following paragraphs, we shall discuss the effects of various parameters in light of these sought-for limits.

As we discussed in length earlier, the amount of water in the primary system has a profound influence on the system's response. First of all, there is the distinction between Mode 1 and Mode 2, the division of which is solely detemined by the water inventory. To reiterate, if the water inventory is sufficiently low so that the hotlegs contain only steam, the heat removal is accomplished by Mode 1, natural circulation. With higher water inventory, Mode 2, the percolating mode, will prevail.

The amount of water also dictates the flow rate in the primary loop. As mentioned in the last section, the primary flow rate during a Mode 1 operation is an order of magnitude smaller than that during a Mode 2 operation because the principal mechanism of heat removal for Mode 1 involves phase changes that are highly effective. For the various submodes of Mode 2, the situation is much more subtle. Because primary flow rate was not directly measured in our experiments, an indirect way of estimating the primary flow rates, or at least their relative magnitude from one test to another, must be devised in order to correlate water inventory with primary flow rates. Such an estimator is provided by the coldleg temperature. It is reasonable to expect that the lower the primary flow rate, the lower the coldleg temperature as a result of prolonged heat transfer, provided the secondary coolant inlet temperature and its flow rate are kept constant. Using the coldleg temperature as an indicator of the primary flow rate, we set out to examine consecutive tests during which water was either added or drained from the primary system. We found three such test sequences and discovered that the higher the water inventory, the lower the primary flow rate, and vice versa.

Referring to Table 5-2, water was added between Tests 13 and 14, and again between Tests 14 and 15, while all other test parameters were kept unchanged. The active loop coldleg temperature of these three tests decreased monotonically, indicating decreases in the primary flow rate. Similar behavior is seen in the test sequence of Tests 16 and 17.

The reverse is also true. When water was drained between Tests 4 and 5, the coldleg temperature took a jump upward, indicating an increase in primary flow rate. The change between Tests 4 and 5 is particularly dramatic, in the sense that the transition actually crosses a modal boundary from Mode 2c to Mode 2b (cf. temperature profiles in Appendix C). Recalling that the analysis presented in Section 7 concludes that $\dot{m}_p/\dot{m}_s < 1$ for Mode 2c and $\dot{m}_p/\dot{m}_s = 1$ for Mode 2b, the experimental evidence that the primary flow rate increased from Test 4 (Mode 2c) to Test 5 (Mode 2b) is complementary to the theory. What remains to be explained is why an increase in water inventory would cause a decrease in primary flow rate, everything else being equal. We suspect that has to do with the nature of the two-phase flow in the vertical hotleg, but a satisfactory theory is still wanting.

When the primary flow rate is decreased, the coolant passing the heaters will absorb more heat, thus resulting in higher vessel temperature and pressure. This fact is indeed borne out by the three test sequences mentioned above. So for all Mode 2 operations, the amount of water in the primary system has yet another effect--namely, the higher the water inventory, the higher the system temperature and pressure.

In discussing the effect of <u>noncondensable gas</u>, namely, nitrogen, it is necessary to separate Mode 1 from Mode 2. For Mode 1, the existence of nitrogen in the upper half of the primary loop has no effect on the natural circulation (except in dictating the elevation of the condensation section) until the condensation region is pushed above the top tube sheet. When that happens, system pressure starts to go up. The increase in pressure compresses the finite amount of N_2 to a smaller volume thus permitting the steam to come in contact with condensing surfaces in the top of the steam generator. Eventually, a new equilibrium is reached. The above process is evidenced in Tests 9 through 12, and again in Tests 31 through 35. In view of this evidence, we conclude that there exists no inherent upper limit for N_2 in Mode 1; a practical limit is set by the permissible pressure of the system. For Mode 2, it appears that any amount of N_2 will raise the system pressure. The more the N_2, the higher the equilibrium pressure will be (e.g., compare Tests 41 and 42; also 43A, 44, and 45). During Test 19, a sufficient

amount of N_2 was added such that the system pressure rose beyond 65 psig (550 kPa) with no sign of leveling off. The test was terminated because the integrity of the test facility was jeopardized.

Referring again to test sequences 41-42 and 43A-44-45, the active-loop coldleg temperature decreased in both of the two test sequences, implying a decrease in primary flow rate. In either sequence, the drop in $\dot{m}_p$ was sufficient to cross modal boundaries. Thus, between Tests 41 and 42, the natural circulation changed from Mode 2b to Mode 2c; and between Tests 44 and 45, it changed from Mode 2a to Mode 2b. In every respect, the adding of nitrogen gas during a Mode 2 operation displays the same effects as adding water; that is, it raises the system temperature and pressure, lowers the primary flow rate, and pushes the mode of natural circulation to a higher hierarchy.

The effect of nitrogen in the coldleg was briefly examined in Tests 36 and 37. The existence of a sufficiently large N_2 bubble in the raised portion of the coldleg interrupts the flow in the primary loop. The system responds with a rising pressure. Again, the increased pressure compresses the nitrogen bubble and reduces its volume. (Eventually, a water bridge was established and circulation was restored.)

The effect of secondary flow rate on system pressure follows the notion that the higher the flow rate, the lower the pressure, and vice versa. Results from nine Mode 1 tests are plotted in Figure 7-1. This figure shows not only the noted trend, but also the high sensitivity of pressure response to change in flow rate. All of these are true for Mode 2 tests as well. But, because of the uncontrollable fluctuations in water inventory in the active loop, in the power input, and in the secondary flow rate, plus the compounded effect of transition from one submode to another, consistent quantitative results are unavailable.

The effect of power input also follows the theory; that is, the higher the power input, the higher the system pressure, and vice versa. Among the Mode 1 tests, Tests 20 and 21 have all other conditions basically the same except the power input. In Test 20, the system equilibrated at 25.3 psia (174 kPa) in response to a power input of 8.06 Btu/s (8.49 kW). When the power was reduced to 5.90 Btu/s (6.22 kW) in Test 21, the system pressure dropped to 15.8 psia (109 kPa). Table 5-2 indicates that Test 8 is a low-power test. Unfortunately, Test 8 followed the previous test by only one hour 24 minutes, not enough to allow the metal parts of the model to cool down to a new equilibrium temperature. Hence the recorded

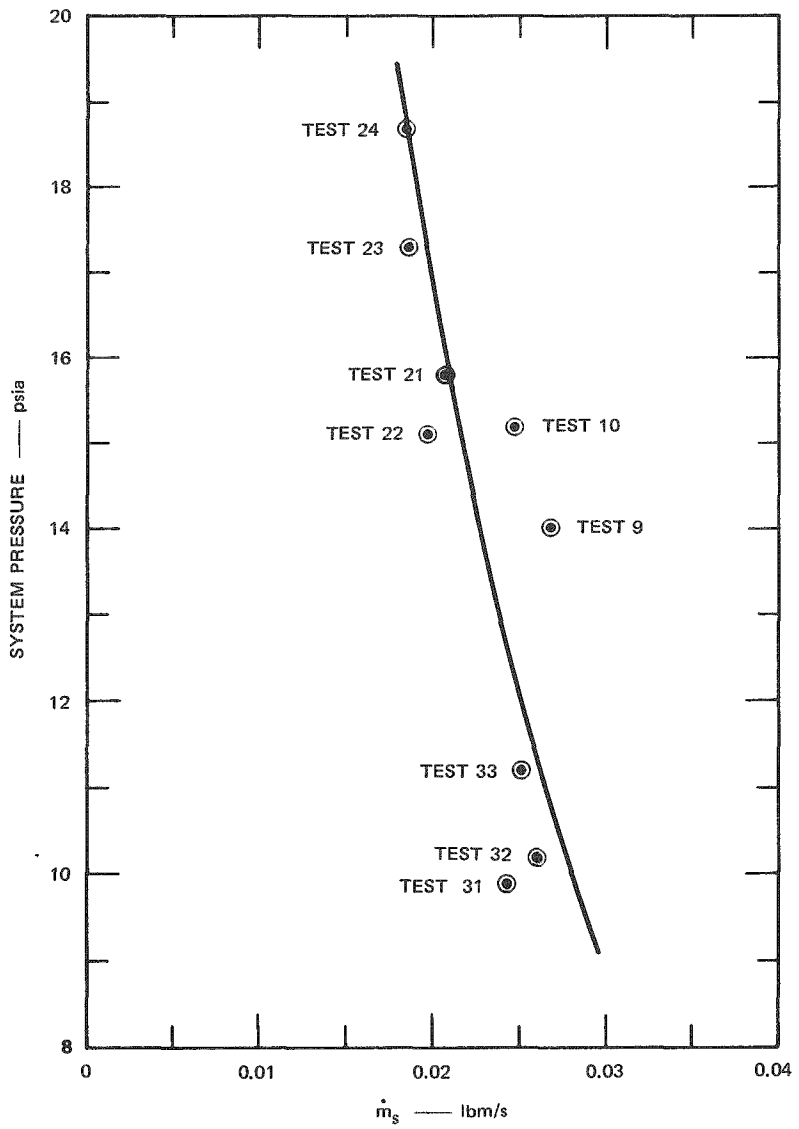

Figure 7-1. Pressure as a Function of Secondary Flow Rate--Mode 1

pressure should not be considered an equilibrium pressure. (The evidence of none-quilibrium lies in the calculated heat removal efficiency of that test, which is greater than 100 percent.) Among the Mode 2 tests, Tests 46 and 50 demonstrate the effect of power convincingly. In Test 46, the system pressure is 16.2 psia (112 kPa) in response to a power input of 5.90 Btu/s (6.22 kW); while in Test 50, the corresponding values are 17.5 psia (121 kPa) and 9.38 Btu/s (9.89 kW).

The effect of creating a leak passage between the reactor vessel and the coldleg was investigated in Tests 23 and 24. In Test 23, creating such a leakage raised

the equilibrium pressure by about 2 psi (14 kPa). But then, in Test 24, resealing the leakage did not restore the system pressure to its original value: instead, the system pressure went up one more psi. Hence, the effect of cross-connection is uncertain; but, in any case, the effect appears to be minimal.

Our model was run with both loops operating in Tests 24, 28, and 30. The unexpected results of these tests were that the right steam generator persistently registered lower temperatures, although its cooling water flow was less than that of the left steam generator. The reason became apparent later, when we tried to accomplish all the cooling using the right steam generator alone. The system pressure shot up linearly from -1 psig (94 kPa) to 14 psig (198 kPa) in 40 minutes--a symptom that indicated little cooling was occurring. After some diagnostic investigation, we discovered that a slight difference in elevation (~ 0.25 inch) between the right hotleg nozzle and the left hotleg nozzle on the reactor vessel, coupled with the orientation of the three heating elements in the reactor vessel effectively preventing the two-phase mixture from flowing into the right steam generator. Although the true effect of a two-loop operation is unknown, we have no reason to suspect any complication in a two-loop operation.

During the last five tests of the series, a model "pressurizer" was added to the test facility. It was made of a 4-inch (10-cm) diameter glass cylinder, approximately 3.5-ft (1-m) high. However, this pressurizer was not designed to have the capability to regulate the pressure of the system, but simply to act as a drain tank with a connection to the left hotleg. The few tests in which the pressurizer was involved should be considered as tests with varying water inventory. The true effect of a pressurizer is yet to be determined.

Section 8

CONCLUSIONS

Based on our present understanding of the two-phase natural circulation experiments described in this report, we draw the following conclusions:

- In our test facility, configured after TMI-2, two-phase natural circulation is effective in removing the heat generated in the model reactor vessel, even in the presence of significant amounts of noncondensable gases.
- Steady-state two-phase natural circulation modes can be established, provided one allows the primary system to seek its own equilibrium pressure. If one attempts to regulate the system pressure via changes in secondary flow rate, pressure oscillations may occur.
- Never in our test series did we observe superheated steam. The highest temperature recorded always corresponds to the saturation temperature of the reactor vessel pressure.
- There exist two distinct modes of natural circulation. Mode 1 is in operation when the water level in the primary system is below the hotleg nozzle elevation. Mode 2, a percolating mode, exists when the water level is above the hotleg nozzle. Mode 2 consists of three submodes; the choice among them appears to be dictated by the water inventory, the amount of noncondensable gas in the primary system, and the secondary flow rate. The secondary coolant temperature profiles corresponding to these three submodes agree with the analytically predicted profiles corresponding to the conditions $\dot{m}_p/\dot{m}_s$ greater than, equal to, or less than one.
- Compared with single-phase natural circulation, two-phase natural circulation is more tolerant of the presence of noncondensable gas. In that respect, Mode 1 is much more tolerant of noncondensable gas than Mode 2. Either mode responds to the existence of excess noncondensable gas with increases in system temperature and pressure. The ultimate limits of the permissible amount of noncondensable gas are likely to be determined by the design limits of the facility. All indications are that a system that can withstand a reasonable pressure will tolerate a volume of noncondensable gas equal to a significant fraction of the primary system volume.

Appendix A

EMPIRICAL FORMULAS FOR CALCULATING VOLUME OF WATER IN THE PRIMARY SYSTEM

Appendix A

EMPIRICAL FORMULAS FOR CALCULATING VOLUME OF WATER IN THE PRIMARY SYSTEM

In all of our tests, the two coldlegs are always water solid unless noncondensable gas is deliberately injected into them. So, in any given test, the amount of water in the system is uniquely determined by the water levels in the reactor vessel and in the two steam generators.* This relationship was empirically determined by correlating the water levels before the model was drained and the volume of water drained from the model. Two independent formulas were found to be needed, one for water level in the model above the hotlegs and one for water level below the hotlegs. The two formulas are given below:

Water level in model above hotleg ports:

$$V_w(\text{in}^3) = 1427 + 9.58(z_A + z_B) + 28.89z_{RV} \quad ; \tag{A-1}$$

Water level in model below hotleg ports:

$$V_w(\text{in}^3) = 1360 + 6.49(z_A + z_B) + 28.89z_{RV} \quad ; \tag{A-2}$$

where z_A and z_B are levels in the left and right steam generators, and z_{RV} is the level in the reactor vessel in inches, as measured according to the scale affixed to the model.† Values of V_w listed in Table 6-2 are calculated from these two equations.

---

*The possible existence of a two-phase mixture in these three components does not alter the validity of this statement, because the sightgauges always indicate the collapsed levels.

†Zero of the scale is at 20 inches (51 cm) above the bottom of the reactor vessel.

Appendix B

CALCULATION OF GROSS HEAT LOSS COEFFICIENT OF THE TEST FACILITY

Appendix B

CALCULATION OF GROSS HEAT LOSS COEFFICIENT OF THE TEST FACILITY

Despite heavy insulation of the model, heat loss to the ambient during the experiments was significant because of the large total surface area and the necessarily exposed sightgauges. An attempt to estimate component heat loss, such as that from one steam generator (using data supplied by the fiberglass insulation manufacturer), was unsuccessful because of the low aspect ratio of these components and the nonuniform insulation that was necessary to accommodate instrumentation. Nevertheless, based on a simple analysis and some experimental correlations of the data, we were able to derive a gross heat-loss coefficient of the test facility.

The analysis assumes a simple energy balance model in which the power input is equal to the heat removed by the secondary coolant plus the gross heat loss,

$$P_{in} = \dot{m}_s C_p (T_o - T_i) + P_{loss} \quad , \tag{B-1}$$

where T_o and T_i are the coolant outlet and inlet temperatures. Steady-state condition is assumed. We further assume that the gross heat loss, P_{loss}, is proportional to the difference between the saturation temperature of the primary system and the ambient temperature,

$$P_{loss} = k(T_{SAT} - T_a) \quad , \tag{B-2}$$

where k, the proportionality constant, is defined as the gross heat loss coefficient that has a unit of (Btu/s)/^{o}F or kW/^{o}C.

We noticed that in all of the Mode 1 natural circulation tests, the secondary coolant outlet temperature is only a few degrees lower than the vessel

temperature, which is equal to the saturation temperature. Hence, within about 5 percent accuracy, one may assume

$$T_o = T_{SAT} \quad . \tag{B-3}$$

Combining the last three equations and solving for T_{SAT}, one obtains a relation between T_{SAT} and $\dot{m}_s$, with k as a parameter:

$$T_{SAT} = \frac{P_{in} + kT_a + \dot{m}_s C_p T_i}{\dot{m}_s C_p + k} \quad . \tag{B-4}$$

T_{SAT} can be expressed as system pressure via the Clausius-Clapeyron relation, or the steam table. An empirical correlation between p and $\dot{m}_s$ for nine of the Mode 1 tests was shown in Figure 7-1. A curve based on Eq. B-4 and using 0.021 (Btu/s)/^{o}F (0.040 kW/^{o}C) for k is plotted in Figure 7-1. The good agreement between the analytical result and the experimental data led us to believe that k = 0.021 (Btu/s)/^{o}F (0.040 kW/^{o}C) is a fair representation of the gross heat loss coefficient of our test facility.

Appendix C

SKIN TEMPERATURE PROFILES OF THE MODEL STEAM GENERATORS

Appendix C

SKIN TEMPERATURE PROFILES OF THE MODEL STEAM GENERATORS

This appendix presents the temperature profiles measured along a vertical slit cut in the fiberglass insulation of each of the two model steam generators. The shapes of these profiles not only gave us a clue to the existence of different modes of natural circulation, but also helped us to clarify the physical process in each of those modes. Profiles of a few tests are missing because the pyrometer used for the measurements failed during those tests.

In each graph, the circles represent the profile of the left steam generator, the x's represent that of the right steam generator. The triangles in the first graph are repeat measurements of some of the points along the left steam generator. Zero elevations on these graphs were arbitrarily chosen. The bottom tube sheet of each steam generator is at an elevation of minus 15 inches, and the top tube sheet at approximately 45 inches. The measurements span nearly the entire lengths of the steam generators.

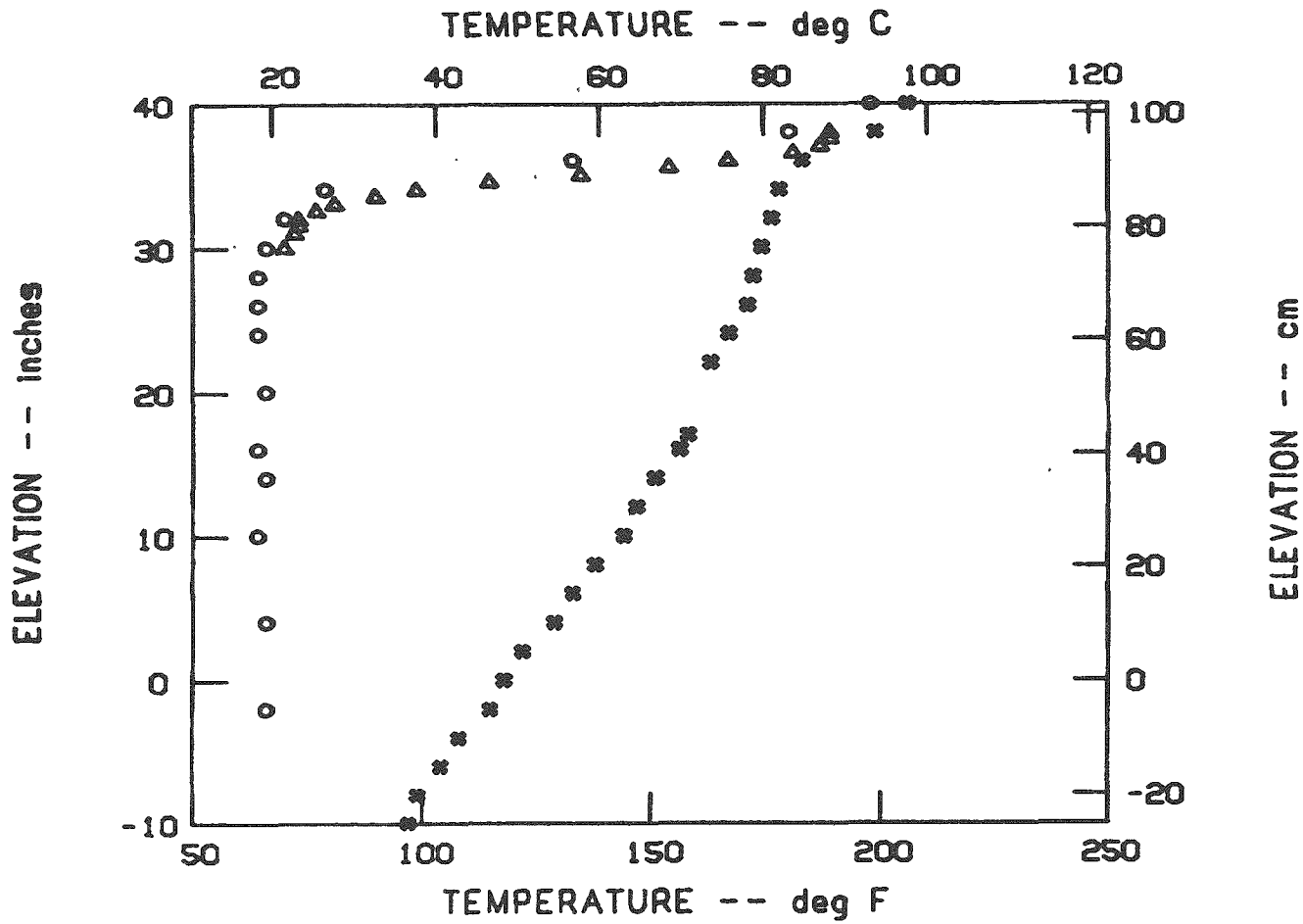

OTSG TEMPERATURE PROFILES: TEST O

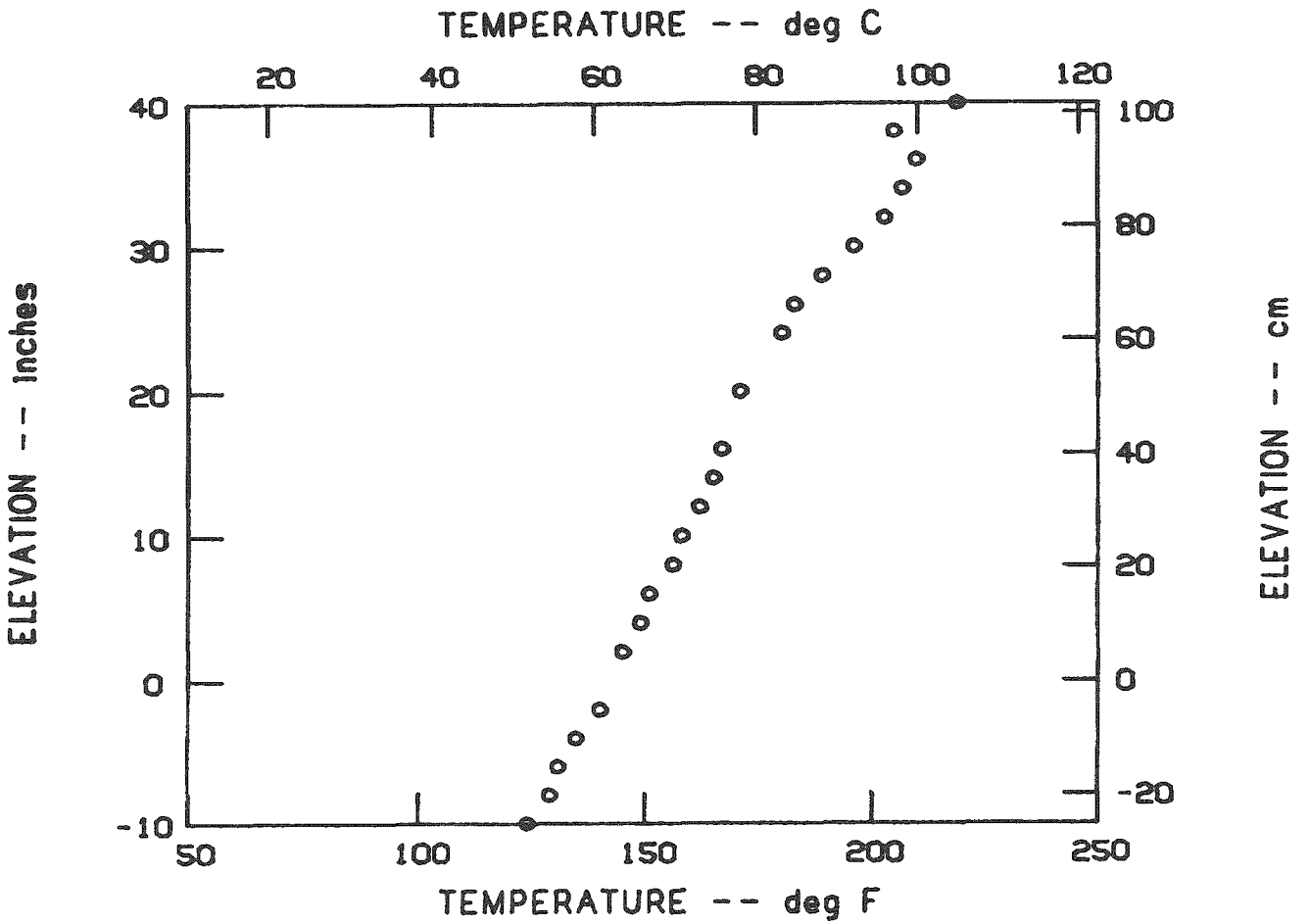

OTSG TEMPERATURE PROFILES: TEST 1

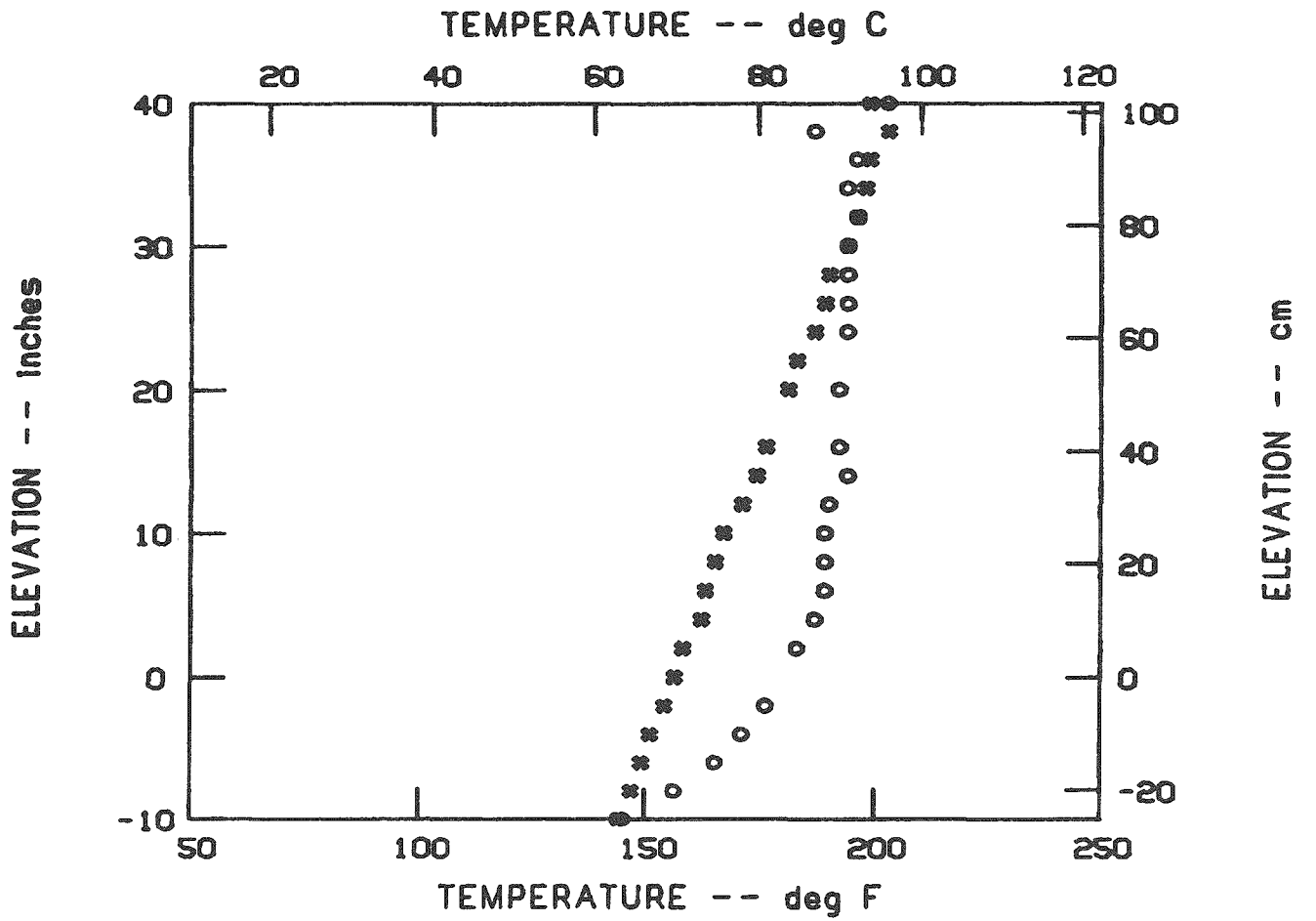

OTSG TEMPERSTURE PROFILES: TEST 2

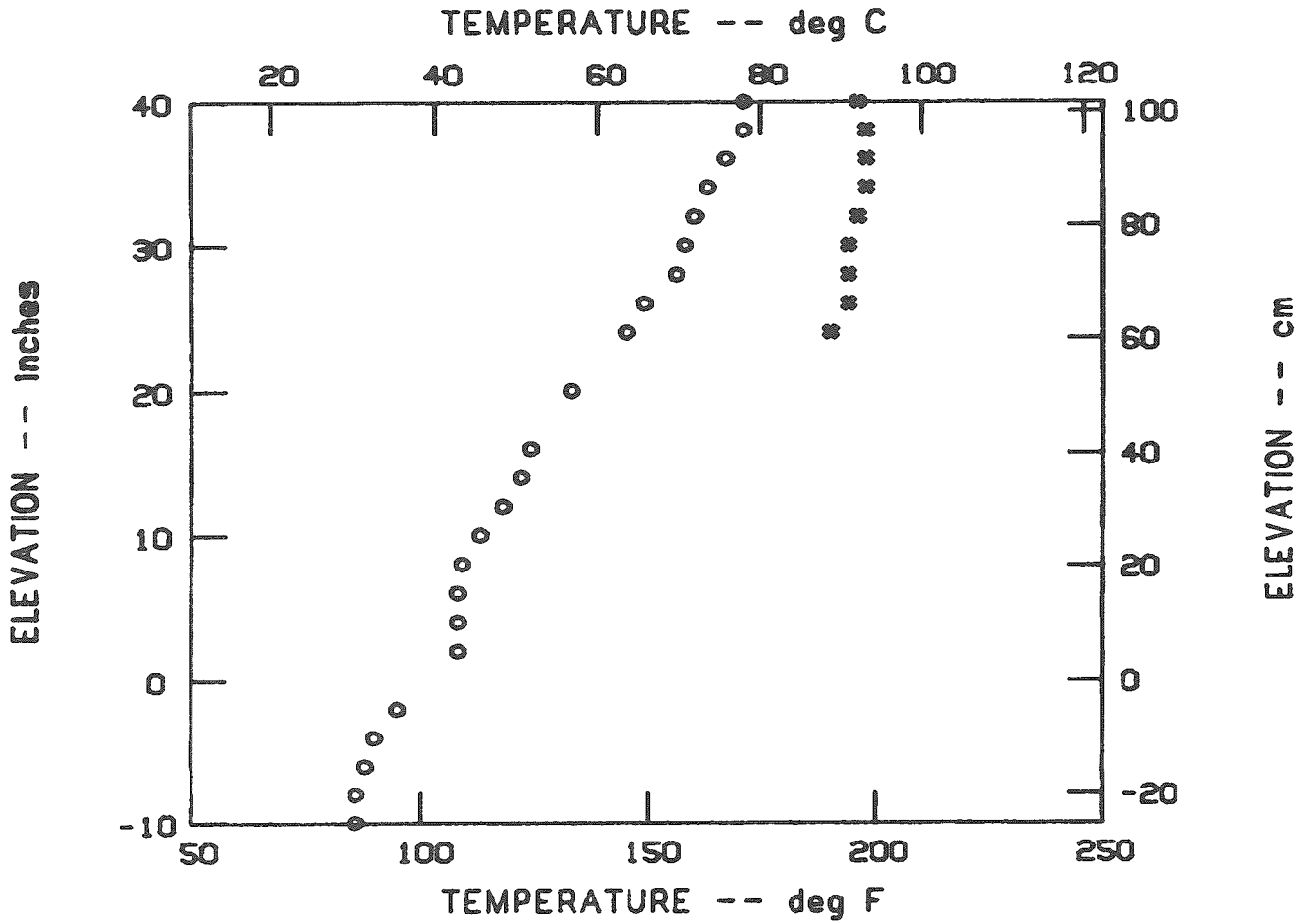

OTSG TEMPERATURE PROFILES: TEST 3

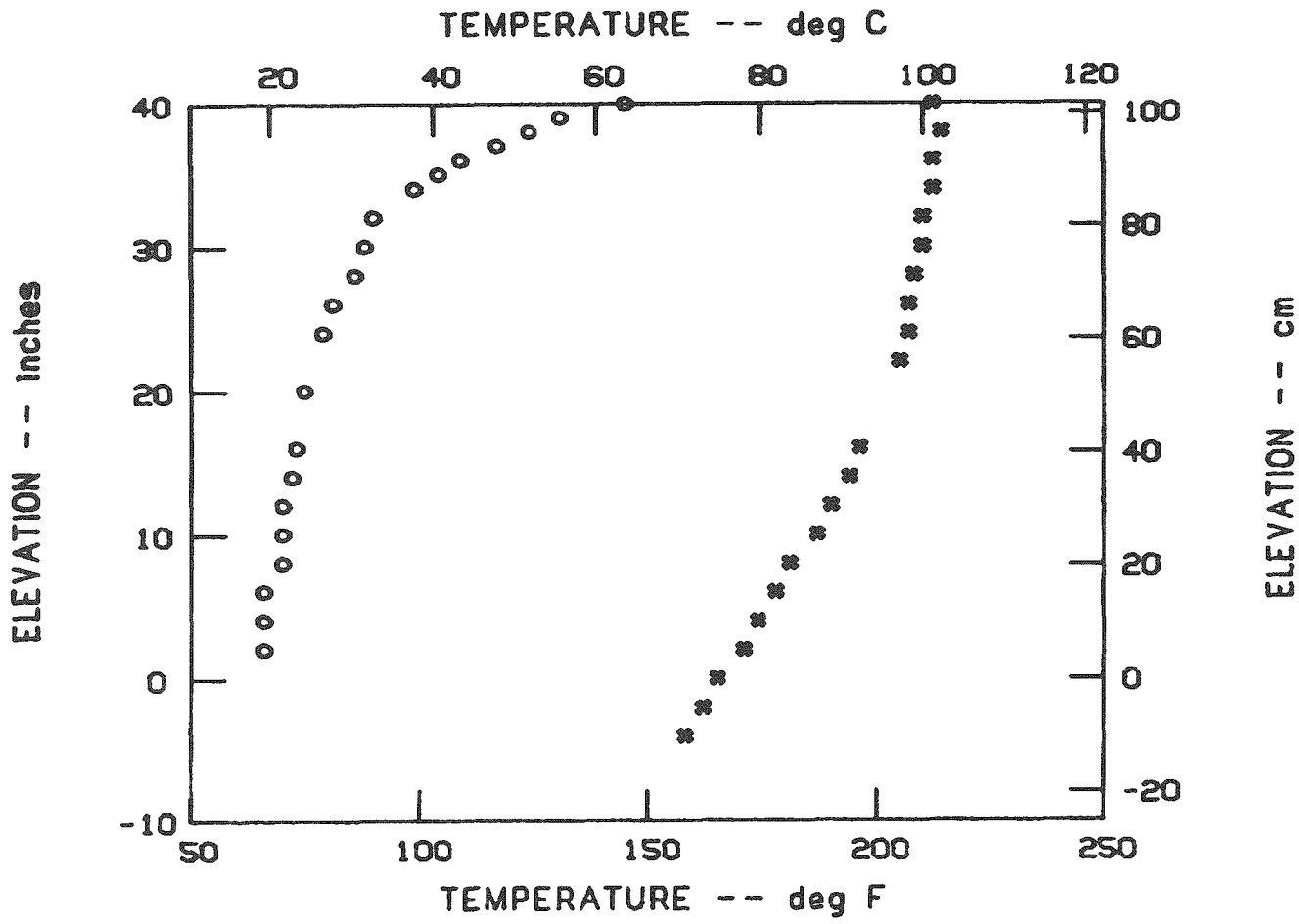

OTSG TEMPERATURE PROFILES: TEST 4

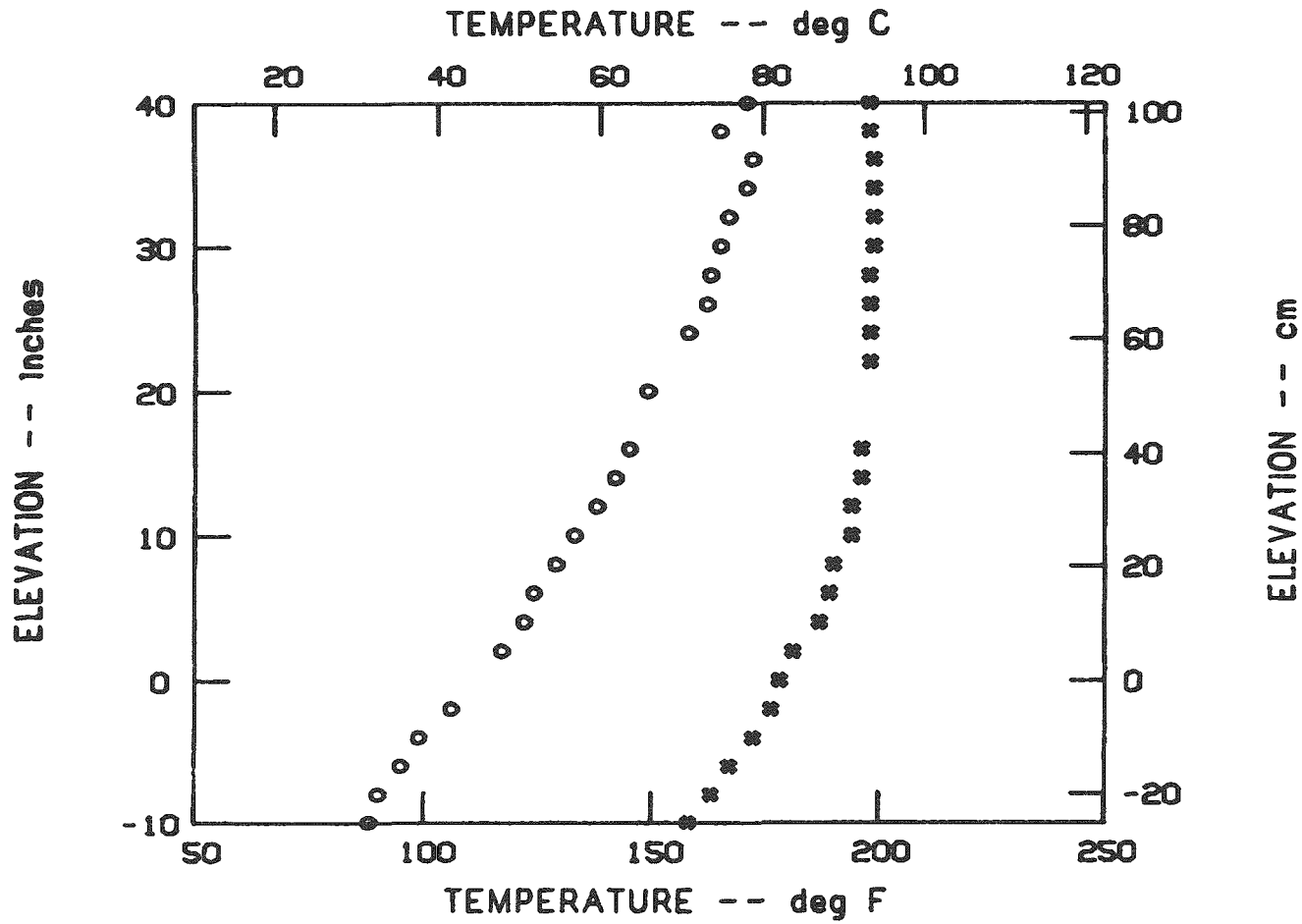

OTSG TEMPERATURE PROFILES: TEST 5

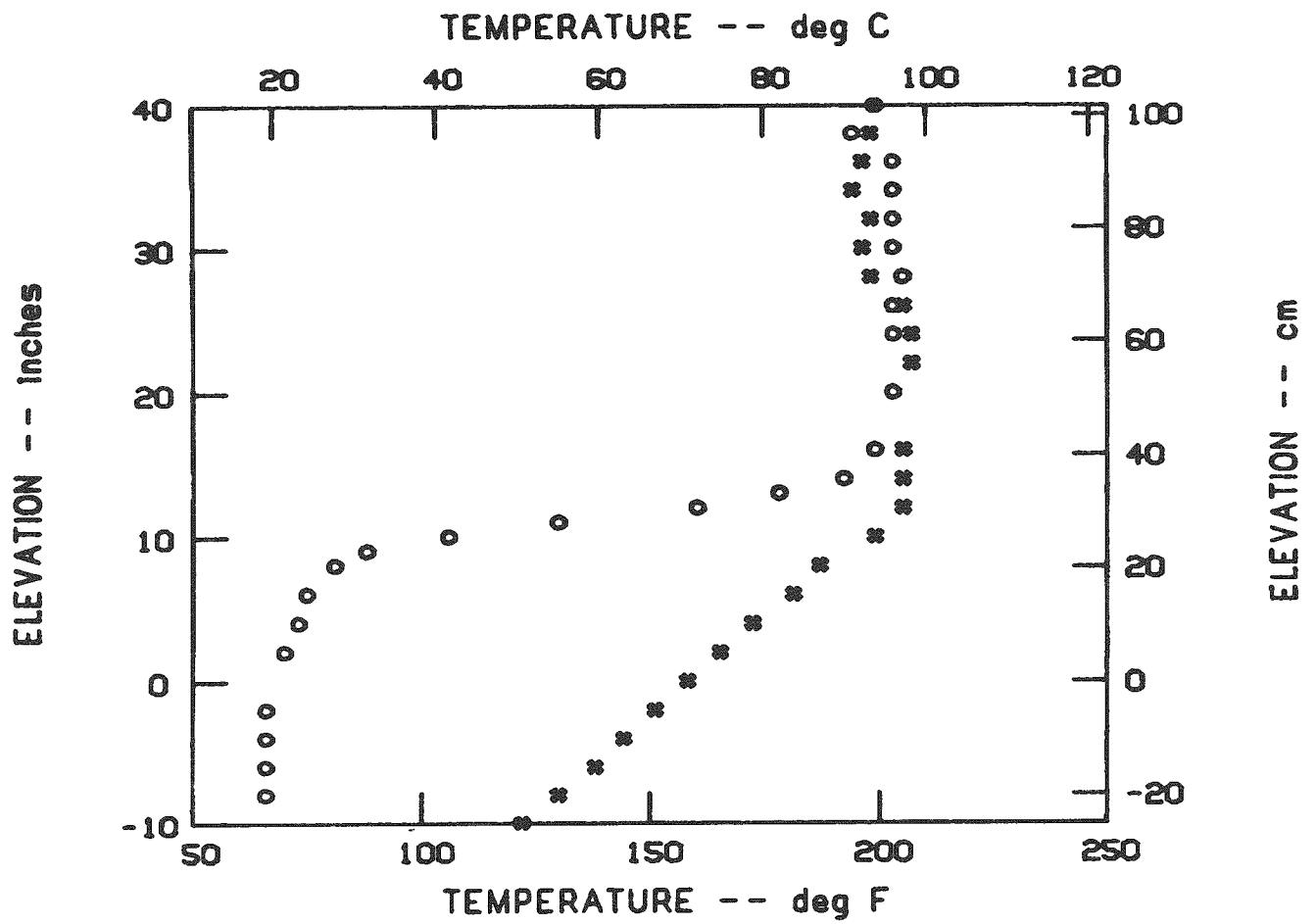

OTSG TEMPERATURE PROFILES: TEST 7

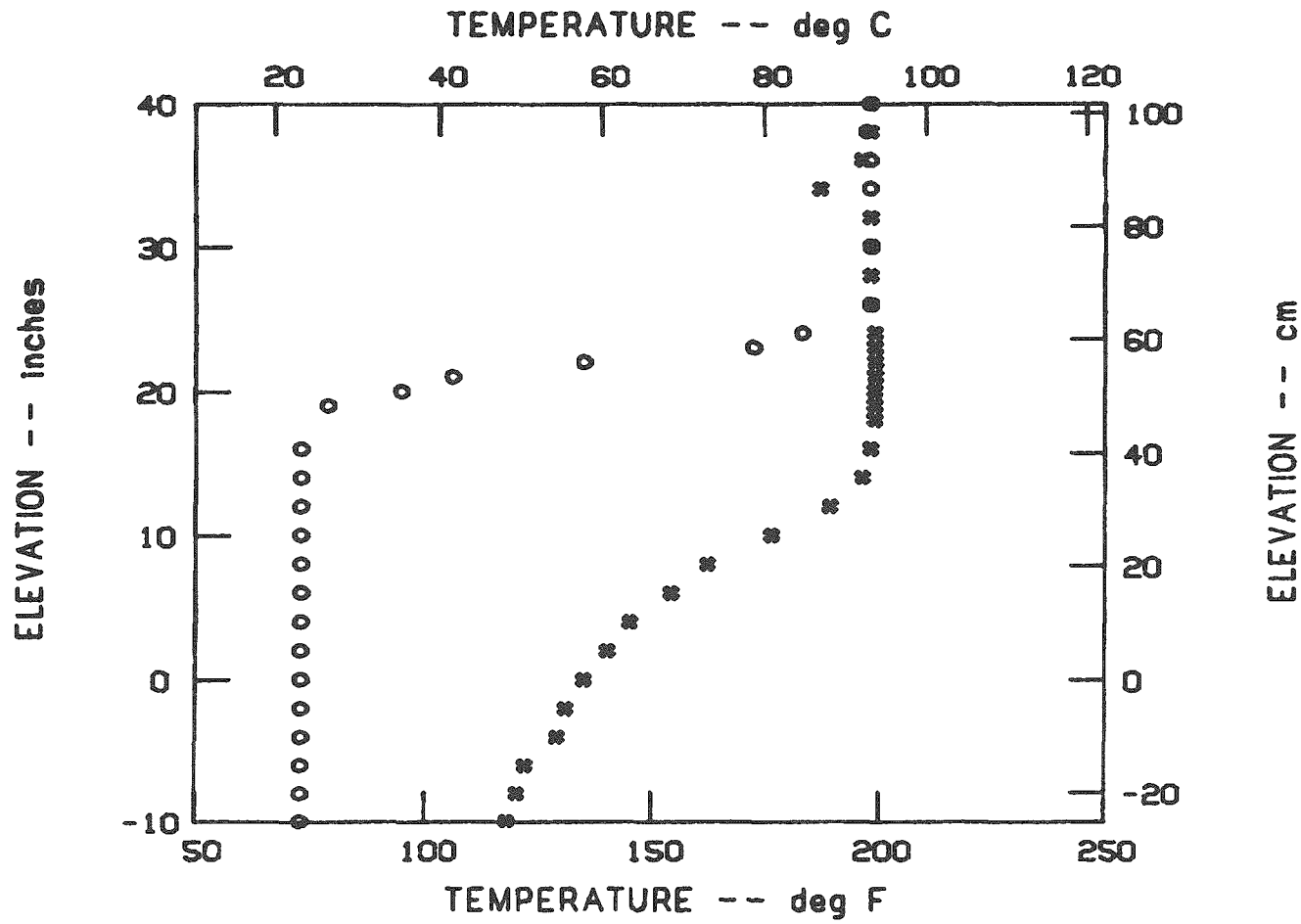

OTSG TEMPERATURE PROFILES: TEST 9

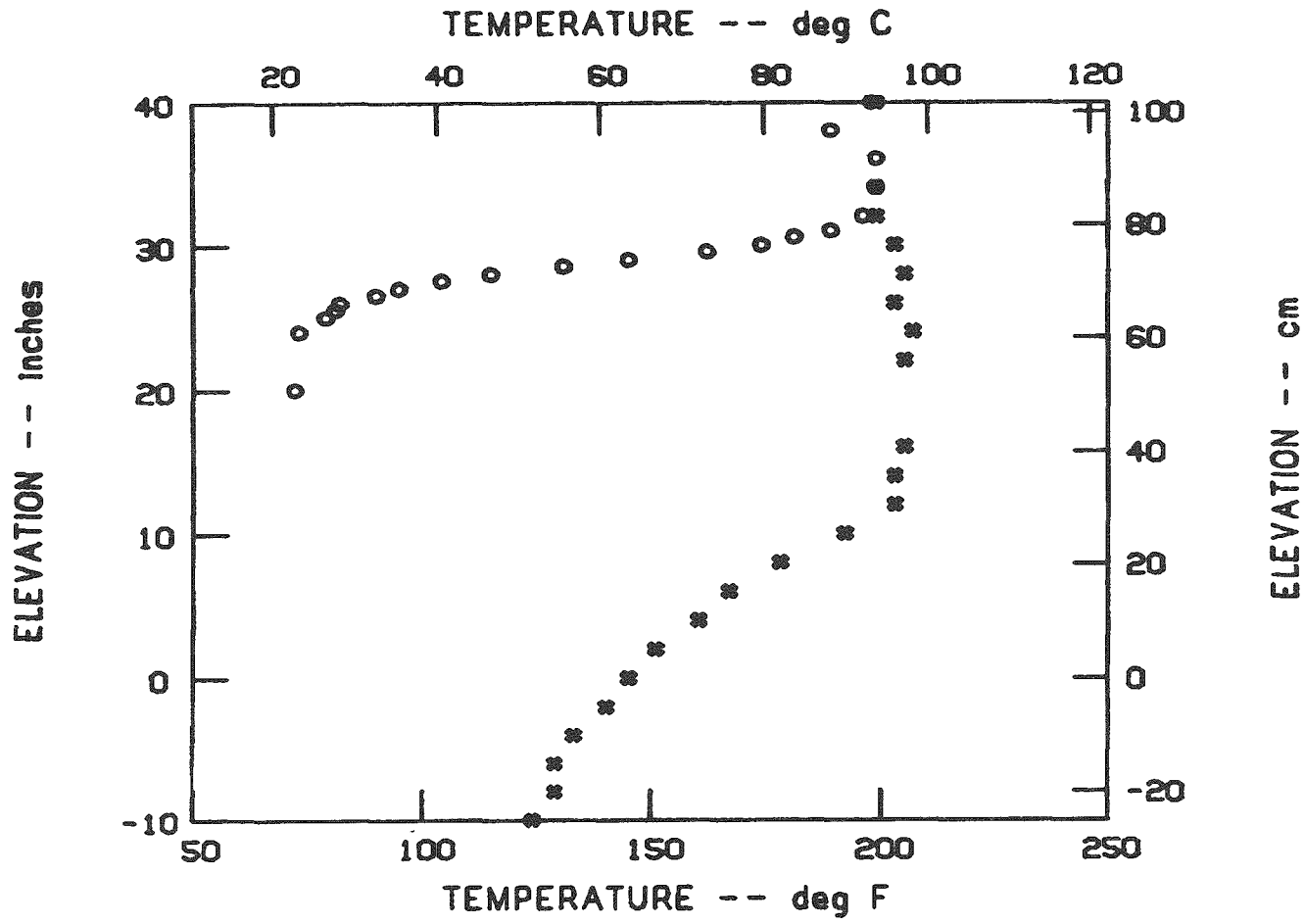

OTSG TEMPERATURE PROFILES: TEST 10

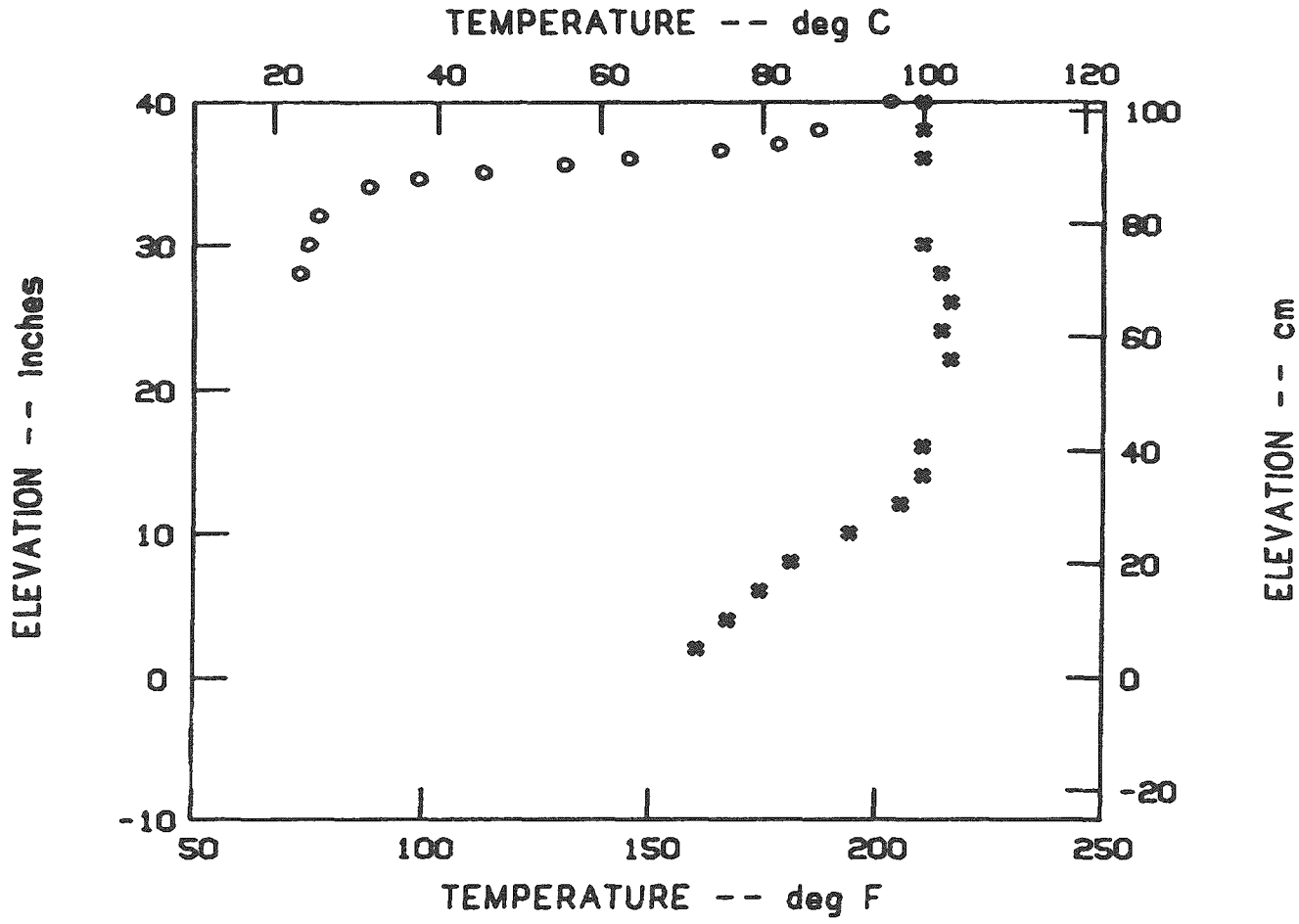

OTSG TEMPERATURE PROFILES: TEST 11

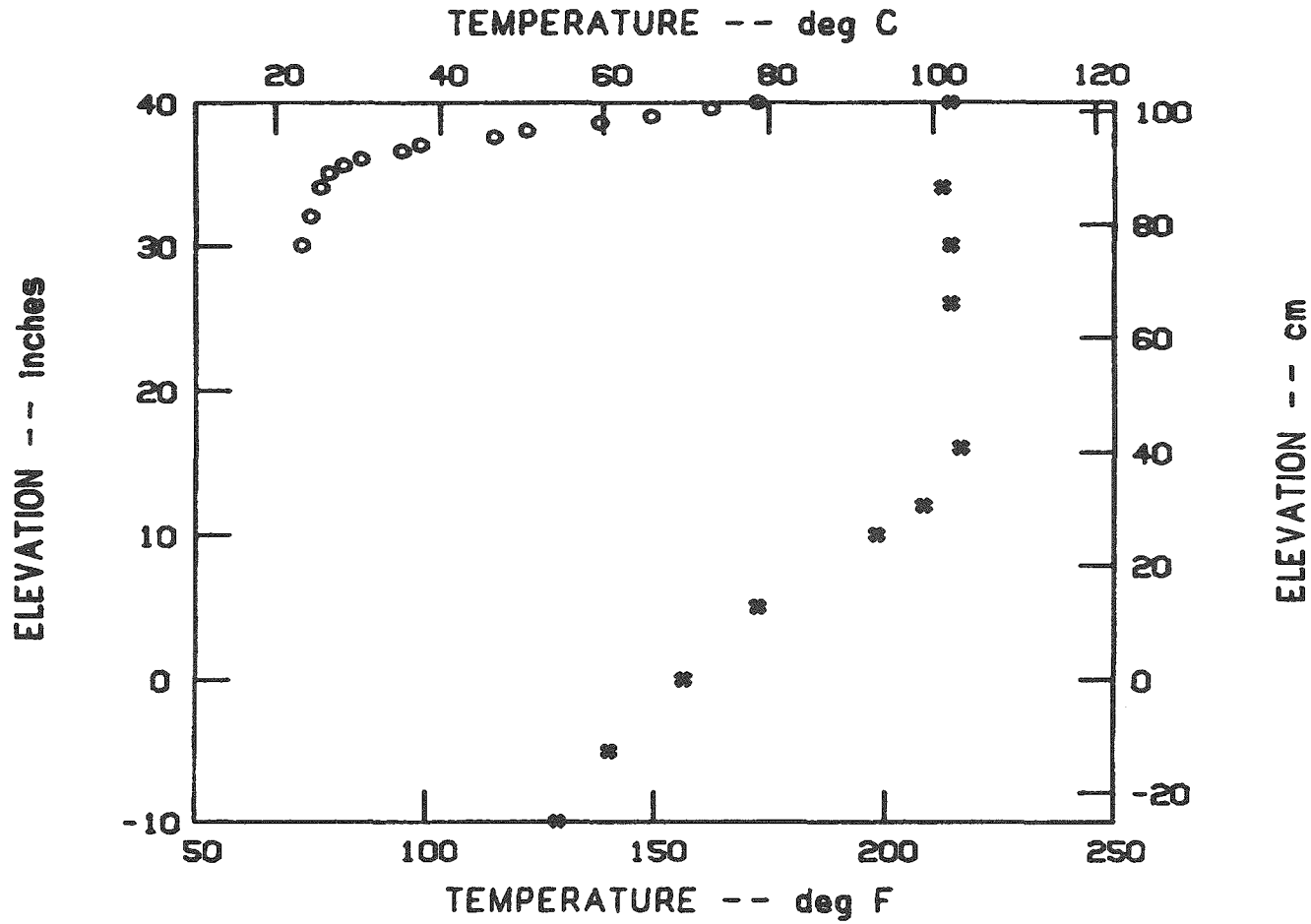

OTSG TEMPERATURE PROFILES: TEST 12

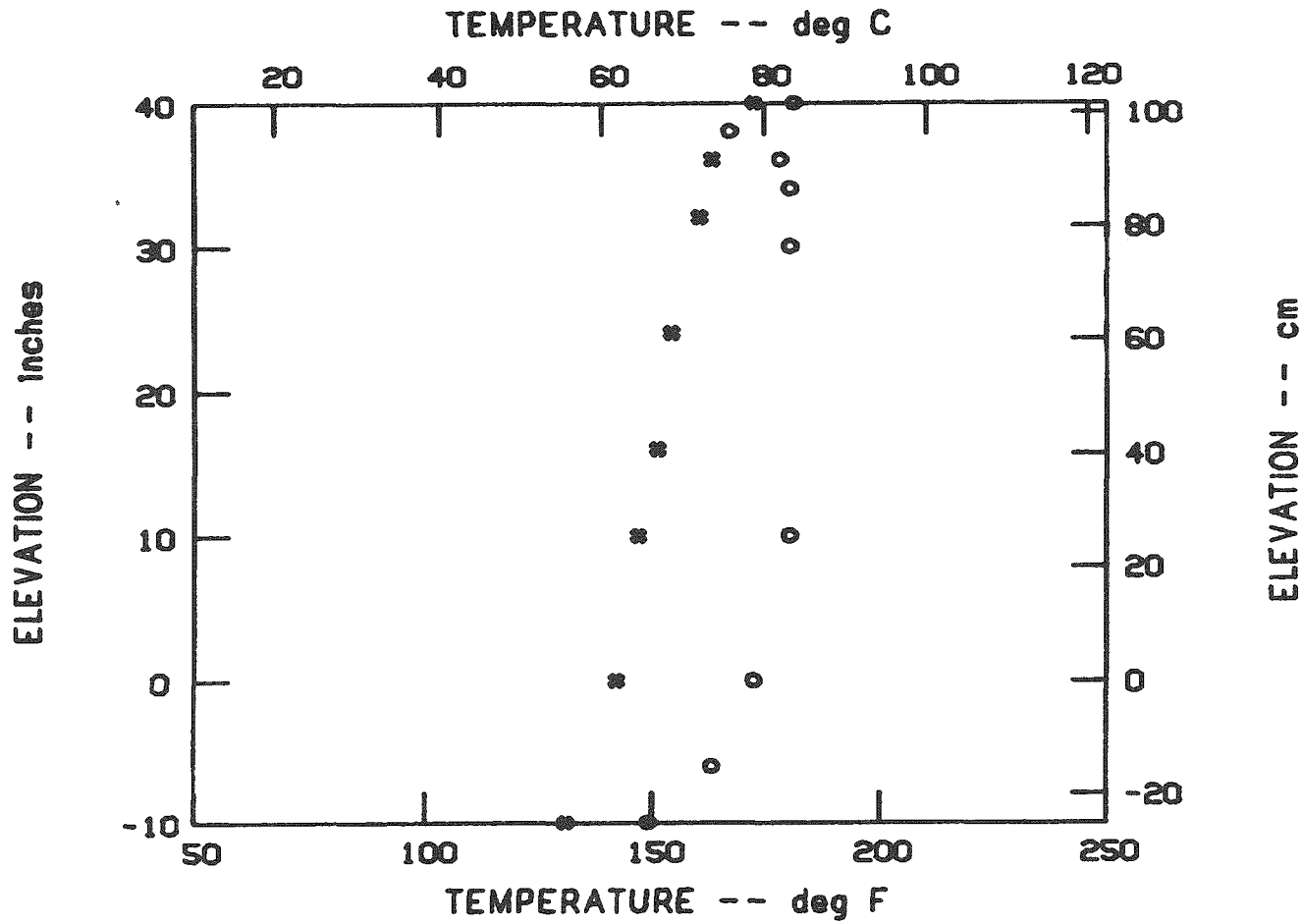

OTSG TEMPERATURE PROFILES: TEST 14

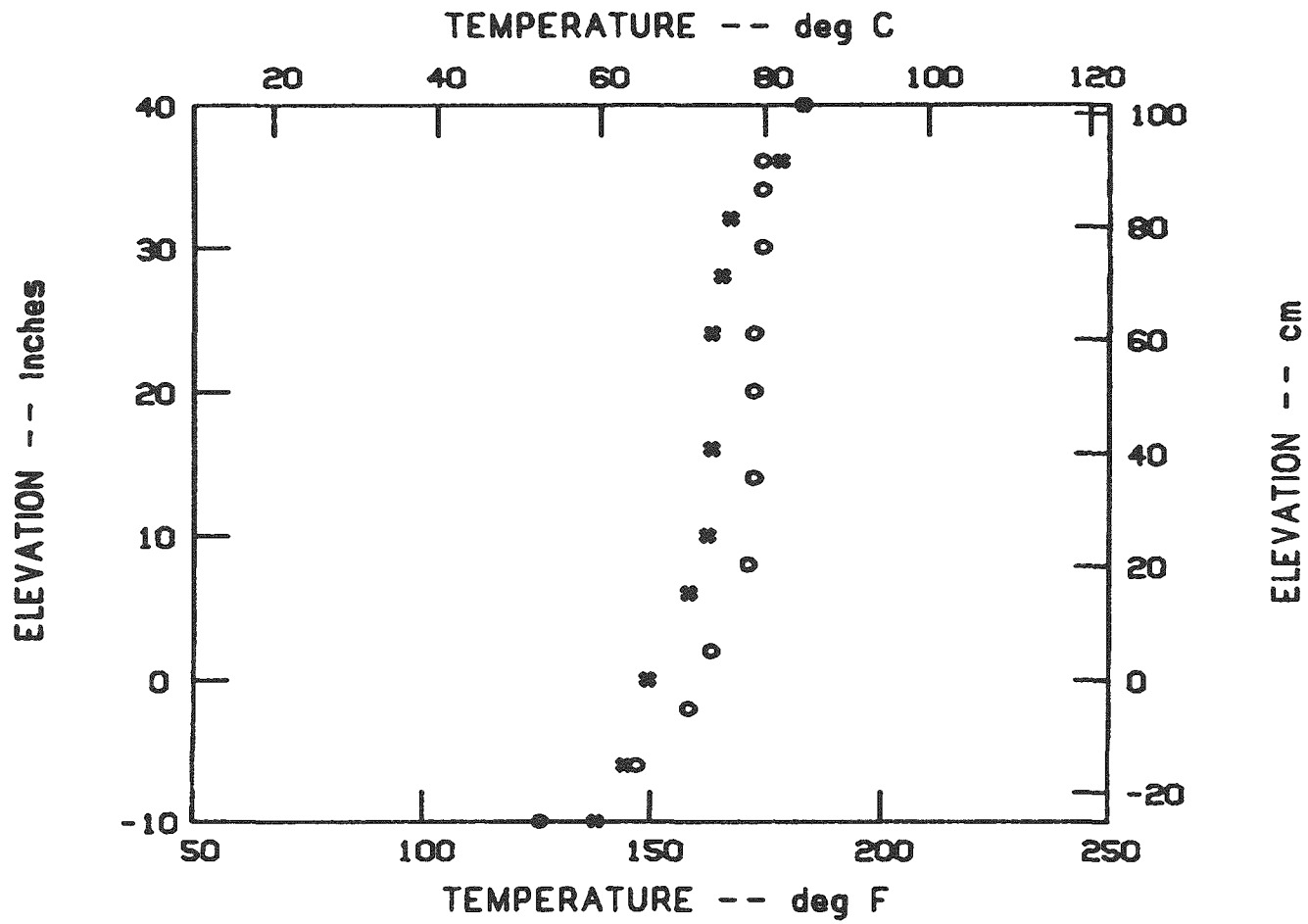

OTSG TEMPERATURE PROFILES: TEST 15

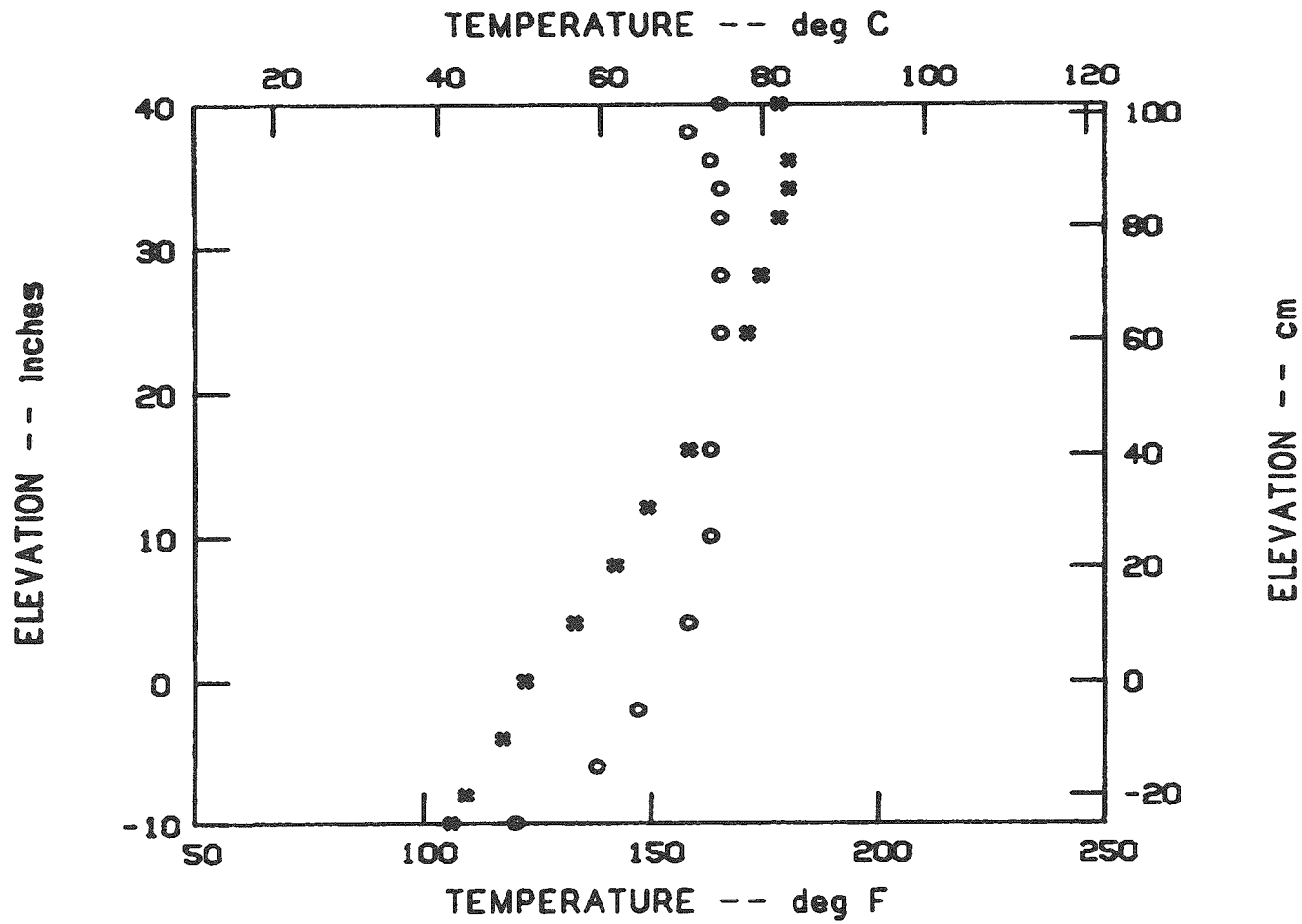

OTSG TEMPERATURE PROFILES: TEST 16

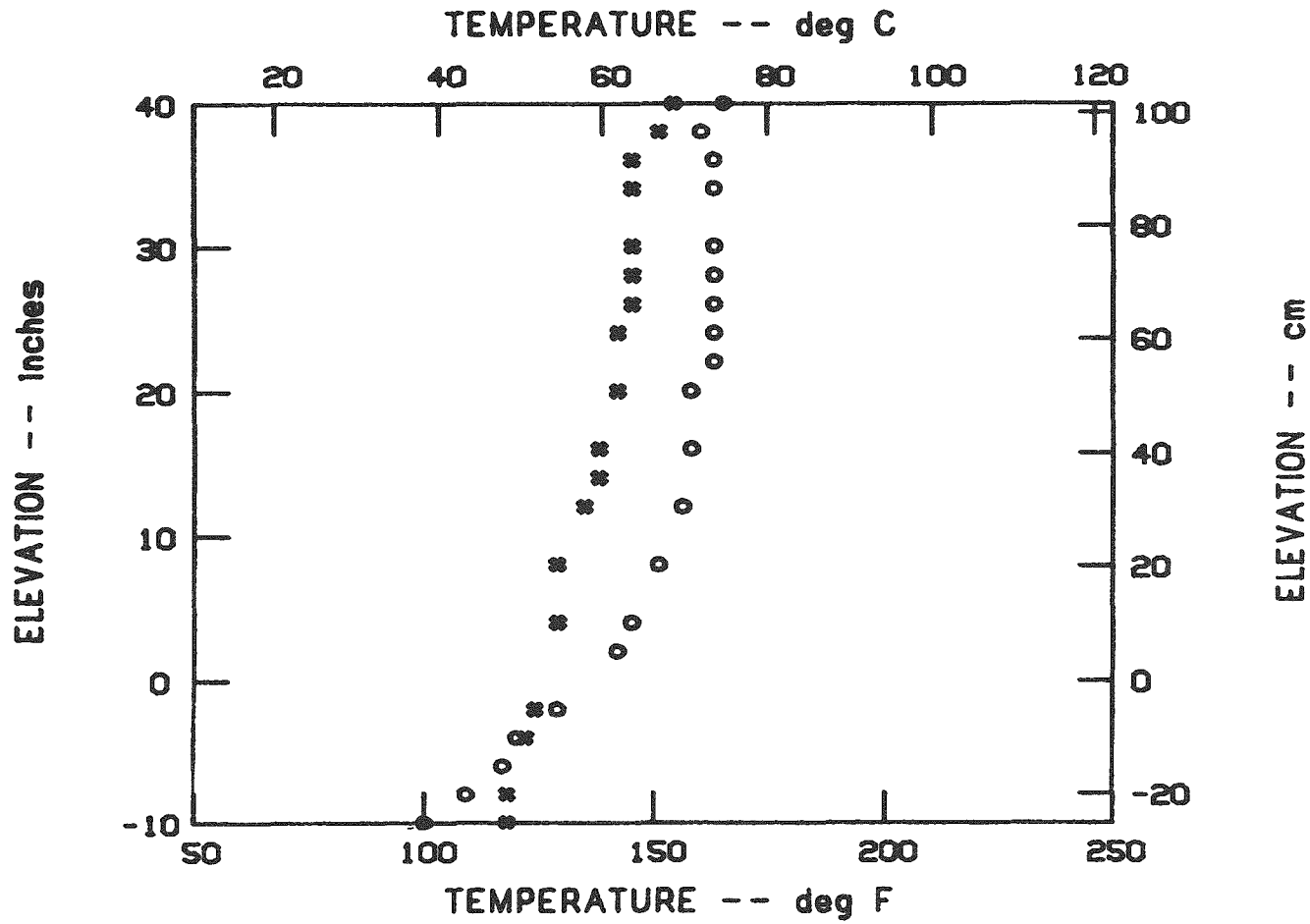

OTSG TEMPERATURE PROFILES: TEST 17

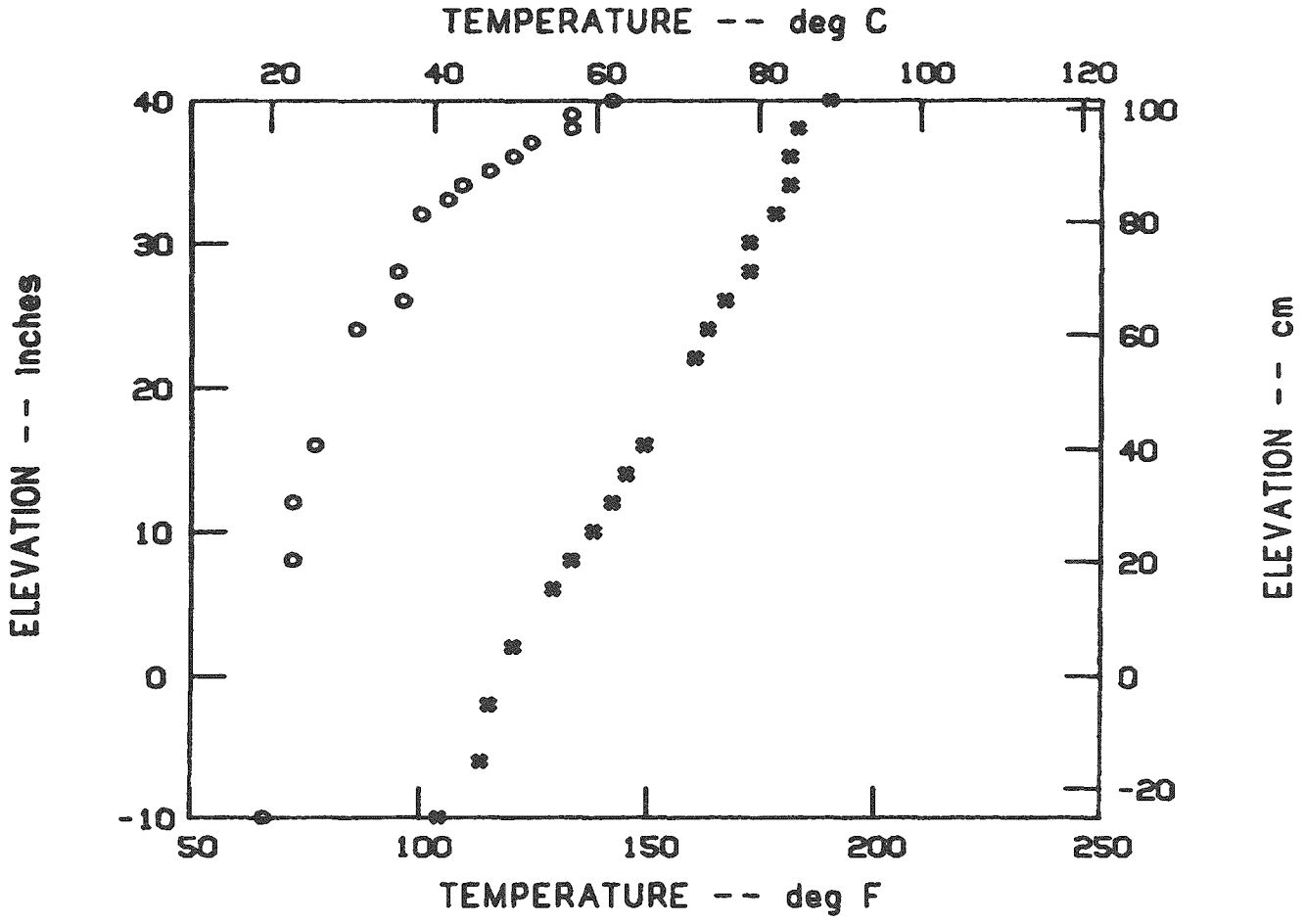

OTSG TEMPERATURE PROFILES: TEST 18

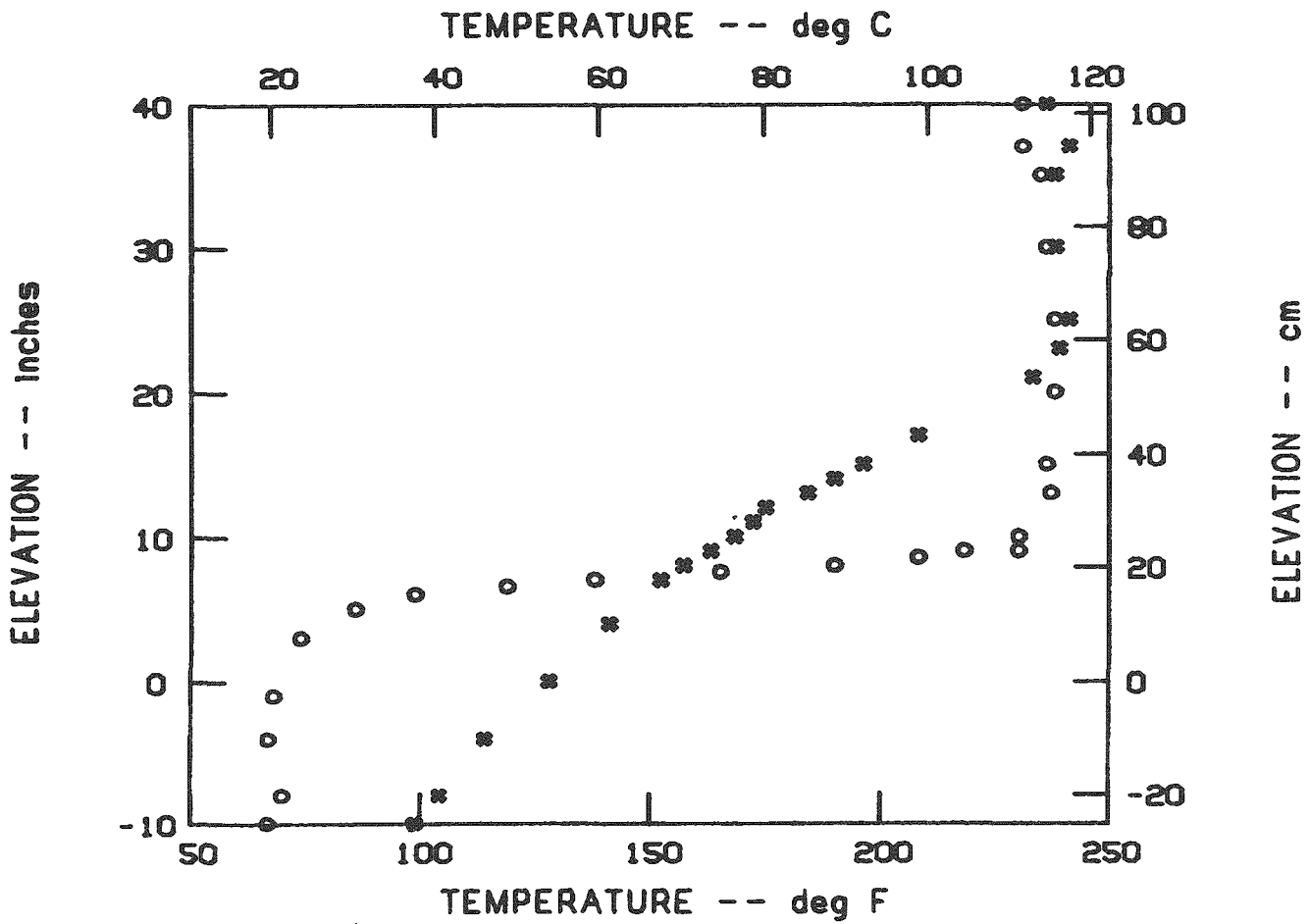

OTSG TEMPERATURE PROFILES: TEST 20

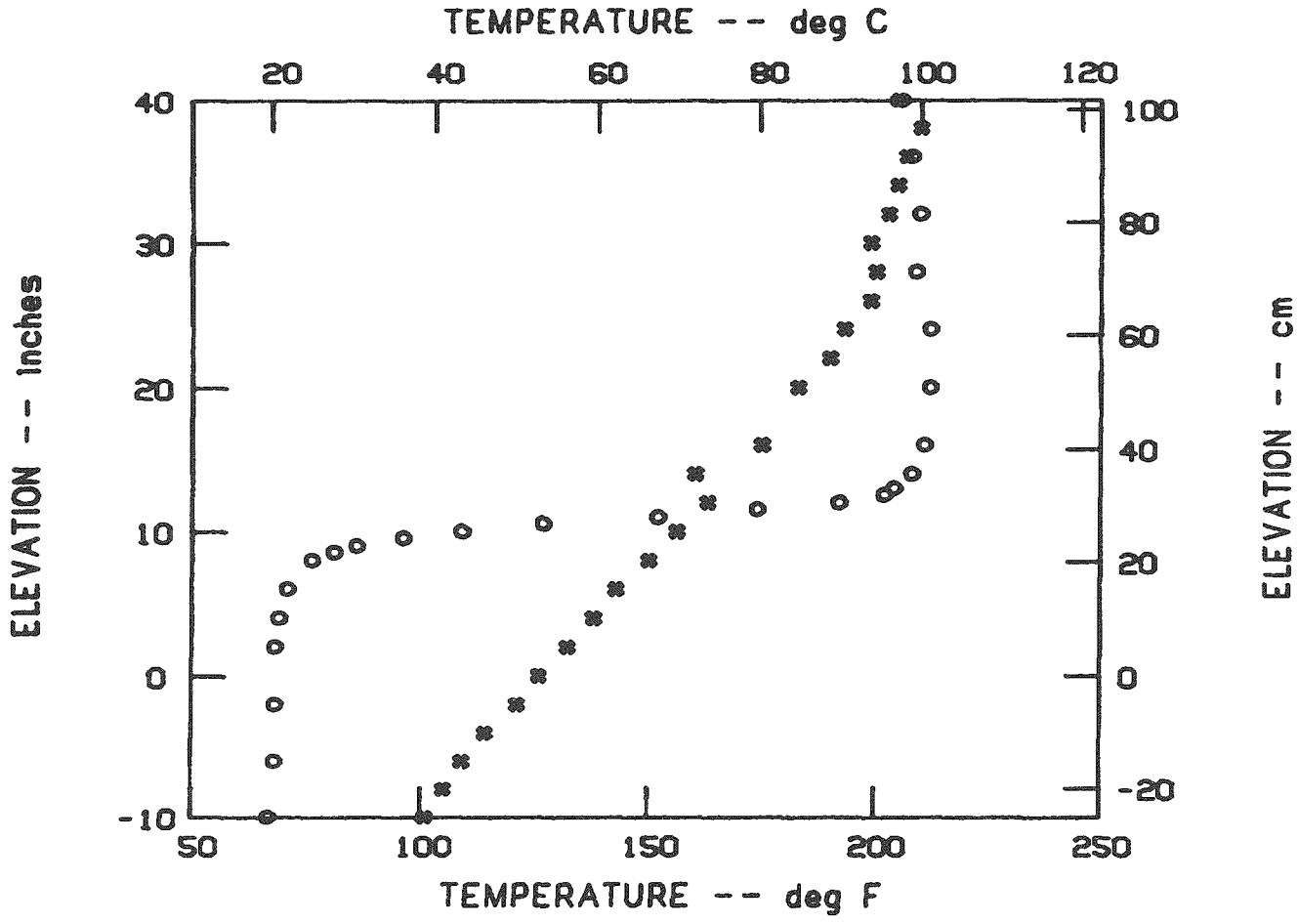

OTSG TEMPERATURE PROFILES: TEST 21

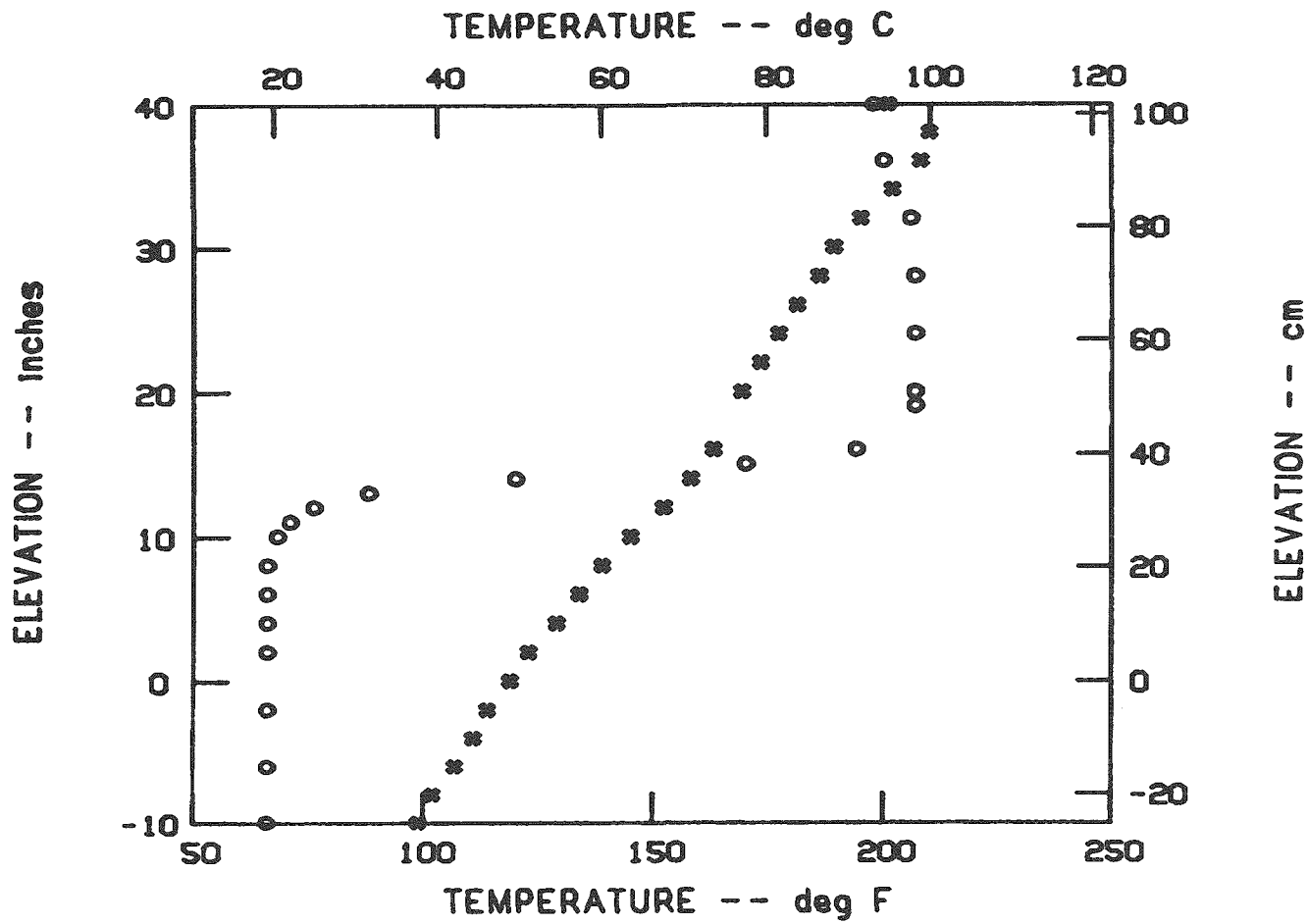

OTSG TEMPERATURE PROFILES: TEST 22

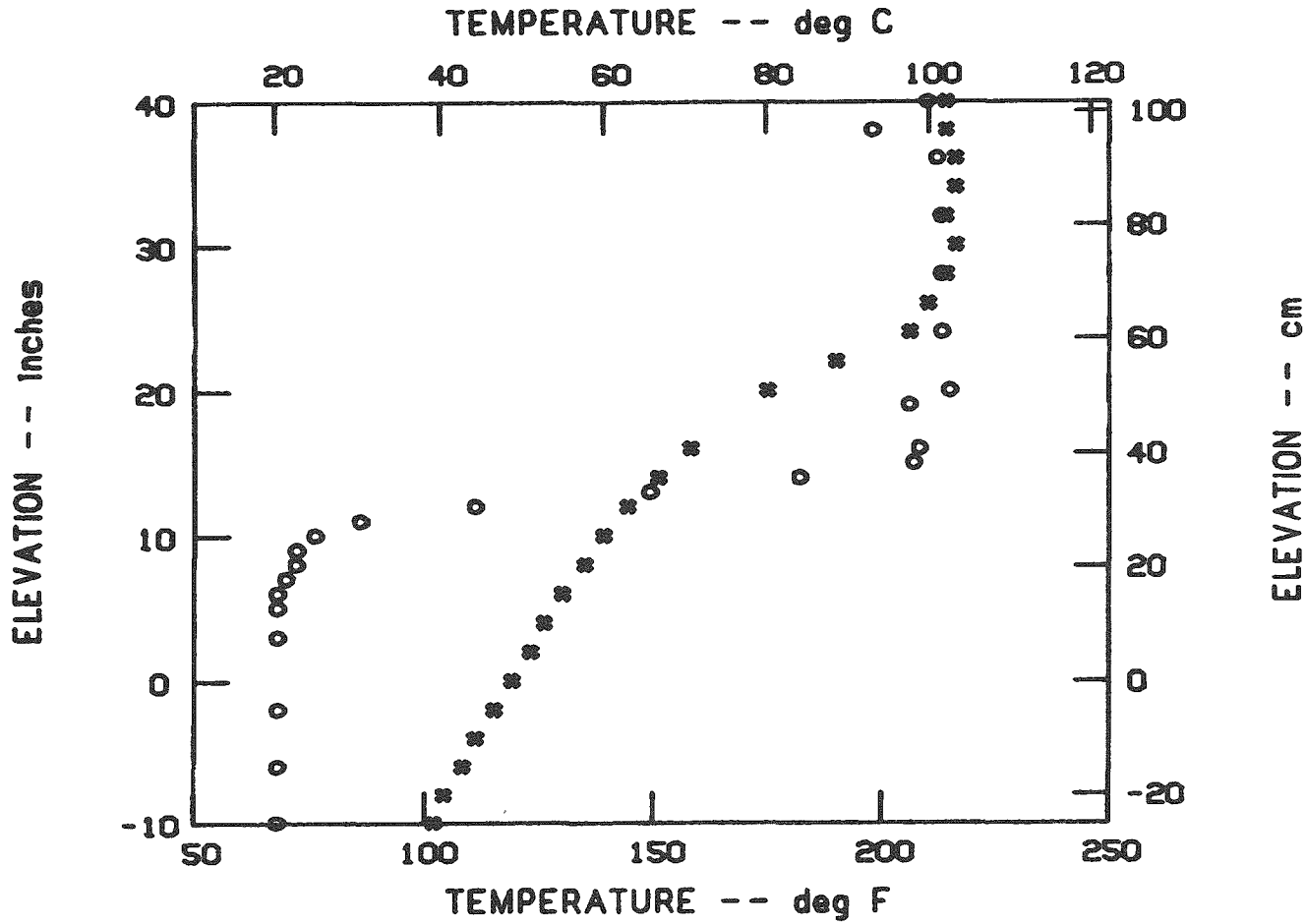

OTSG TEMPERATURE PROFILES: TEST 23

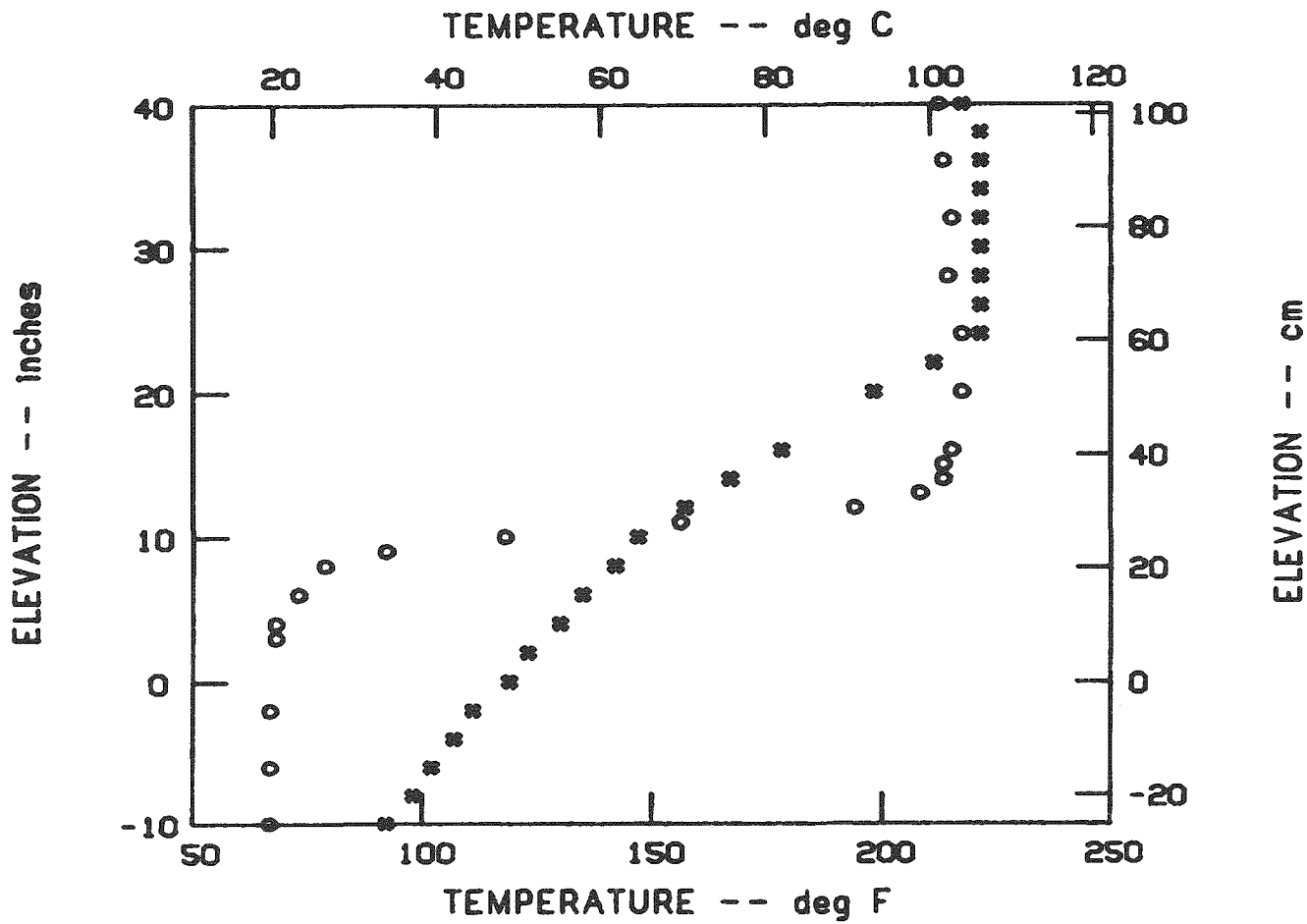

OTSG TEMPERATURE PROFILES: TEST 24

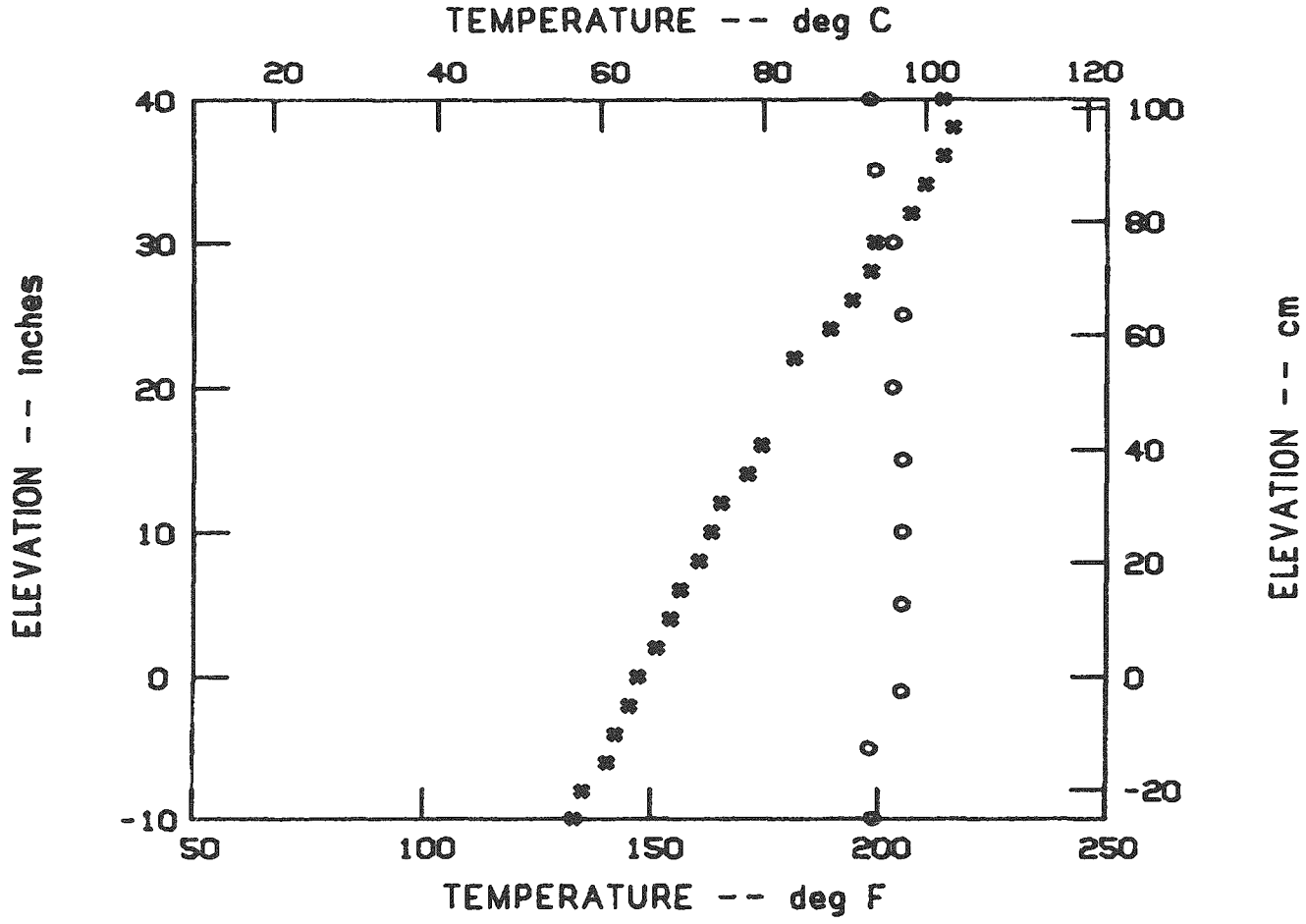

OTSG TEMPERATURE PROFILES: TEST 25

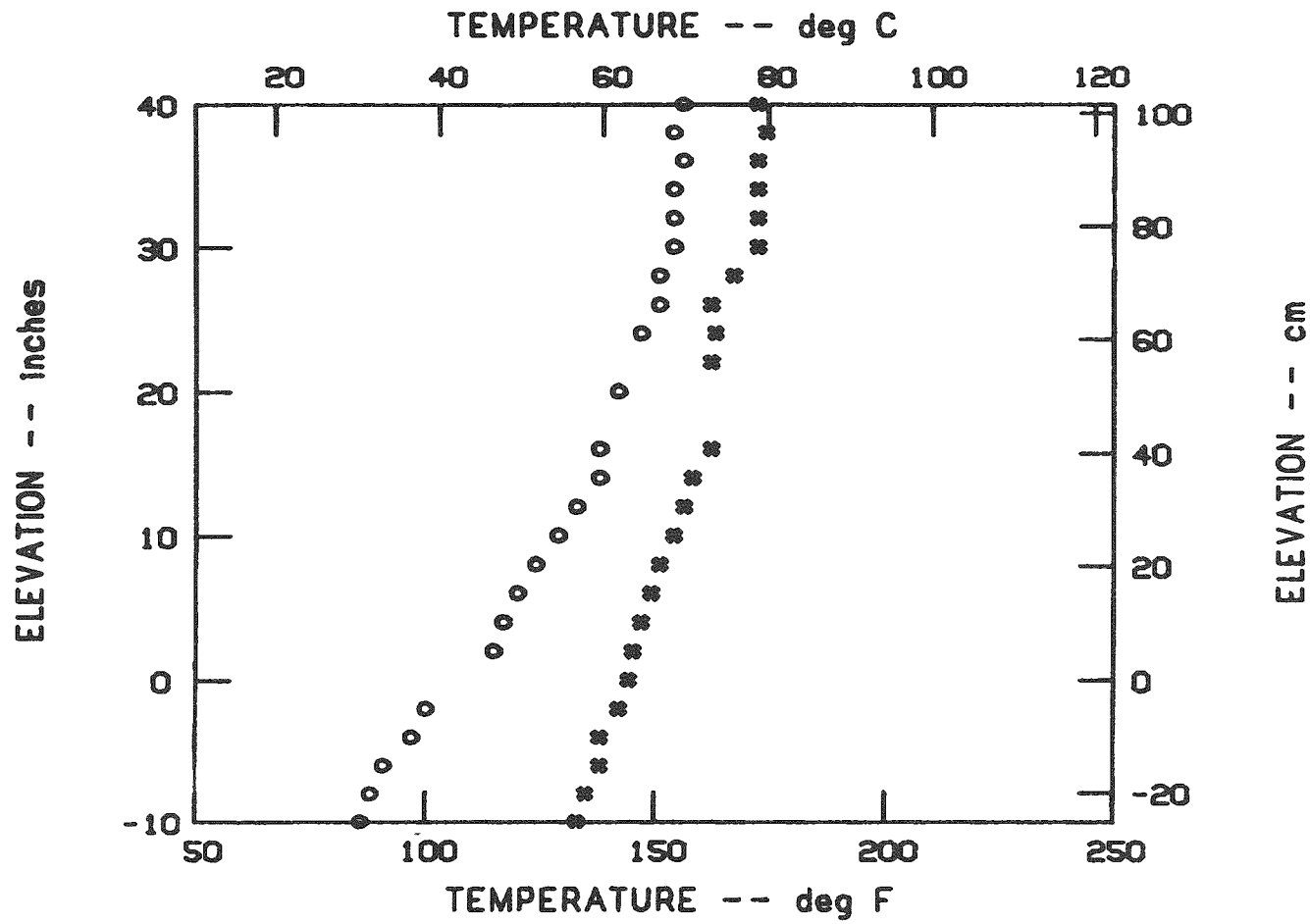

OTSG TEMPERATURE PROFILES: TEST 26

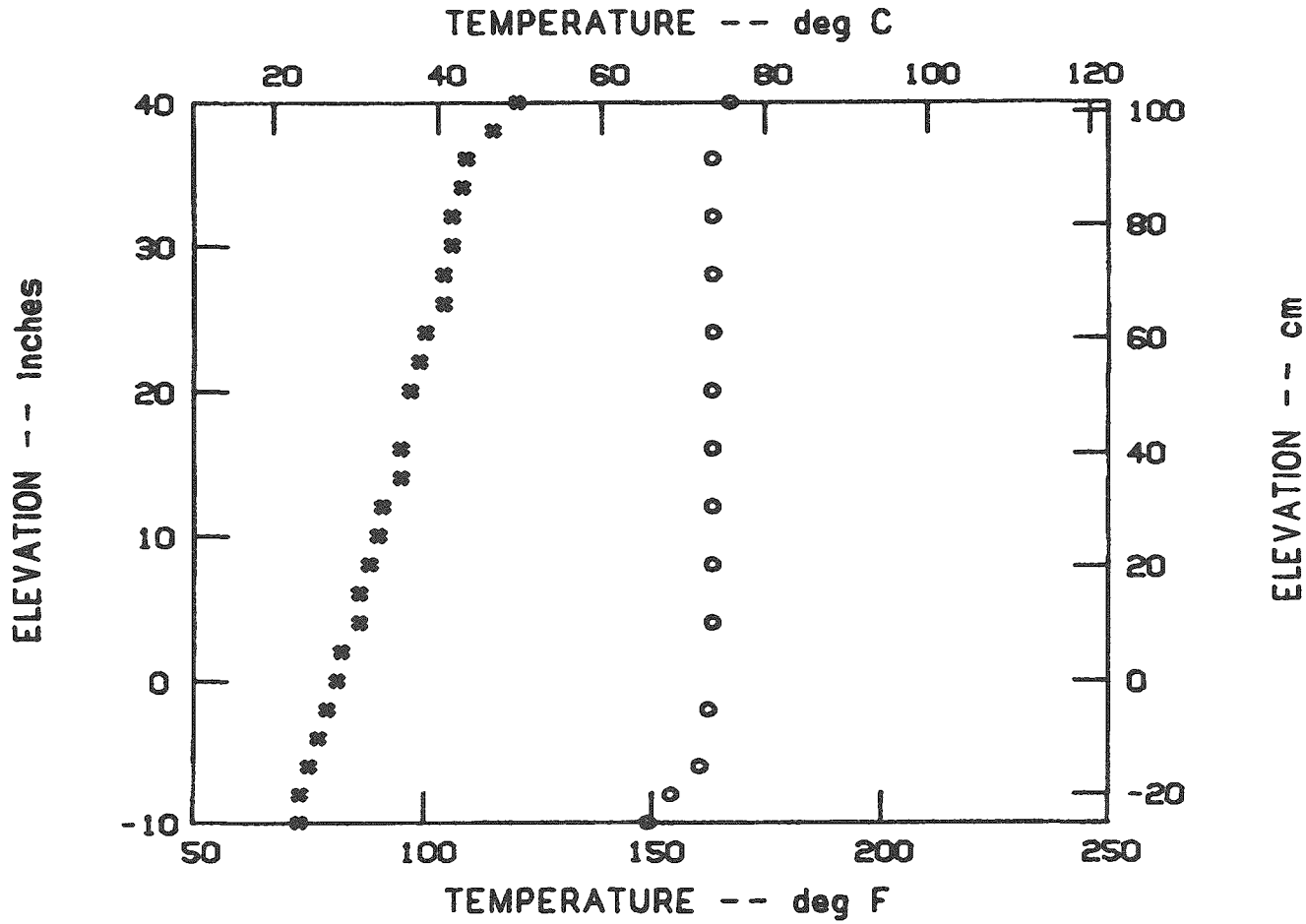

OTSG TEMPERATURE PROFILES: TEST 27

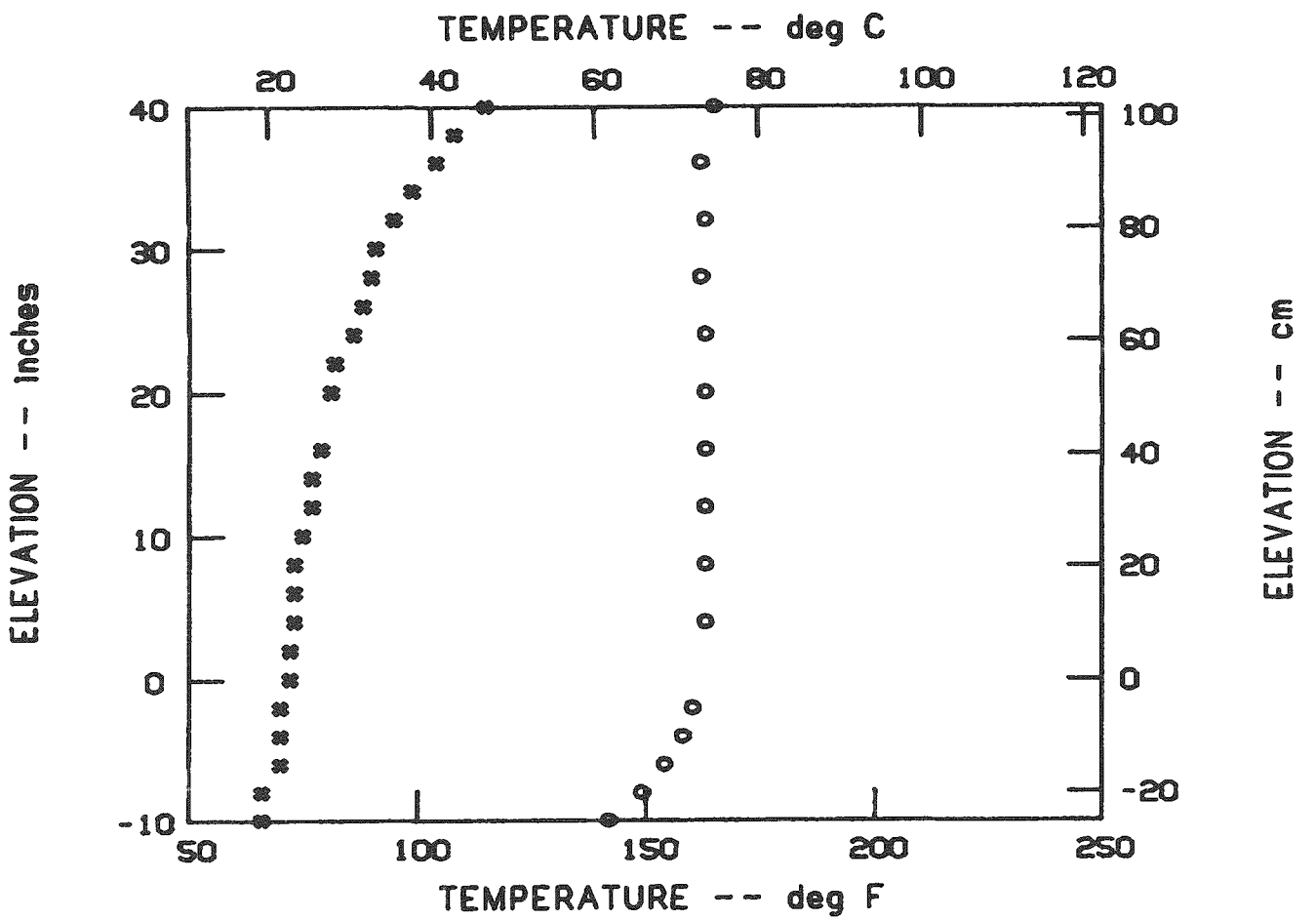

OTSG TEMPERATURE PROFILES: TEST 28

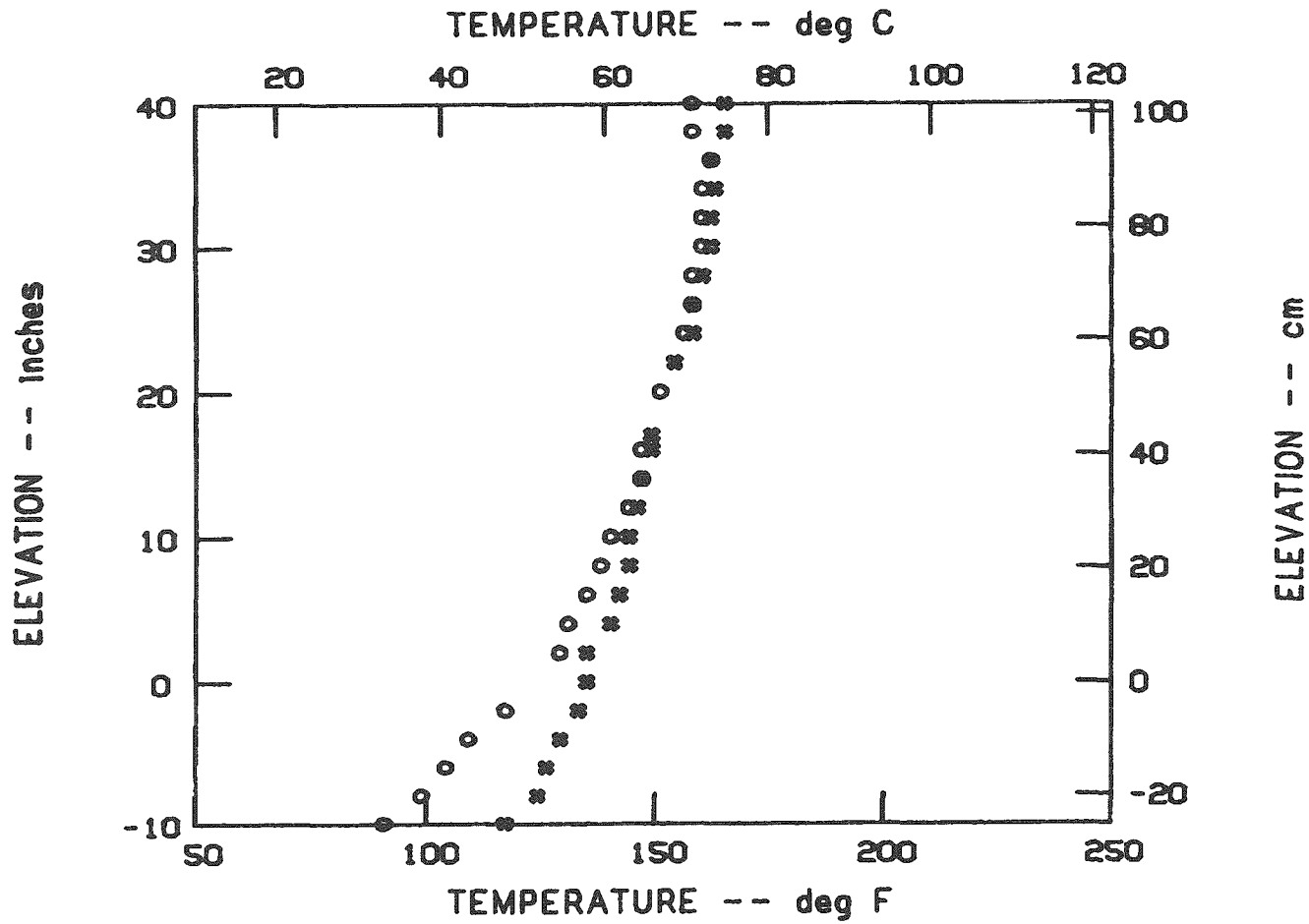

OTSG TEMPERATURE PROFILES: TEST 29

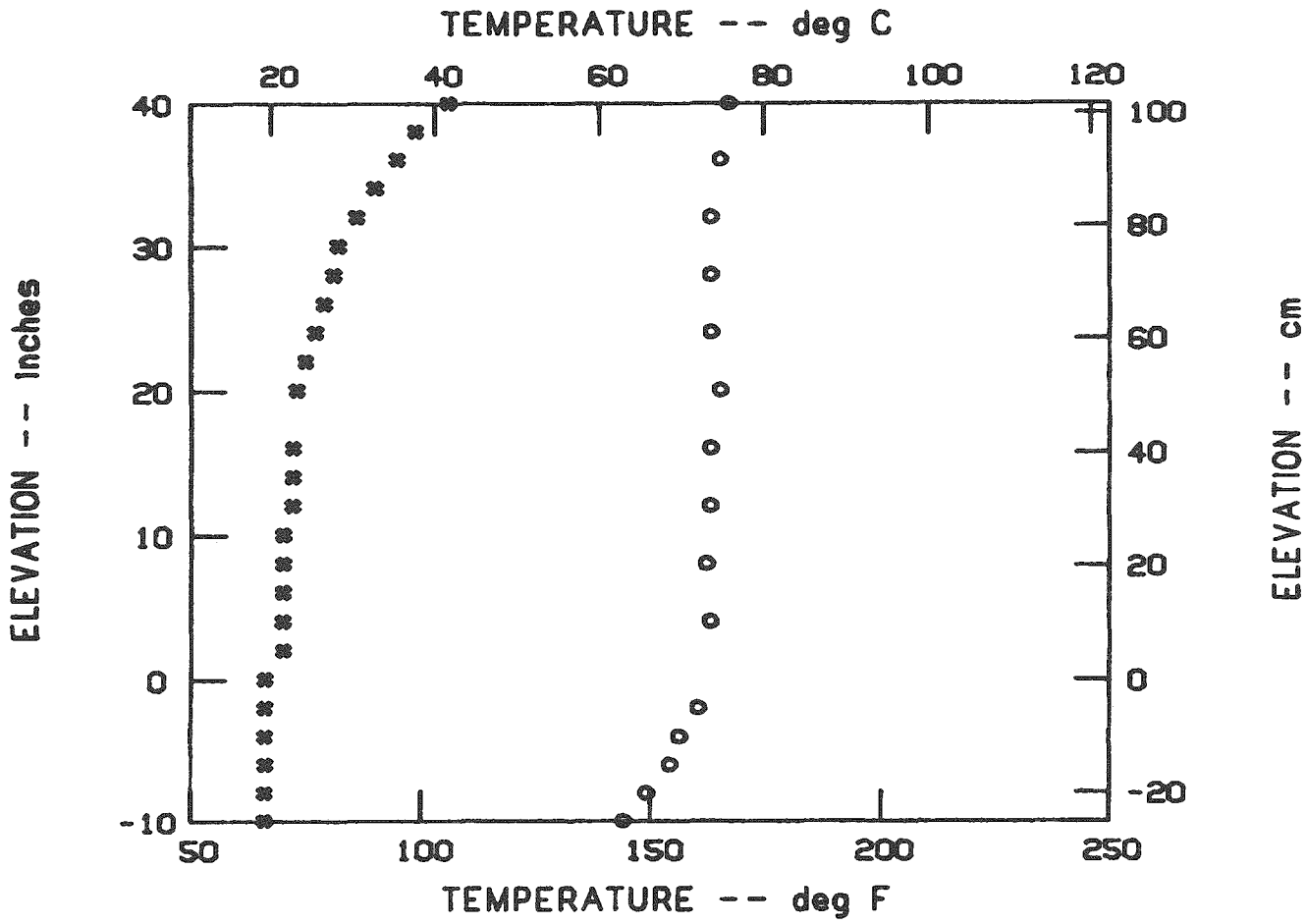

OTSG TEMPERATURE PROFILES: TEST 30

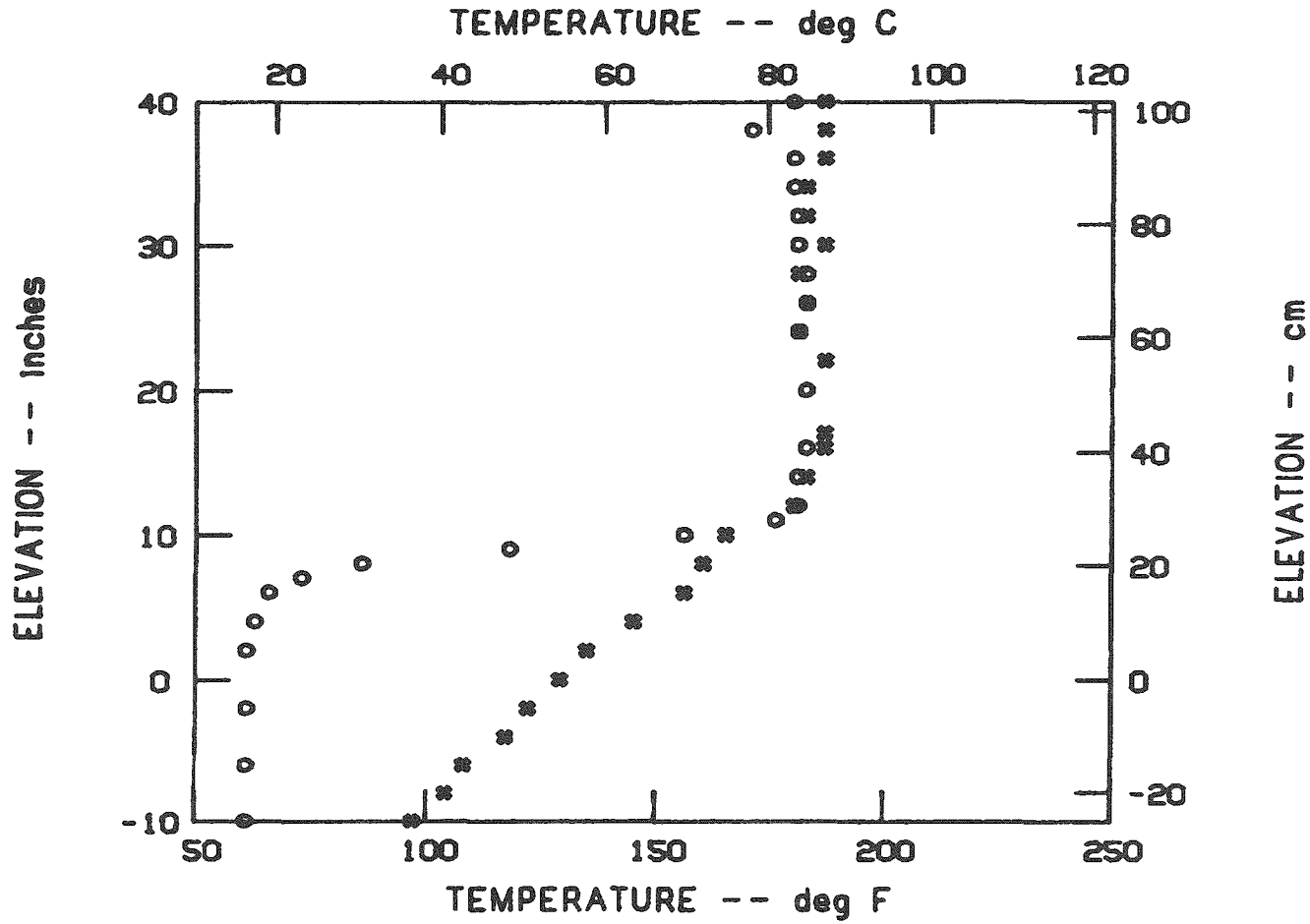

OTSG TEMPERATURE PROFILES: TEST 31

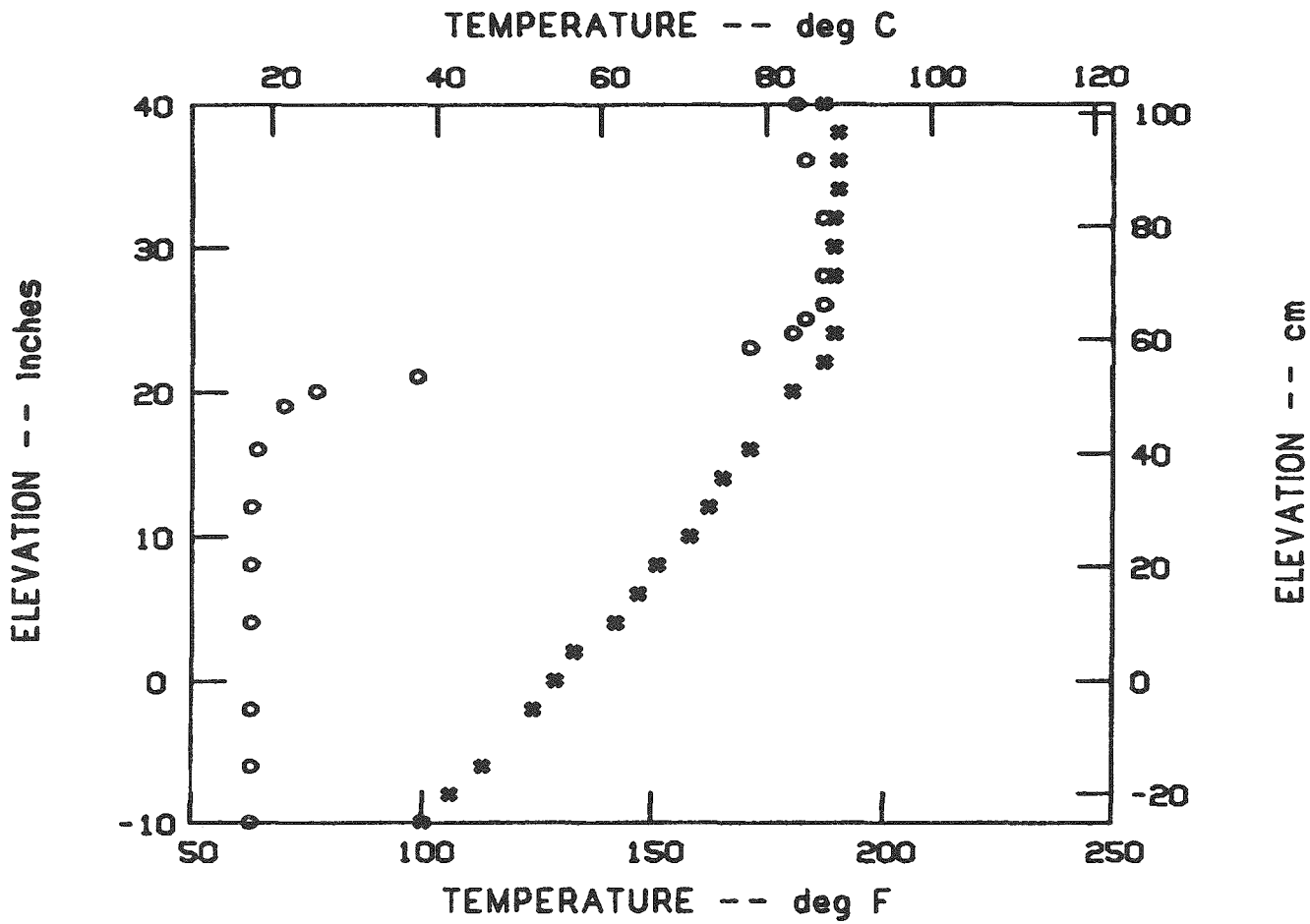

OTSG TEMPERATURE PROFILES: TEST 32

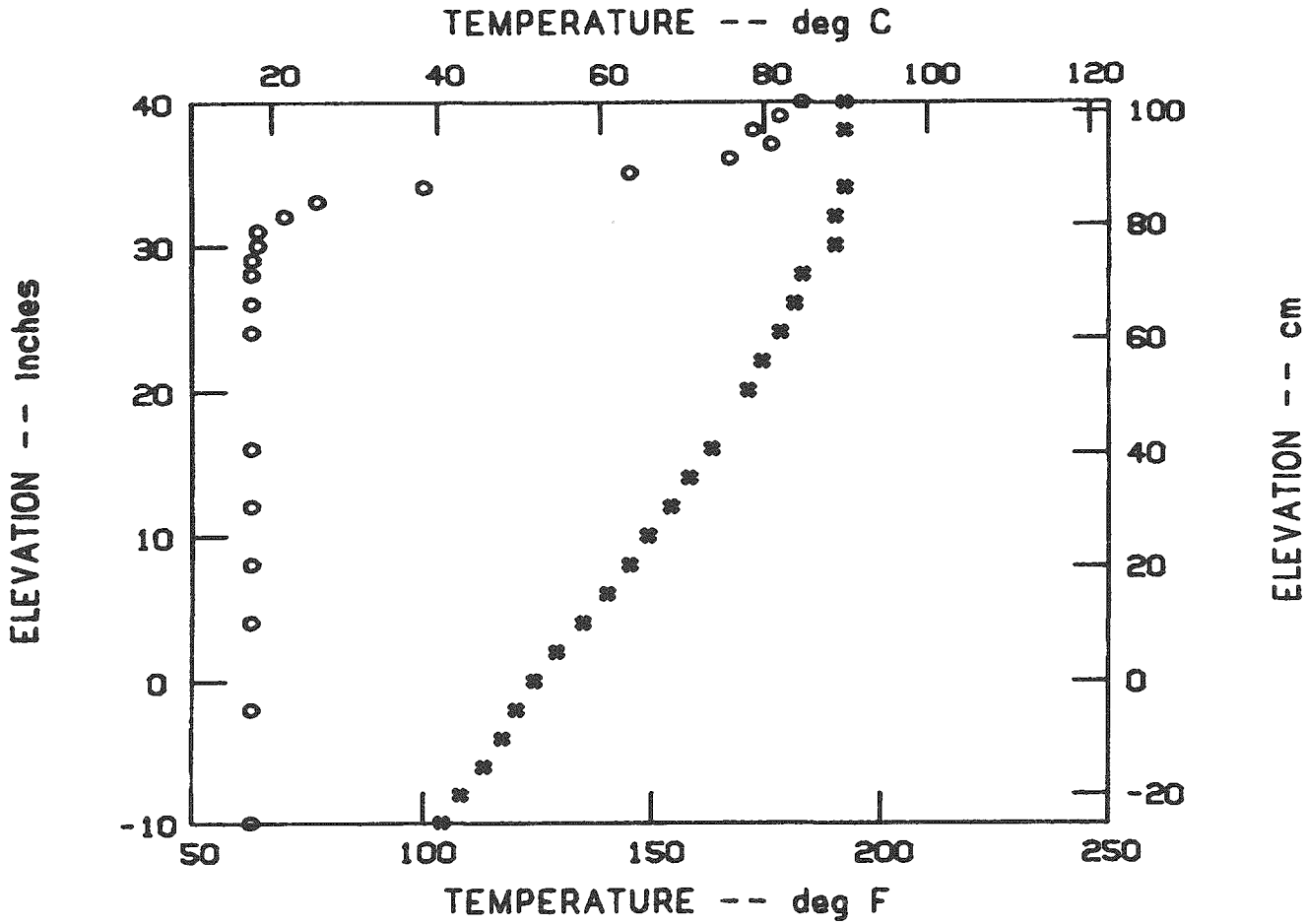

OTSG TEMPERATURE PROFILES: TEST 33

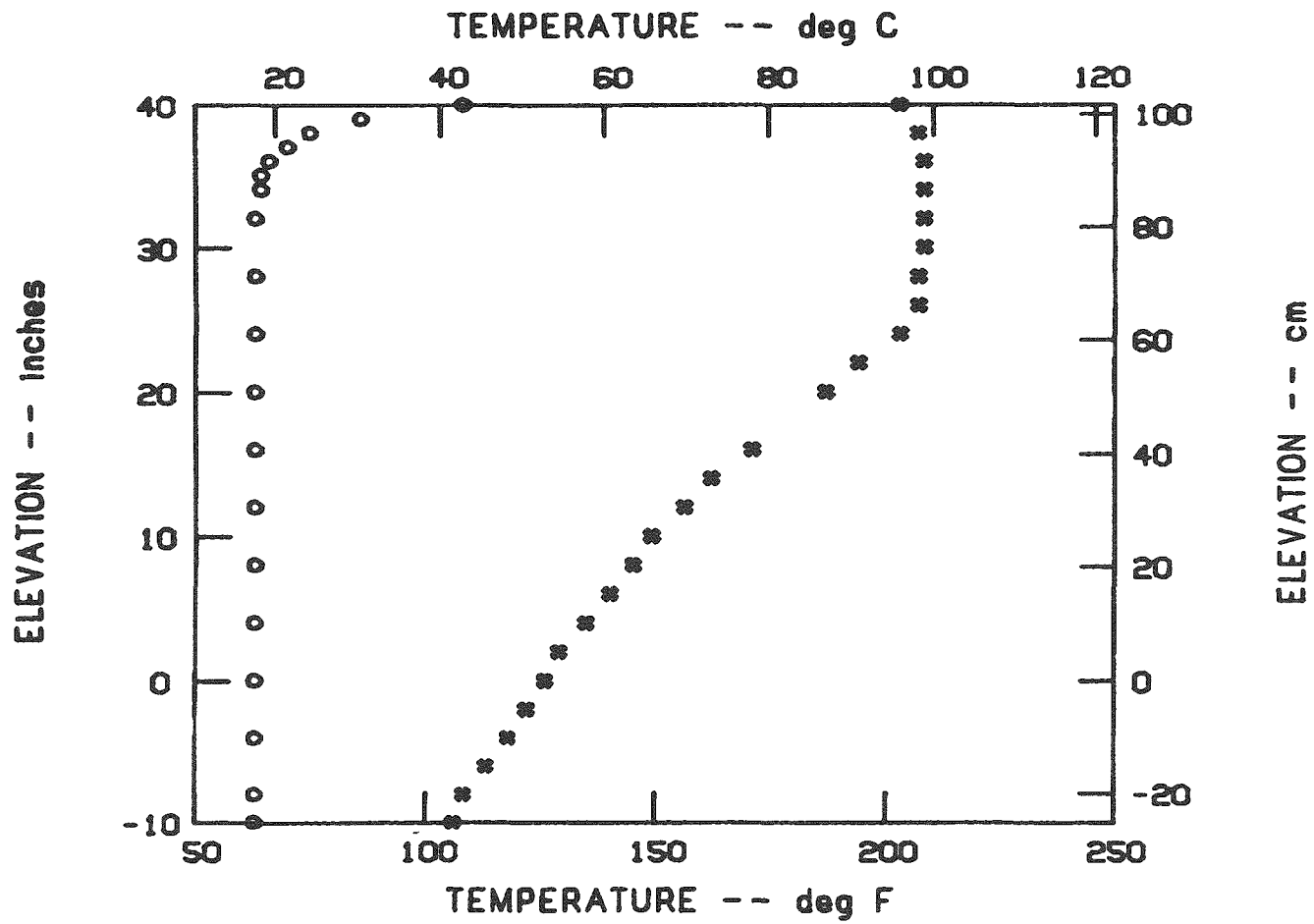

OTSG TEMPERATURE PROFILES: TEST 34

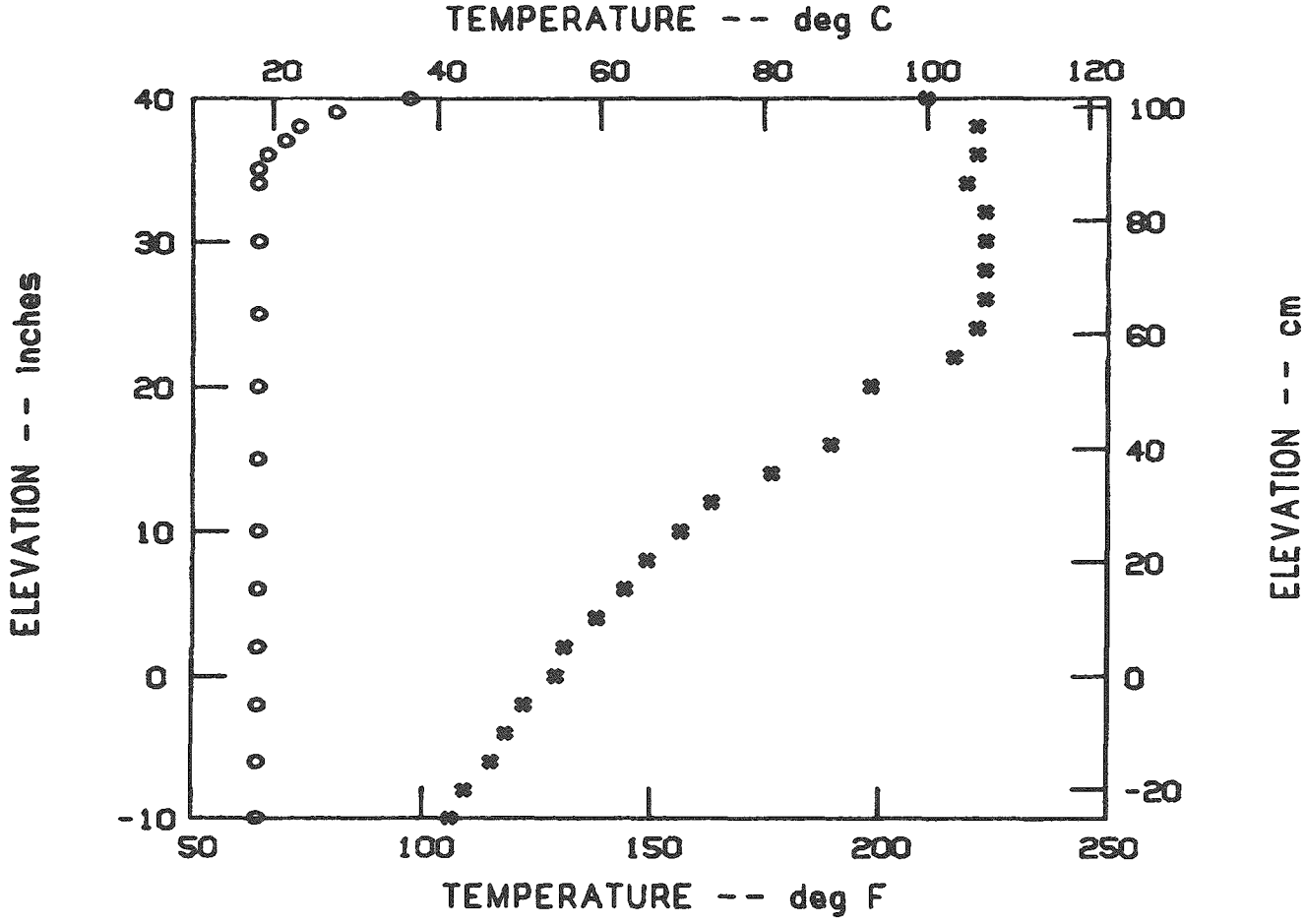

OTSG TEMPERATURE PROFILES: TEST 35

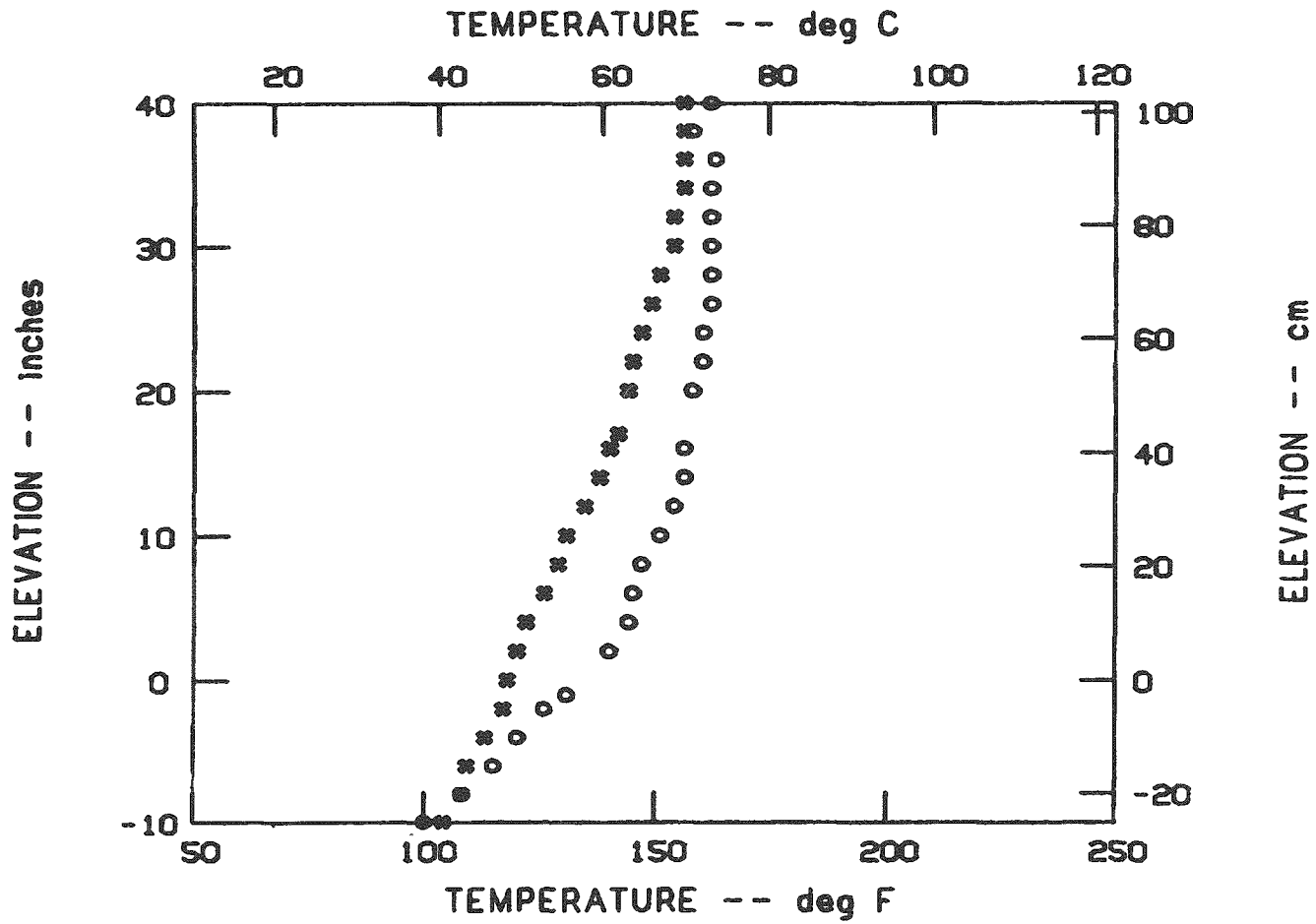

OTSG TEMPERATURE PROFILES: TEST 38

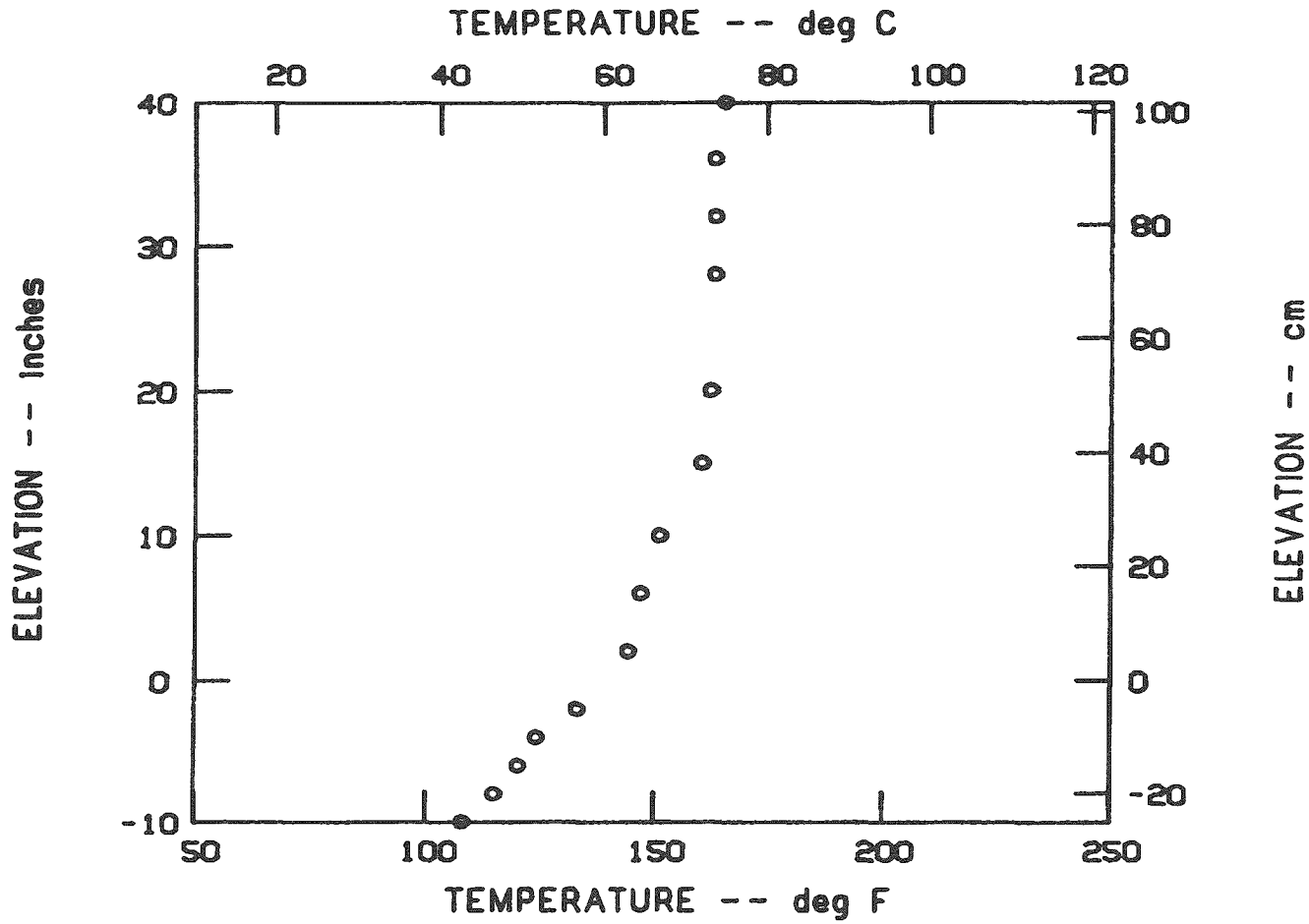

OTSG TEMPERATURE PROFILES: TEST 39

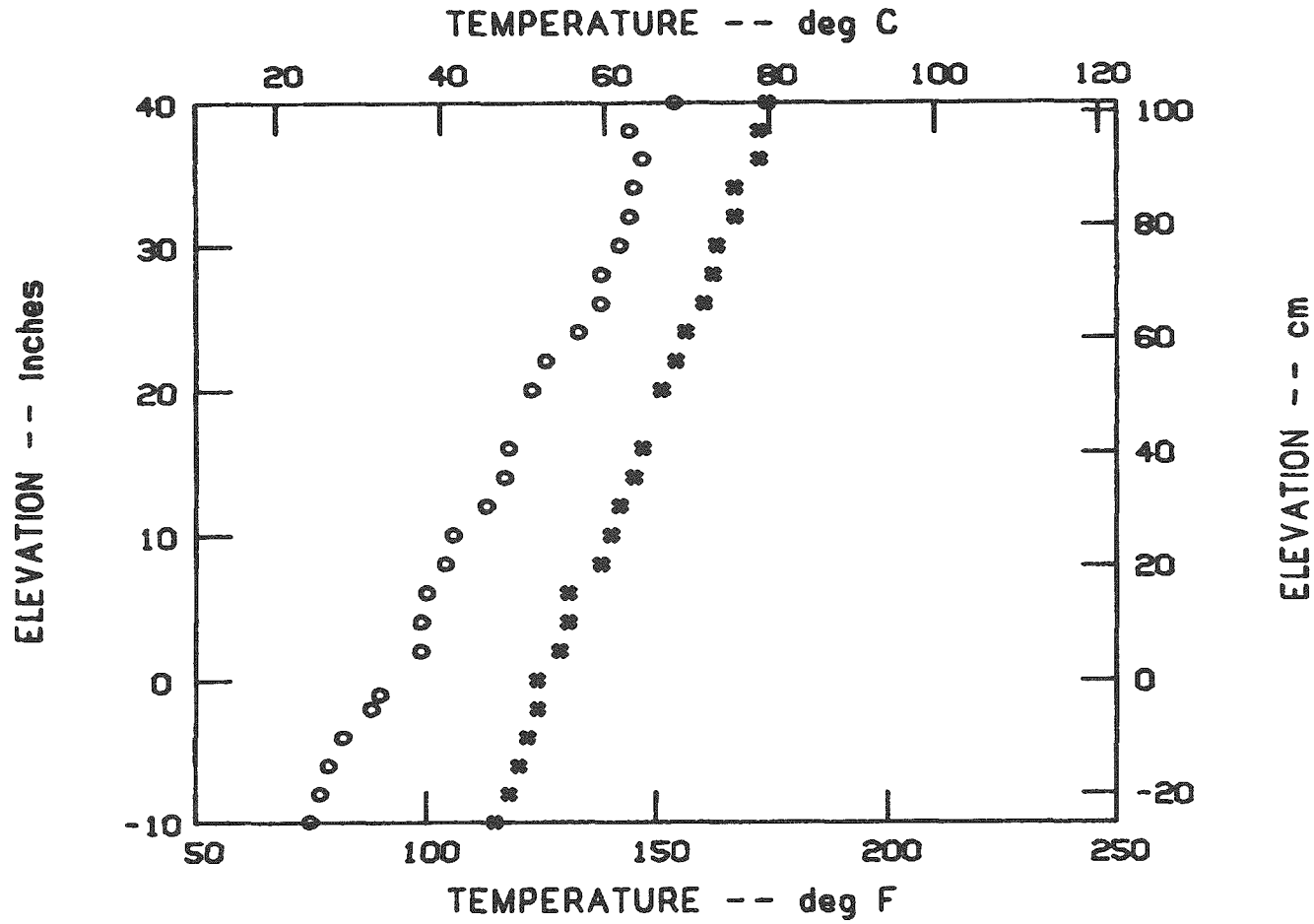

OTSG TEMPERATURE PROFILES: TEST 40

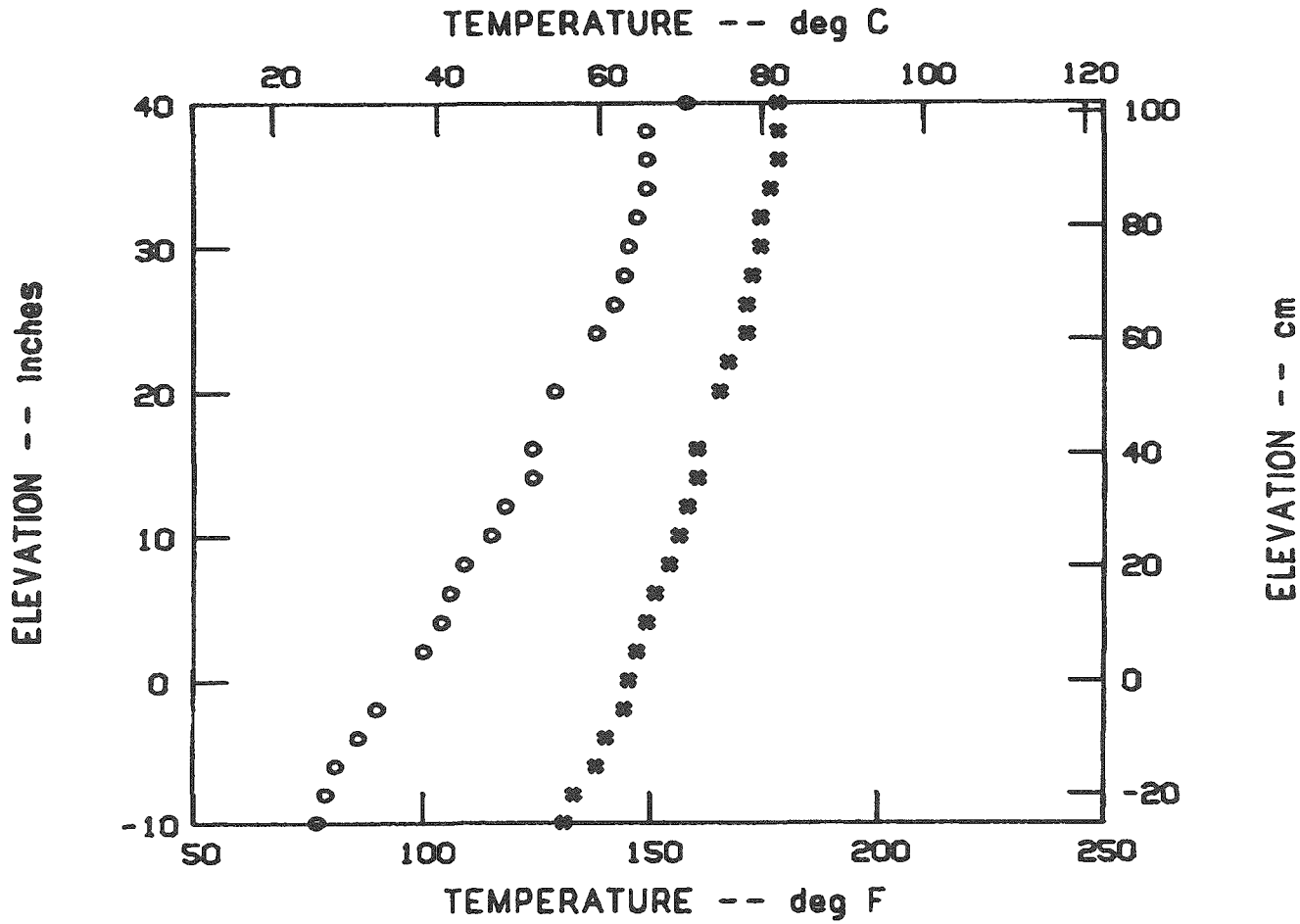

OTSG TEMPERATURE PROFILES: TEST 41

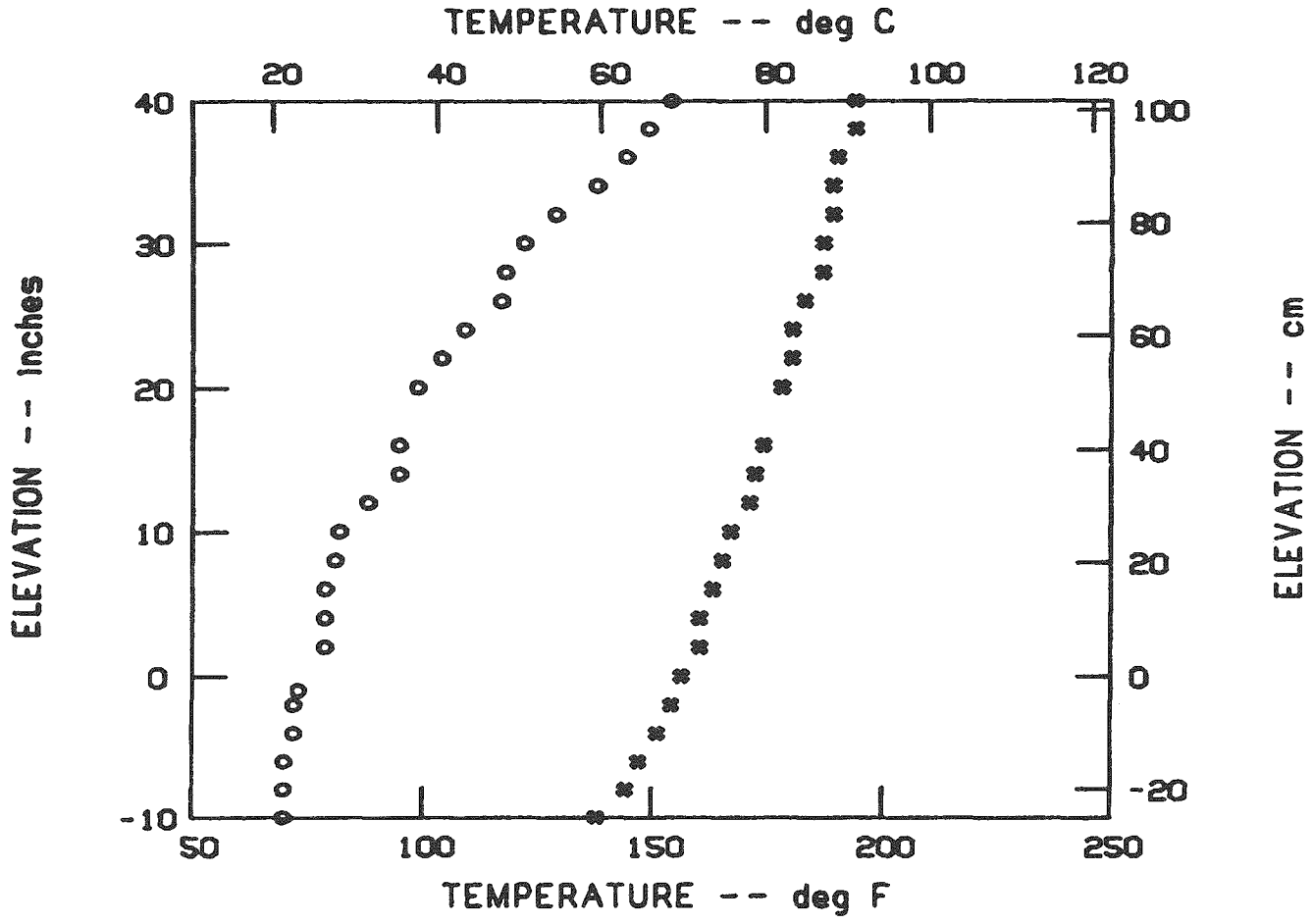

OTSG TEMPERATURE PROFILES: TEST 42

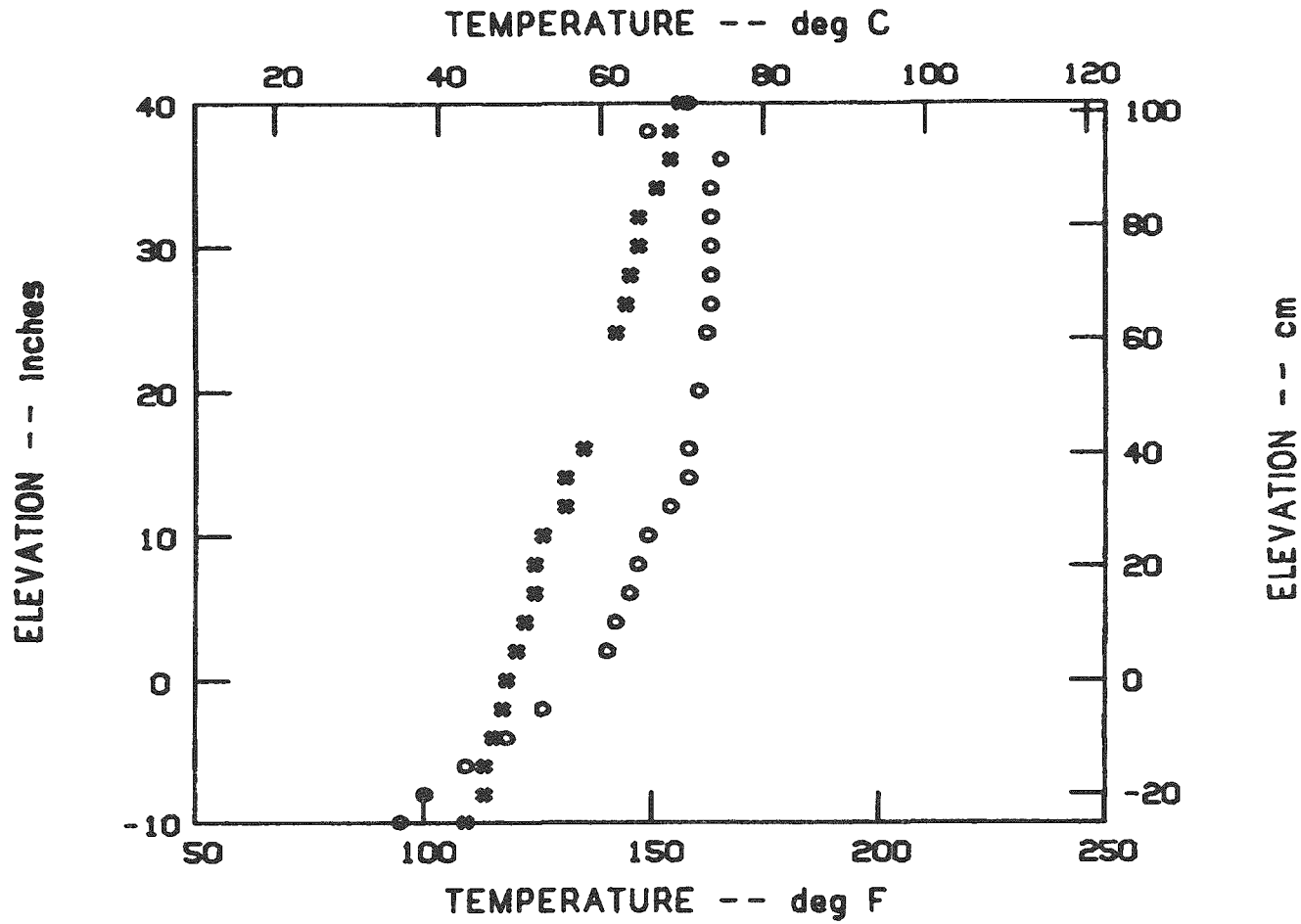

OTSG TEMPERATURE PROFILES: TEST 43

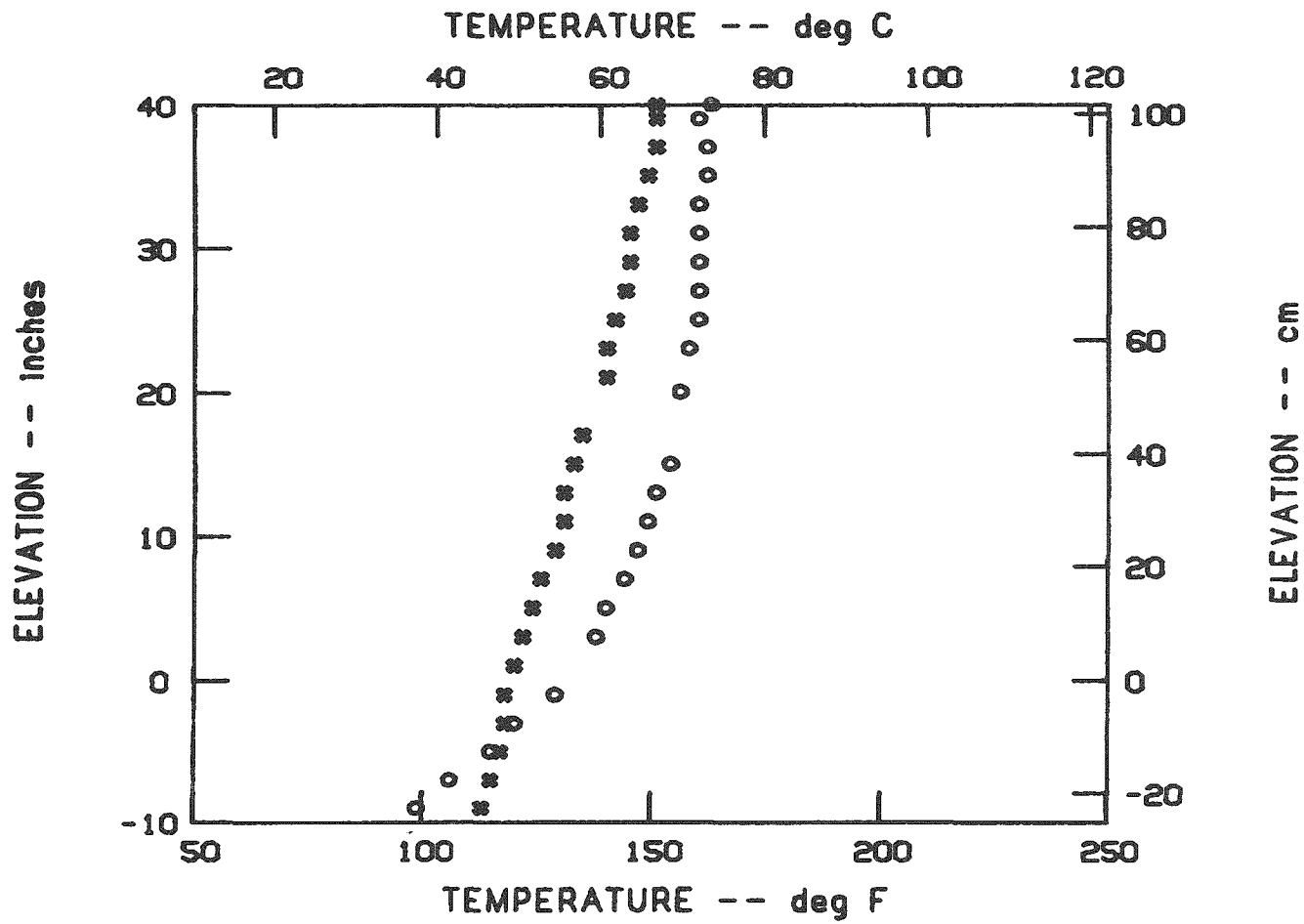

OTSG TEMPERATURE PROFILES: TEST 43A

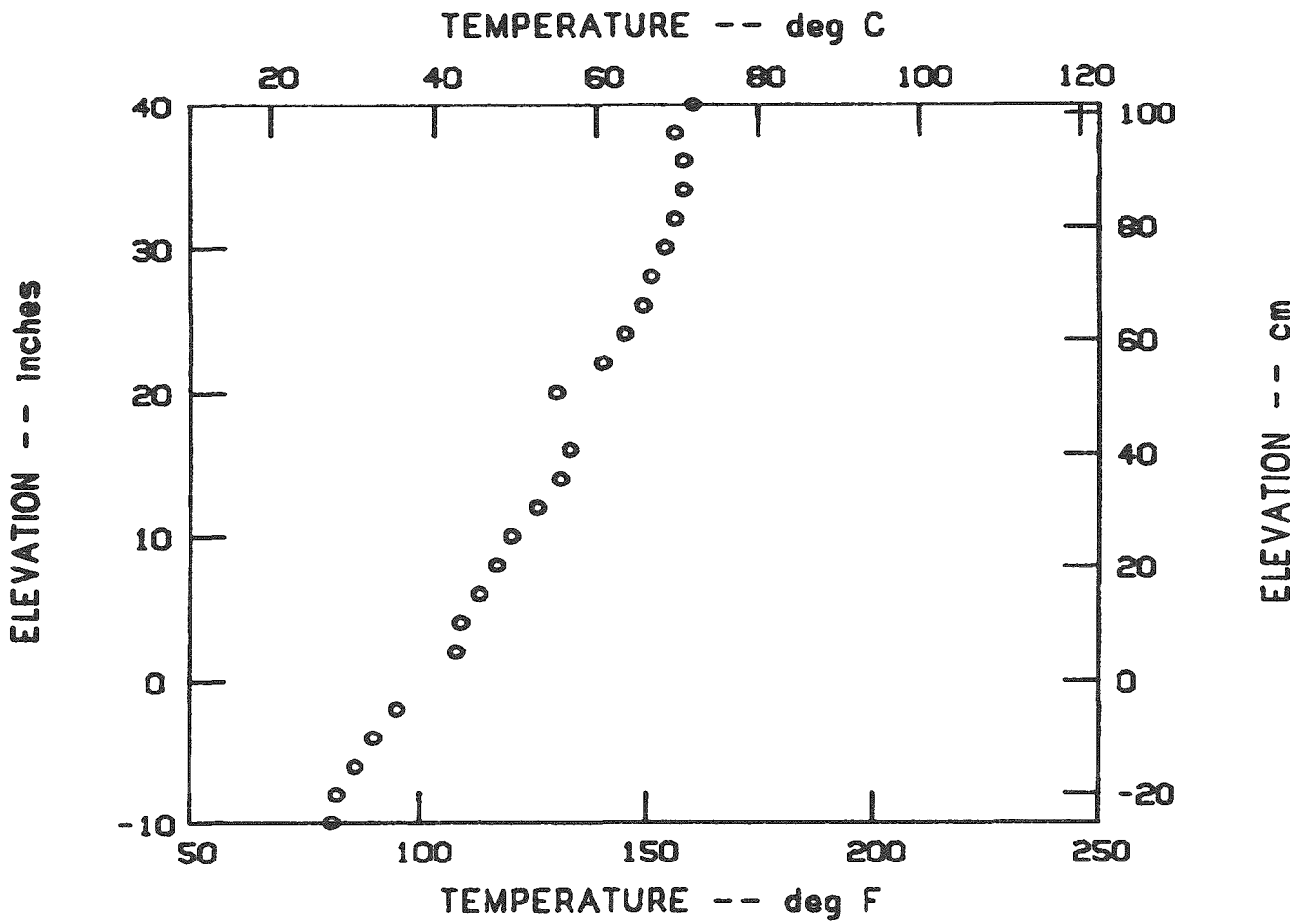

OTSG TEMPERATURE PROFILES: TEST 44

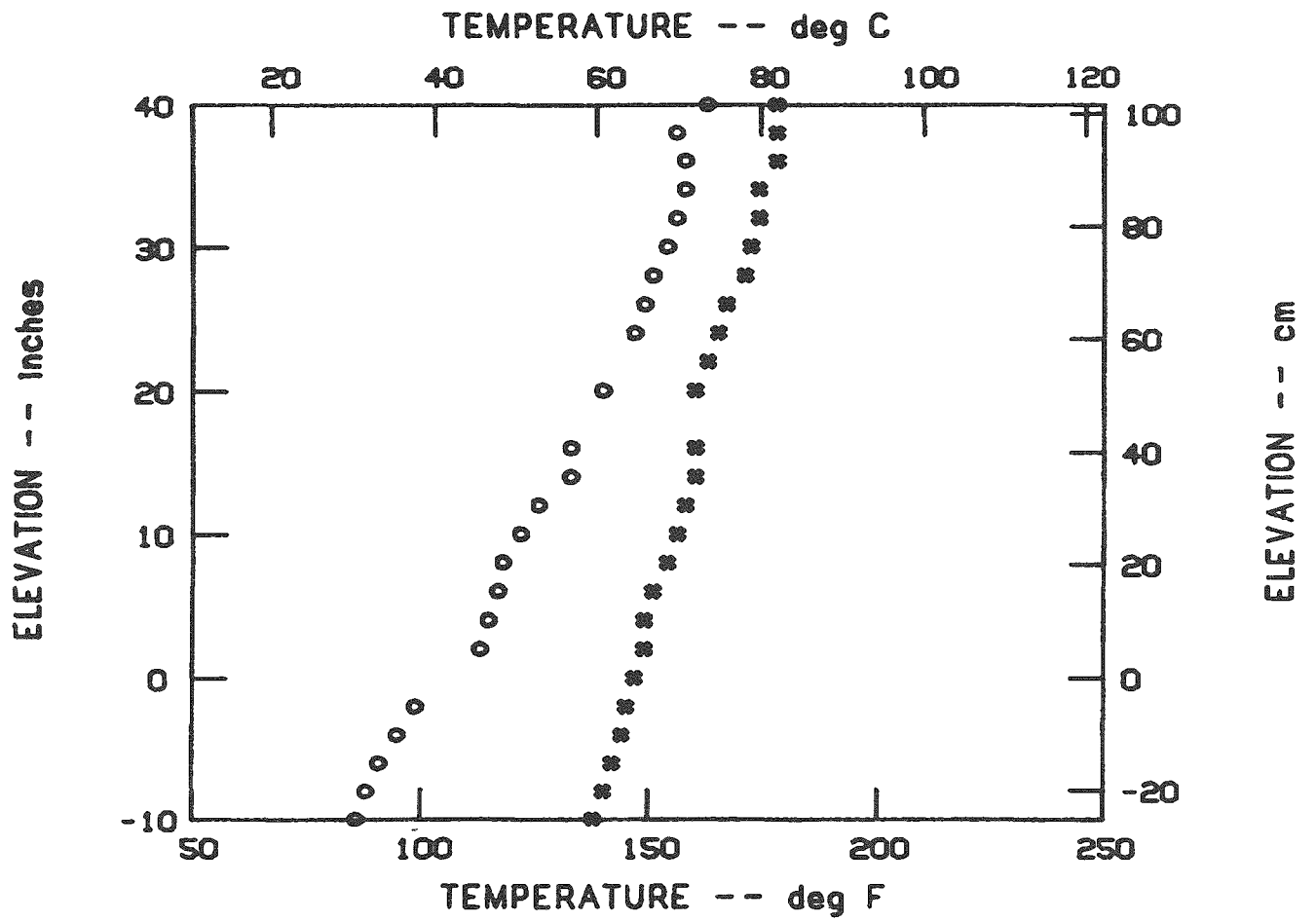

OTSG TEMPERATURE PROFILES: TEST 45

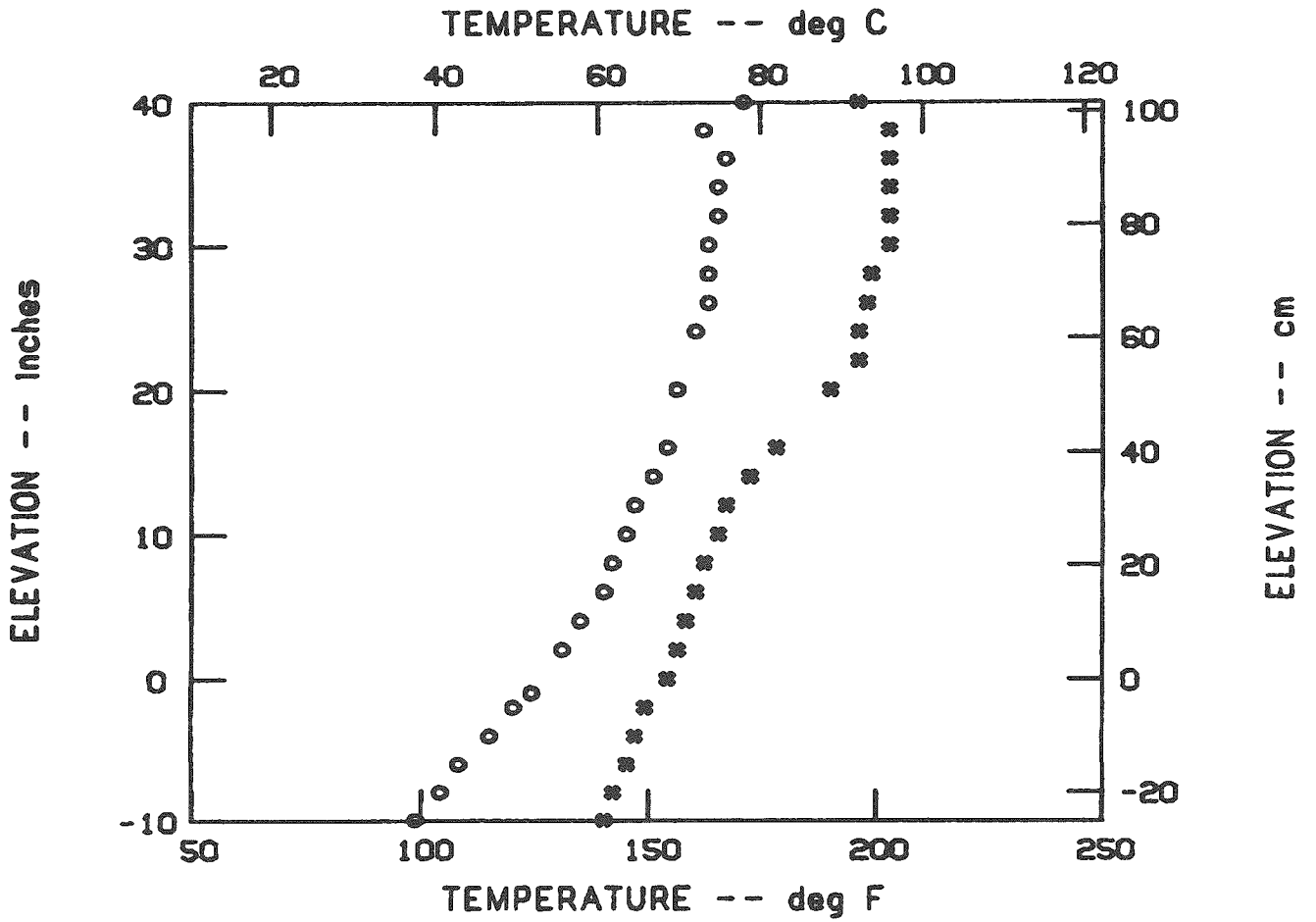

OTSG TEMPERATURE PROFILES: TEST 46

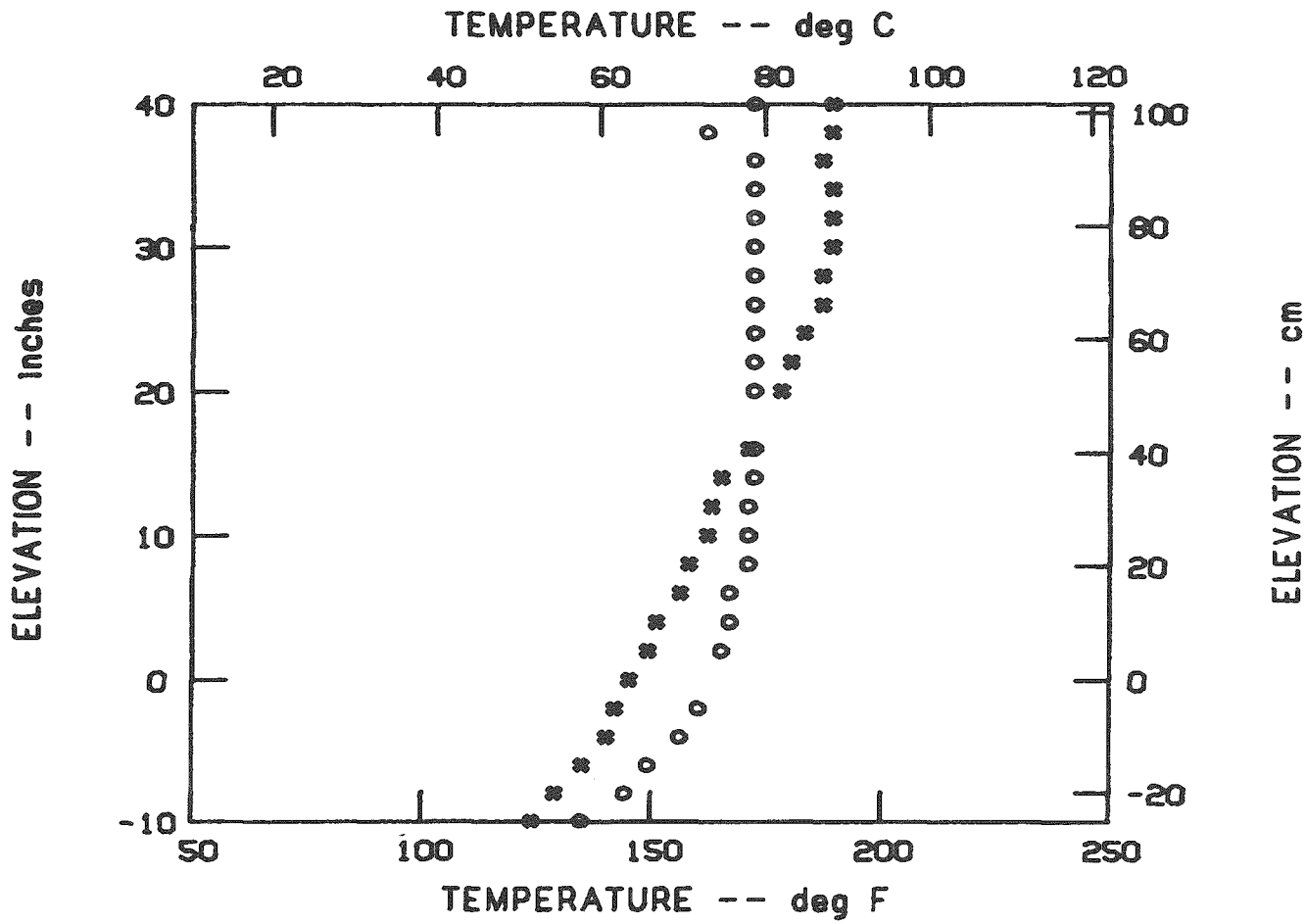

OTSG TEMPERATURE PROFILES: TEST 47

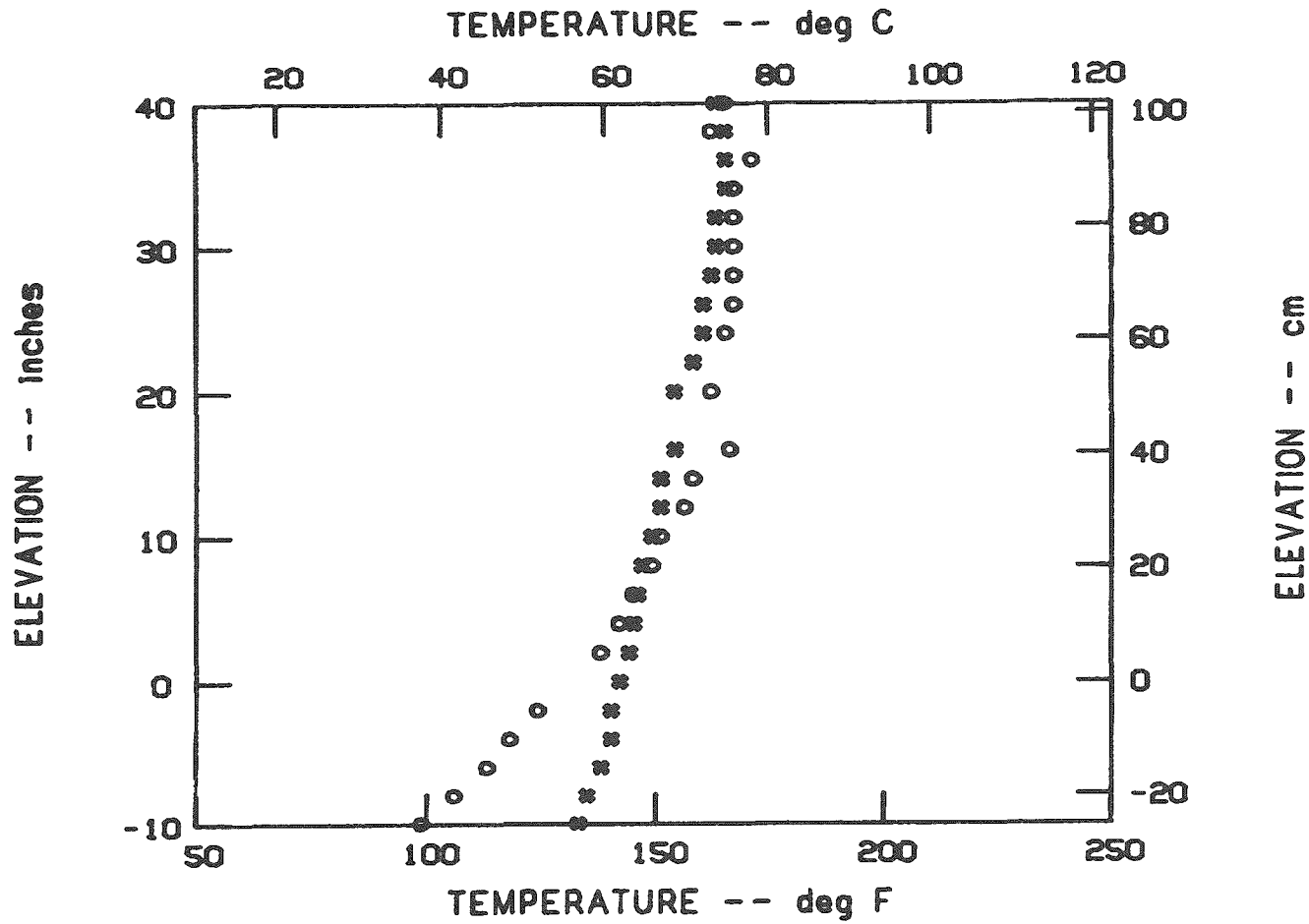

OTSG TEMPERATURE PROFILES: TEST 48

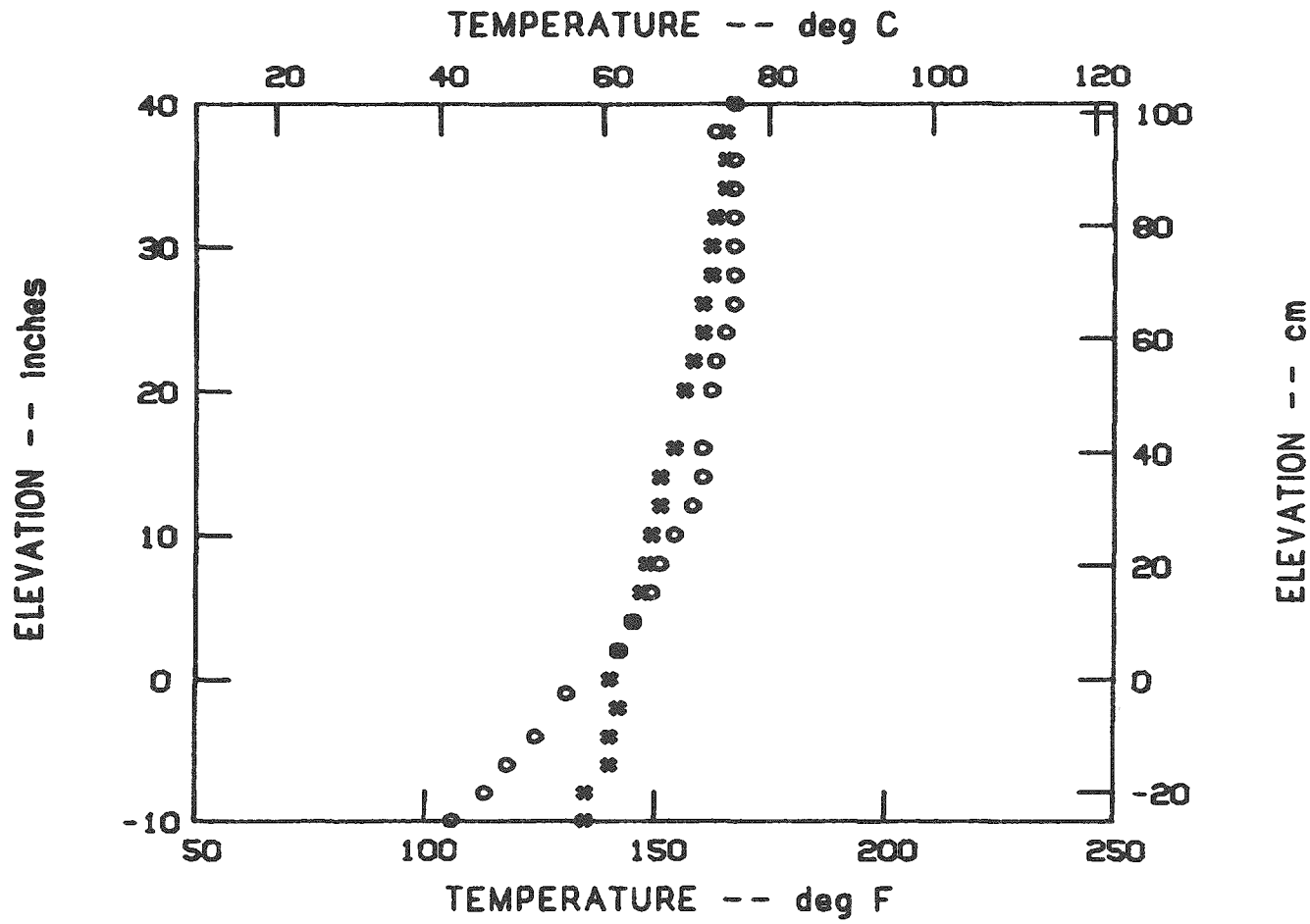

OTSG TEMPERATURE PROFILES: TEST 49

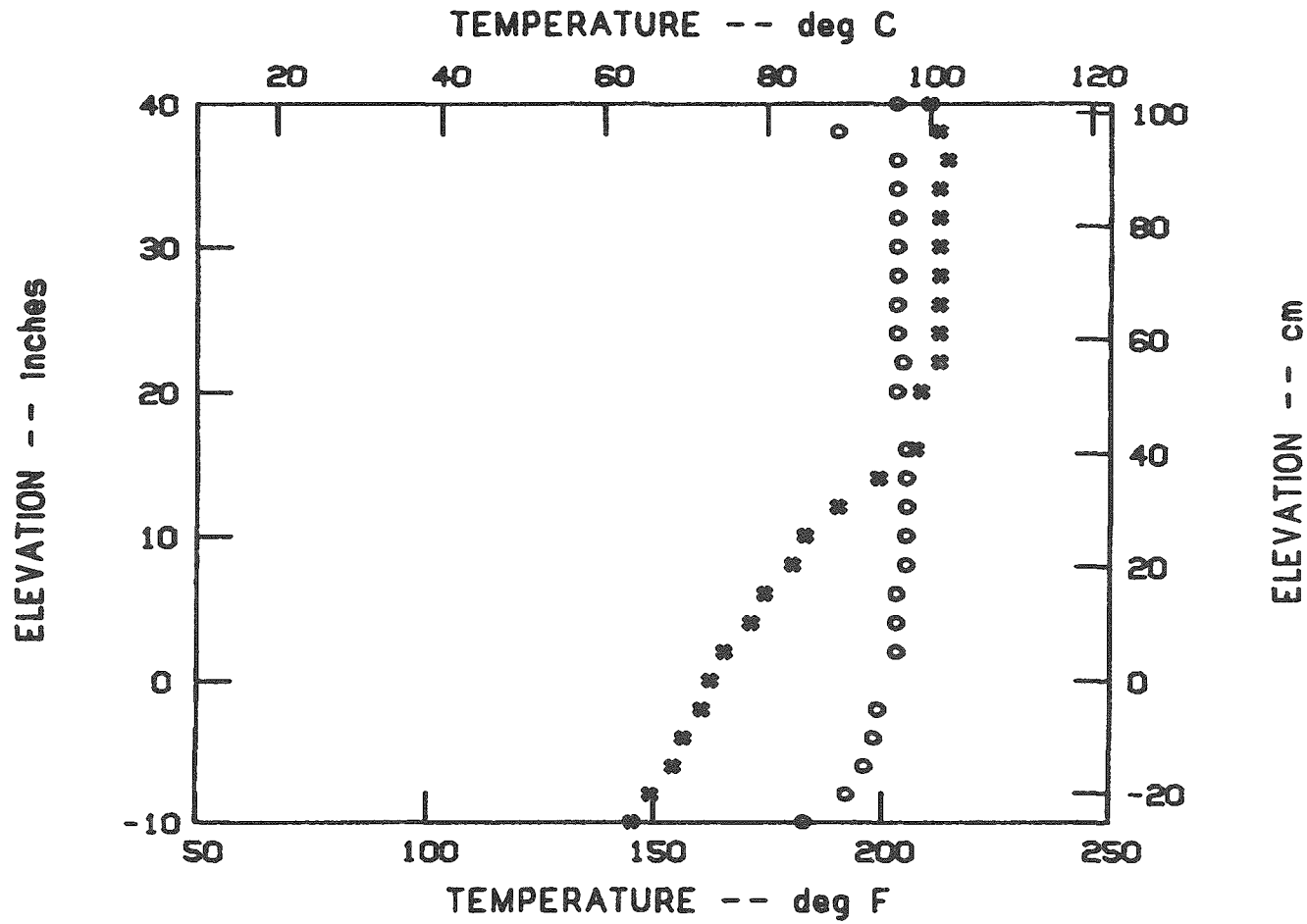

OTSG TEMPERATURE PROFILES: TEST 50

EPRI NP-2069

Below are five index cards that allow for filing according to the four cross-references in addition to the title of the report. A brief abstract describing the major subject area covered in the report is included on each card.

EPRI NP-2069
RP1731-1
Final Report
October 1981

ANALYSIS AND TESTING PROGRAM

EPRI

Two-Phase Natural Circulation Experiments in a Test Facility Modeled After Three Mile Island Unit-2

Contractor: SRI International

A series of natural circulation experiments, conducted in a test facility that was configured after the primary and secondary cooling systems of Three Mile Island Unit-2, are described. Details are provided on the test facility, instrumentation, and effects of various operating parameters. Two different modes of natural circulation are described: Mode 1, which removes the heat via reflux condensation, and Mode 2, which removes the heat by means of two-phase natural circulation in the primary loop. 106 pp.

EPRI Project Manager: J.-P. Sursock

Cross-References:
1. EPRI NP-2069 2. RP1731-1 3. Analysis and Testing Program 4. Two-Phase Flow

ELECTRIC POWER RESEARCH INSTITUTE
Post Office Box 10412, Palo Alto, CA 94303 415-855-2000

EPRI NP-2069
RP1731-1
Final Report
October 1981

TWO-PHASE FLOW

EPRI

Two-Phase Natural Circulation Experiments in a Test Facility Modeled After Three Mile Island Unit-2

Contractor: SRI International

A series of natural circulation experiments, conducted in a test facility that was configured after the primary and secondary cooling systems of Three Mile Island Unit-2, are described. Details are provided on the test facility, instrumentation, and effects of various operating parameters. Two different modes of natural circulation are described: Mode 1, which removes the heat via reflux condensation, and Mode 2, which removes the heat by means of two-phase natural circulation in the primary loop. 106 pp.

EPRI Project Manager: J.-P. Sursock

Cross-References:
1. EPRI NP-2069 2. RP1731-1 3. Analysis and Testing Program 4. Two-Phase Flow

ELECTRIC POWER RESEARCH INSTITUTE
Post Office Box 10412, Palo Alto, CA 94303 415-855-2000

EPRI

EPRI NP-2069
RP1731-1
Final Report
October 1981

Two-Phase Natural Circulation Experiments in a Test Facility Modeled After Three Mile Island Unit-2

Contractor: SRI International

A series of natural circulation experiments, conducted in a test facility that was configured after the primary and secondary cooling systems of Three Mile Island Unit-2, are described. Details are provided on the test facility, instrumentation, and effects of various operating parameters. Two different modes of natural circulation are described: Mode 1, which removes the heat via reflux condensation, and Mode 2, which removes the heat by means of two-phase natural circulation in the primary loop. 106 pp.

EPRI Project Manager: J.-P. Sursock

Cross-References:
1. EPRI NP-2069 2. RP1731-1 3. Analysis and Testing Program 4. Two-Phase Flow

ELECTRIC POWER RESEARCH INSTITUTE
Post Office Box 10412, Palo Alto, CA 94303 415-855-2000

EPRI NP-2069

EPRI

EPRI NP-2069
RP1731-1
Final Report
October 1981

Two-Phase Natural Circulation Experiments in a Test Facility Modeled After Three Mile Island Unit-2

Contractor: SRI International

A series of natural circulation experiments, conducted in a test facility that was configured after the primary and secondary cooling systems of Three Mile Island Unit-2, are described. Details are provided on the test facility, instrumentation, and effects of various operating parameters. Two different modes of natural circulation are described: Mode 1, which removes the heat via reflux condensation, and Mode 2, which removes the heat by means of two-phase natural circulation in the primary loop. 106 pp.

EPRI Project Manager: J.-P. Sursock

Cross-References:
1. EPRI NP-2069 2. RP1731-1 3. Analysis and Testing Program 4. Two-Phase Flow

ELECTRIC POWER RESEARCH INSTITUTE
Post Office Box 10412, Palo Alto, CA 94303 415-855-2000

RP1731-1

EPRI

EPRI NP-2069
RP1731-1
Final Report
October 1981

Two-Phase Natural Circulation Experiments in a Test Facility Modeled After Three Mile Island Unit-2

Contractor: SRI International

A series of natural circulation experiments, conducted in a test facility that was configured after the primary and secondary cooling systems of Three Mile Island Unit-2, are described. Details are provided on the test facility, instrumentation, and effects of various operating parameters. Two different modes of natural circulation are described: Mode 1, which removes the heat via reflux condensation, and Mode 2, which removes the heat by means of two-phase natural circulation in the primary loop. 106 pp.

EPRI Project Manager: J.-P. Sursock

Cross-References:
1. EPRI NP-2069 2. RP1731-1 3. Analysis and Testing Program 4. Two-Phase Flow

ELECTRIC POWER RESEARCH INSTITUTE
Post Office Box 10412, Palo Alto, CA 94303 415-855-2000